salaman.web.cern.ch/

The quest for Lepton Flavour Violation through 0v2β decays in Germanium:

Large Enriched
Germanium Experiment
for Neutrinoless ββ Decay

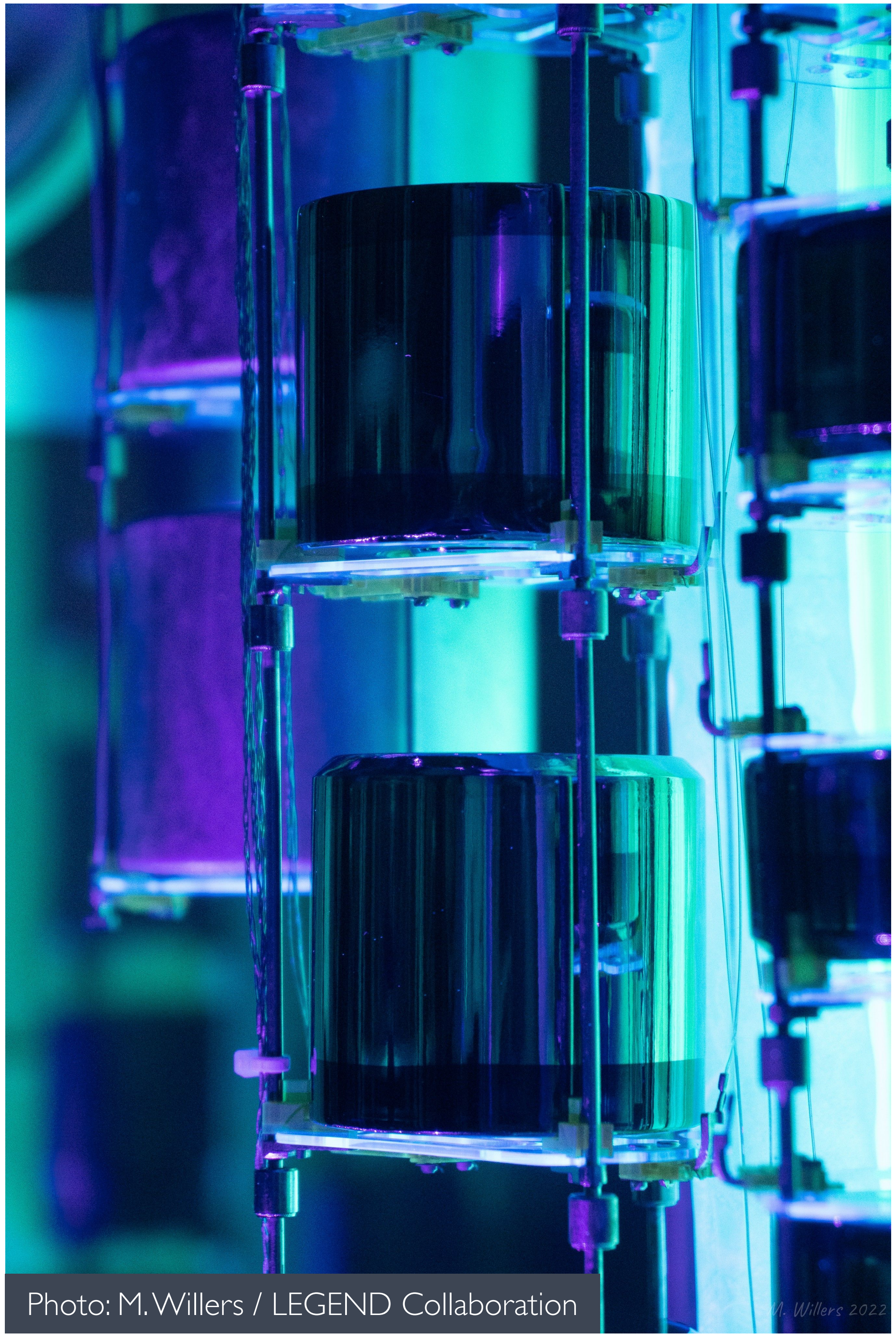
Photo: M. Willers / LEGEND Collaboration

G. Salamanna (Roma Tre University & INFN)
U BHM, June 14th, 2023

The heart of the matter

$$P_{\nu_\alpha \to \nu_\beta}(t) = |\langle \nu_\beta | \nu_\alpha(t) \rangle|^2$$

$$= \delta_{\alpha\beta} - 4 \sum_{i>j} \Re(U^*_{\alpha i} U_{\beta i} U_{\alpha j} U^*_{\beta j}) \sin^2(\frac{\Delta m^2_{ij} L}{4E})$$

$$+ 2 \sum_{i>j} \Im(U^*_{\alpha i} U_{\beta i} U_{\alpha j} U^*_{\beta j}) \sin(\frac{\Delta m^2_{ij} L}{4E}),$$

where $\Delta m^2_{ij} = m^2_i - m^2_j$ and we can rewrite:

$$\frac{\Delta m^2_{ij} L}{4E} \approx 1.267 \frac{\Delta m^2_{ij}[eV^2] \times L[km]}{E[GeV]}.$$

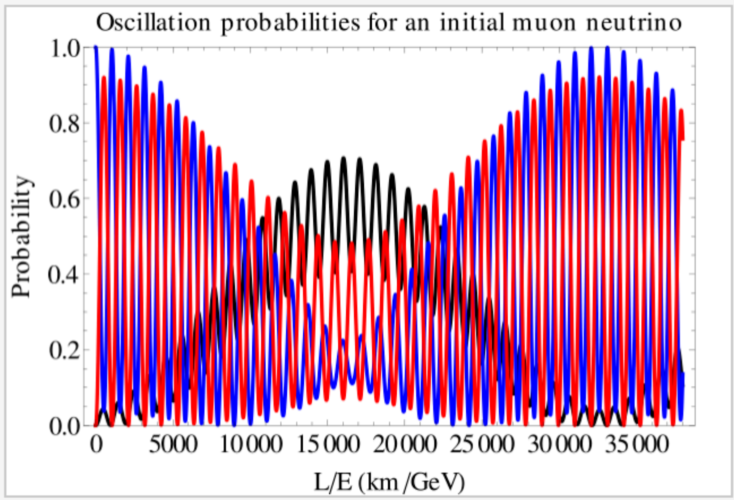

Muon neutrino oscillations, long range

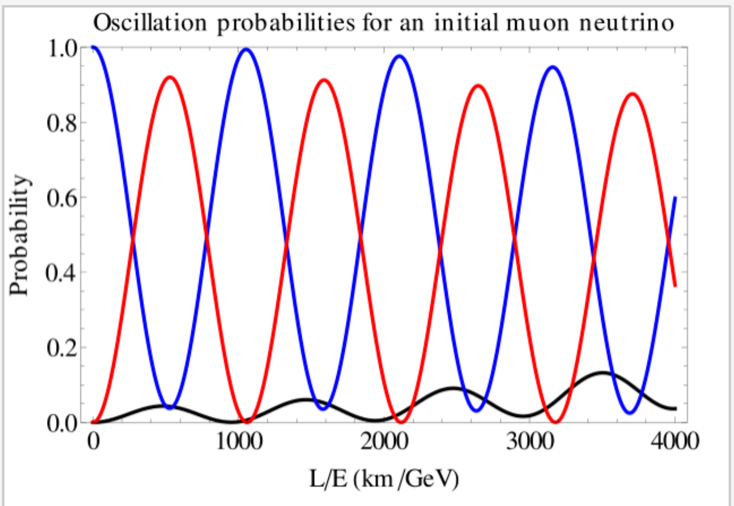

Muon neutrino oscillations, short range

Neutrino oscillations reveal that **(anti-)neutrinos do have a mass**

- …but we also know that "fertile" neutrinos are LH only (V-A coupling with W bosons)
  - Then how do we get a Dirac mass for neutrinos?

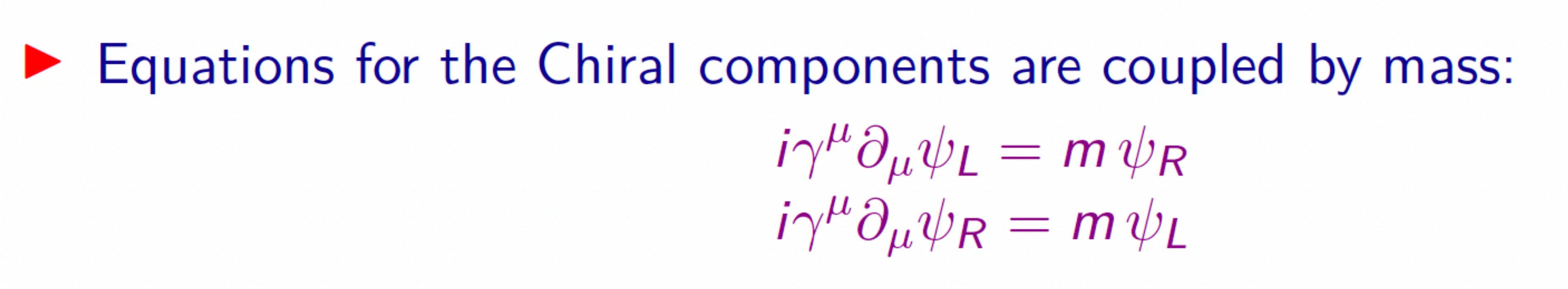

- Equations for the Chiral components are coupled by mass:

$$i\gamma^\mu \partial_\mu \psi_L = m\,\psi_R$$
$$i\gamma^\mu \partial_\mu \psi_R = m\,\psi_L$$

- …but we also know that "fertile" neutrinos are LH only (V-A coupling with W bosons)
  - Then how do we get a Dirac mass for neutrinos?

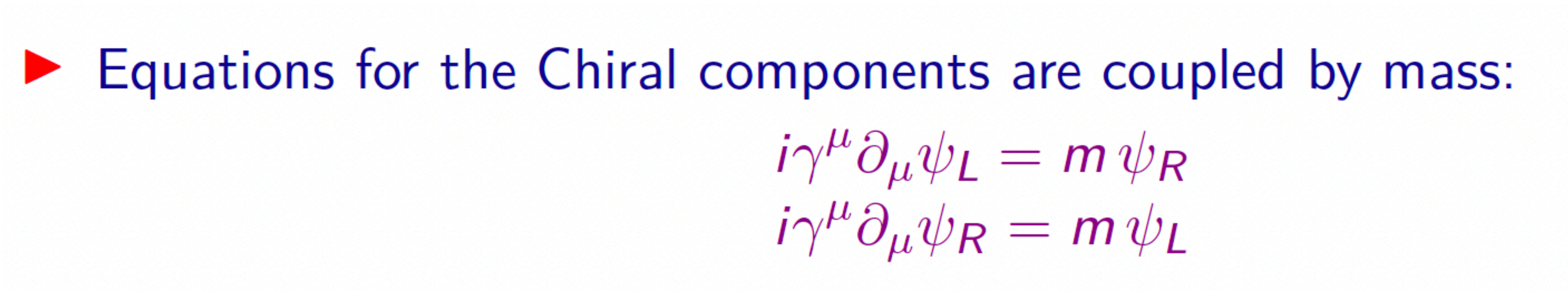

- ► Equations for the Chiral components are coupled by mass:

$$i\gamma^\mu \partial_\mu \psi_L = m\,\psi_R$$
$$i\gamma^\mu \partial_\mu \psi_R = m\,\psi_L$$

Can we get a non-Dirac mass term in the Lagrangian with LH neutrinos only?

- …but we also know that "fertile" neutrinos are LH only (V-A coupling with W bosons)
  - Then how do we get a Dirac mass for neutrinos?

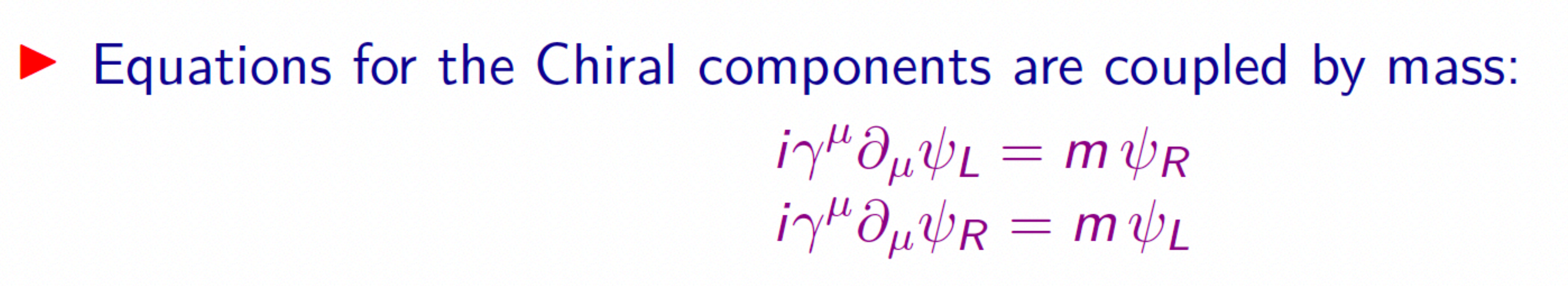

- Equations for the Chiral components are coupled by mass:

$$i\gamma^\mu\partial_\mu\psi_L = m\,\psi_R$$
$$i\gamma^\mu\partial_\mu\psi_R = m\,\psi_L$$

Can we get a non-Dirac mass term in the Lagrangian with LH neutrinos only?

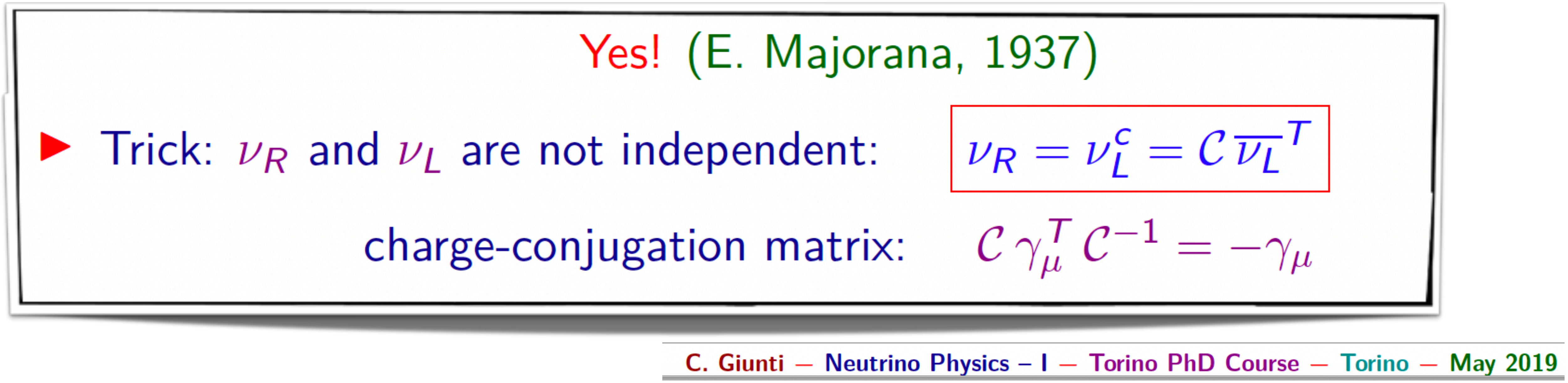

Yes! (E. Majorana, 1937)

- Trick: ν_R and ν_L are not independent: $\boxed{\nu_R = \nu_L^c = \mathcal{C}\,\overline{\nu_L}^T}$

charge-conjugation matrix: $\mathcal{C}\,\gamma_\mu^T\,\mathcal{C}^{-1} = -\gamma_\mu$

C. Giunti — Neutrino Physics – I — Torino PhD Course — Torino — May 2019

Majorana condition

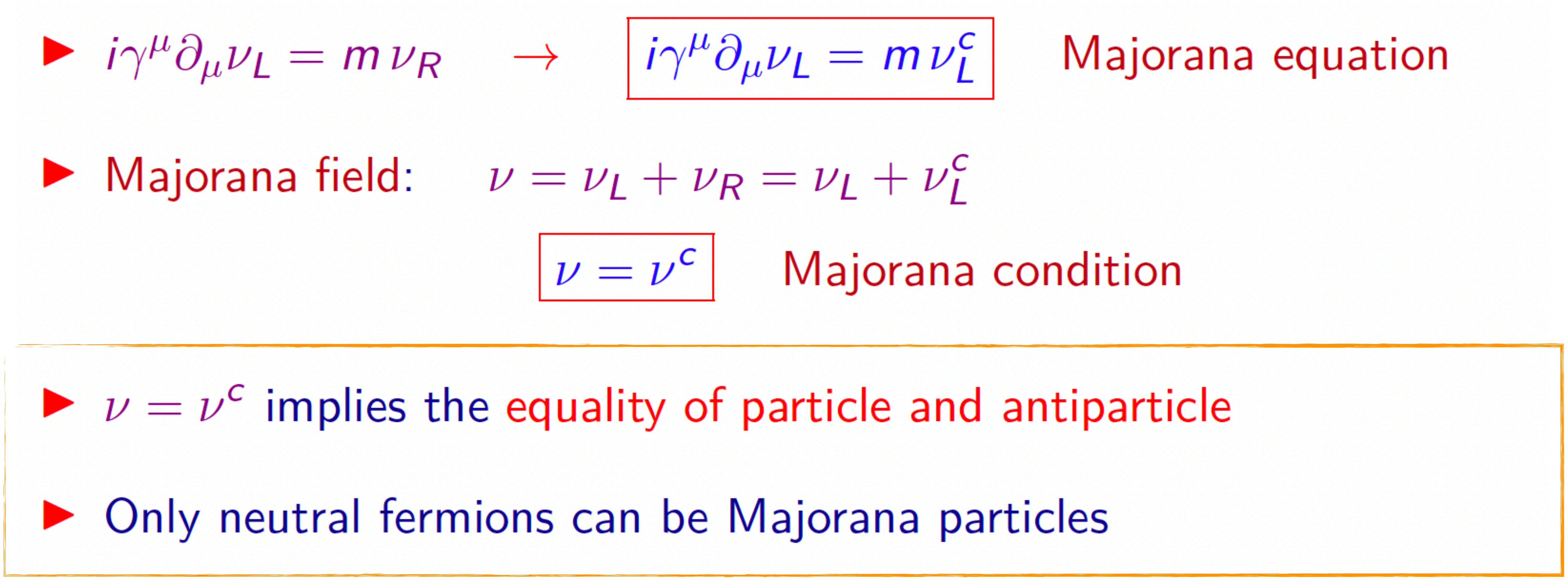

- $i\gamma^{\mu}\partial_{\mu}\nu_L = m\,\nu_R \quad \to \quad \boxed{i\gamma^{\mu}\partial_{\mu}\nu_L = m\,\nu_L^c}$ Majorana equation
- Majorana field: $\nu = \nu_L + \nu_R = \nu_L + \nu_L^c$

  $\boxed{\nu = \nu^c}$ Majorana condition

- $\nu = \nu^c$ implies the equality of particle and antiparticle
- Only neutral fermions can be Majorana particles

- Extra: explains smallness of neutrino mass (see-saw mechanism)
- and provides a candidate for CPV in early Universe

C. Giunti — Neutrino Physics – I — Torino PhD Course — Torino — May 2019 implies…

Total Lepton Number

$$\cancel{L = +1} \quad \longleftarrow \quad \boxed{\nu = \nu^c} \quad \longrightarrow \quad \cancel{L = -1}$$

$$\nu_L \quad \Longrightarrow \quad L = +1 \qquad\qquad \nu_L^c \quad \Longrightarrow \quad L = -1$$

$$\mathscr{L}^{\mathrm{M}} = \overline{\nu_L}\, i\partial\!\!\!/\, \nu_L - \frac{m}{2}\left(\overline{\nu_L^c}\, \nu_L + \overline{\nu_L}\, \nu_L^c\right)$$

Total Lepton Number is not conserved: $\boxed{\Delta L = \pm 2}$

Best process to find violation of Total Lepton Number:

Neutrinoless Double-β Decay

$$\mathcal{N}(A, Z) \to \mathcal{N}(A, Z+2) + 2e^- + \cancel{2\bar{\nu}_e} \qquad (\beta\beta^-_{0\nu})$$

$$\mathcal{N}(A, Z) \to \mathcal{N}(A, Z-2) + 2e^+ + \cancel{2\nu_e} \qquad (\beta\beta^+_{0\nu})$$

NB: other, less preferred BSM explanations for 0ν2β exist (e.g. *https://arxiv.org/pdf/2303.17261.pdf*)

0ν2β decays

$\Delta L=0$

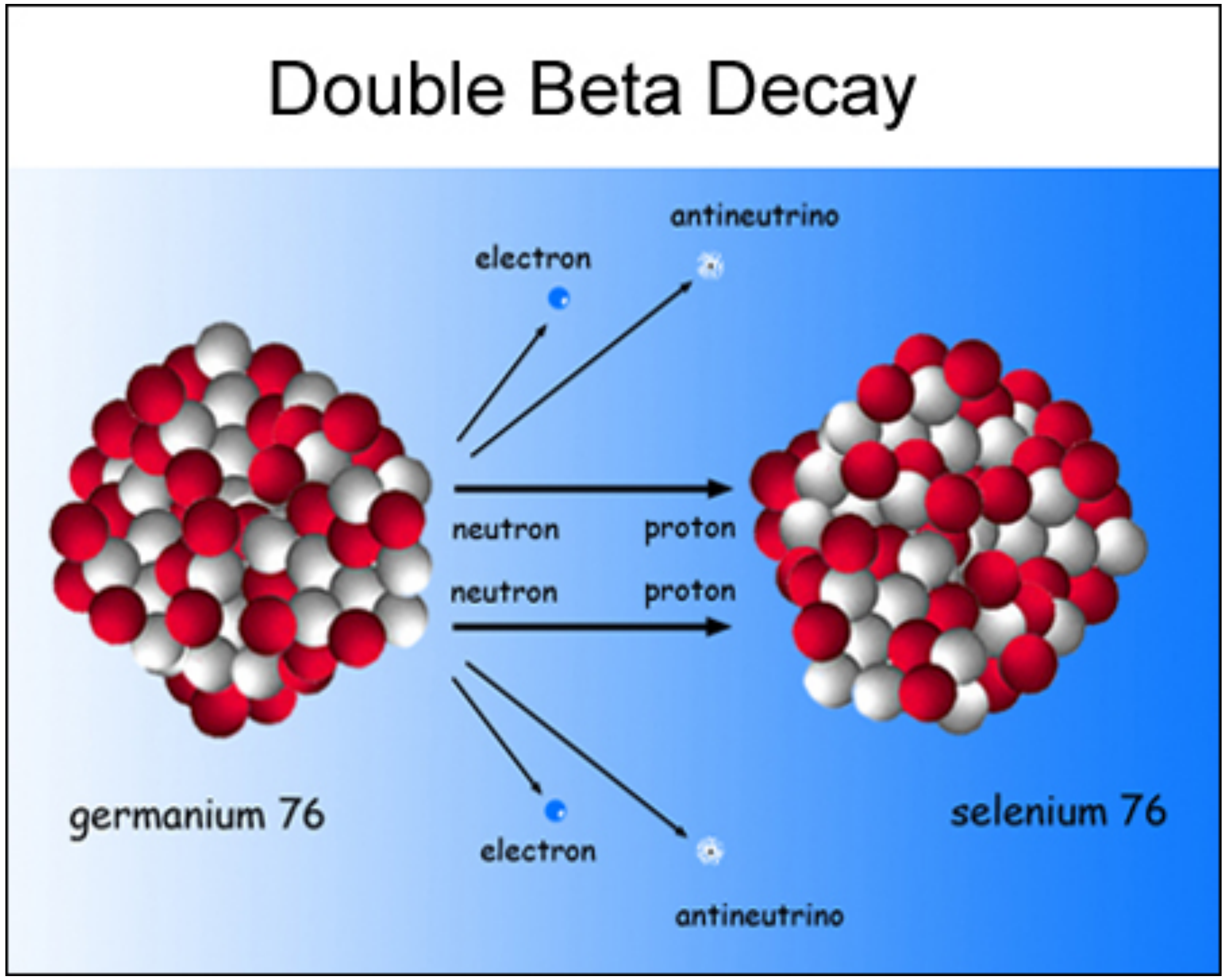

- Two β decays at the same time
- Only a few isotopes able to undergo 2β

$$2\nu\beta\beta : (A, Z) \rightarrow (A, Z+2) + 2e^{-} + 2\nu_e$$

2nd order process, observed, $T_{1/2}$ ~ 10^{19}-10^{24} yrs

^{76}Ge: $T_{1/2}$ ~ 10^{21} yrs

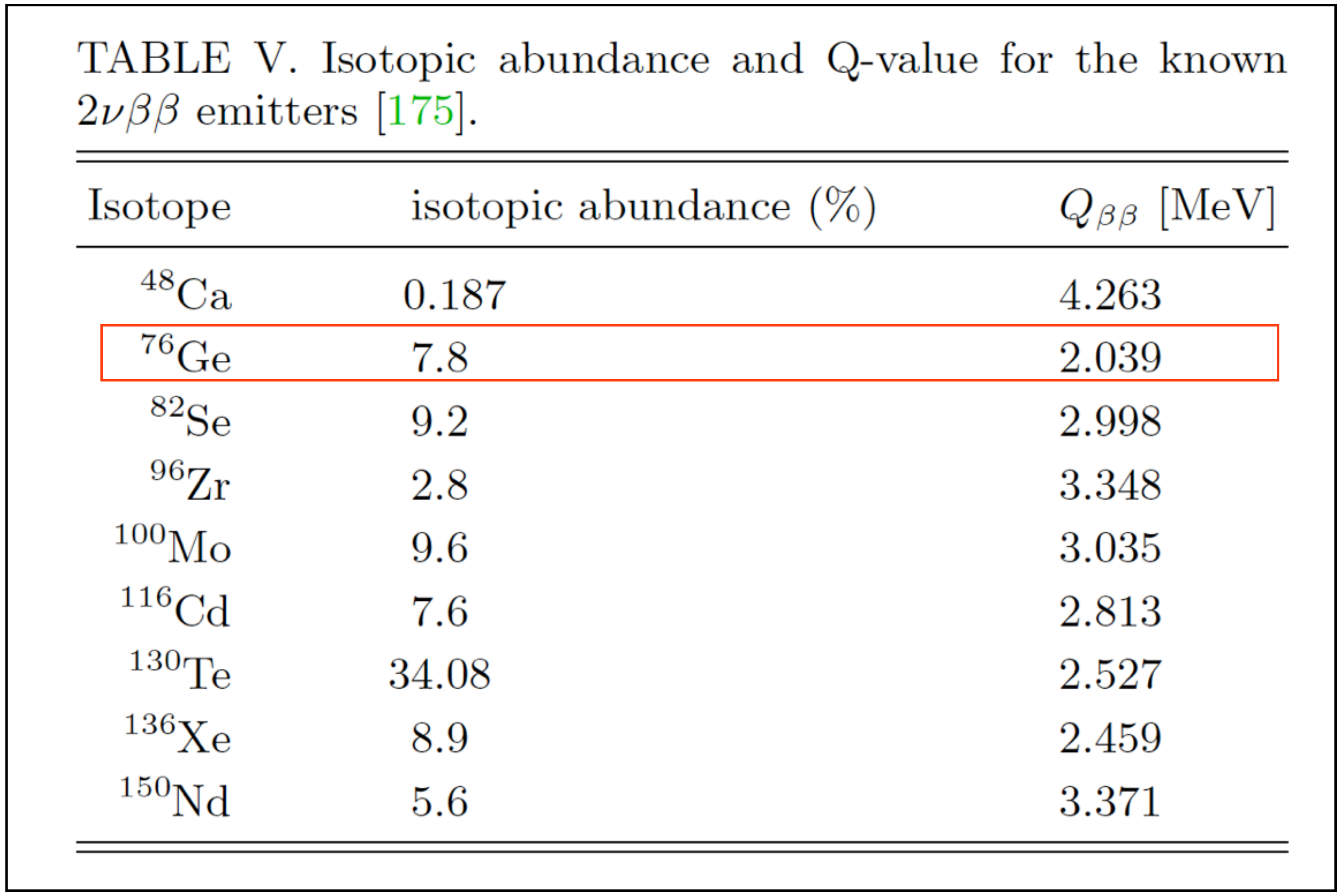

TABLE V. Isotopic abundance and Q-value for the known $2\nu\beta\beta$ emitters [175].

Isotope	isotopic abundance (%)	$Q_{\beta\beta}$ [MeV]
^{48}Ca	0.187	4.263
^{76}Ge	7.8	2.039
^{82}Se	9.2	2.998
^{96}Zr	2.8	3.348
^{100}Mo	9.6	3.035
^{116}Cd	7.6	2.813
^{130}Te	34.08	2.527
^{136}Xe	8.9	2.459
^{150}Nd	5.6	3.371

$$Q_{\beta\beta} = M(Z+2)-M(Z) -2m_e$$

0ν2β decays

ΔL=2

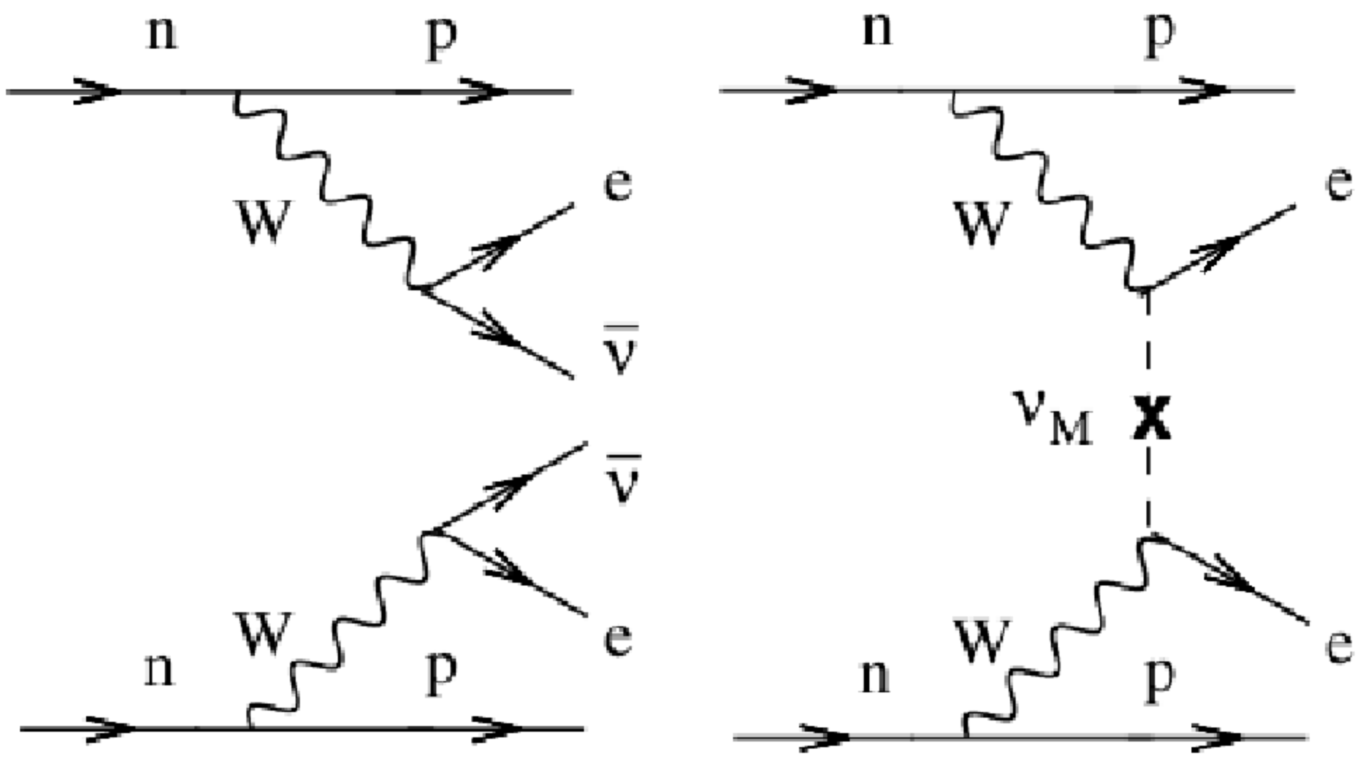

$0\nu\beta\beta : (A, Z) \rightarrow (A, Z{+}2) + 2e^-$

- ⇔ if neutrinos are Majorana fermions

(Majorana mass term)

- Prosaically: $\nu \equiv \bar{\nu}$
- Not only process available, but the one with the highest sensitivity
- BSM (SM only Dirac terms with L-R fermions)

$$\left(T^{0\nu}_{1/2}\right)^{-1} = \underset{\substack{\uparrow \\ \textit{phase space factor}}}{G^{0\nu}(Q_{\beta\beta}, Z)} \; \underset{\substack{\uparrow \\ \textit{nuclear matrix element}}}{\left|M^{0\nu}\right|^2} \left(\frac{\langle m_{ee}\rangle}{m_e}\right)^2$$

$$\langle m_{ee}\rangle = \left|\sum_i U_{ei}^2 m_i\right|$$

effective Majorana neutrino mass

NB: experiments measure $T^{0\nu}_{1/2}$

Connection with mass ordering

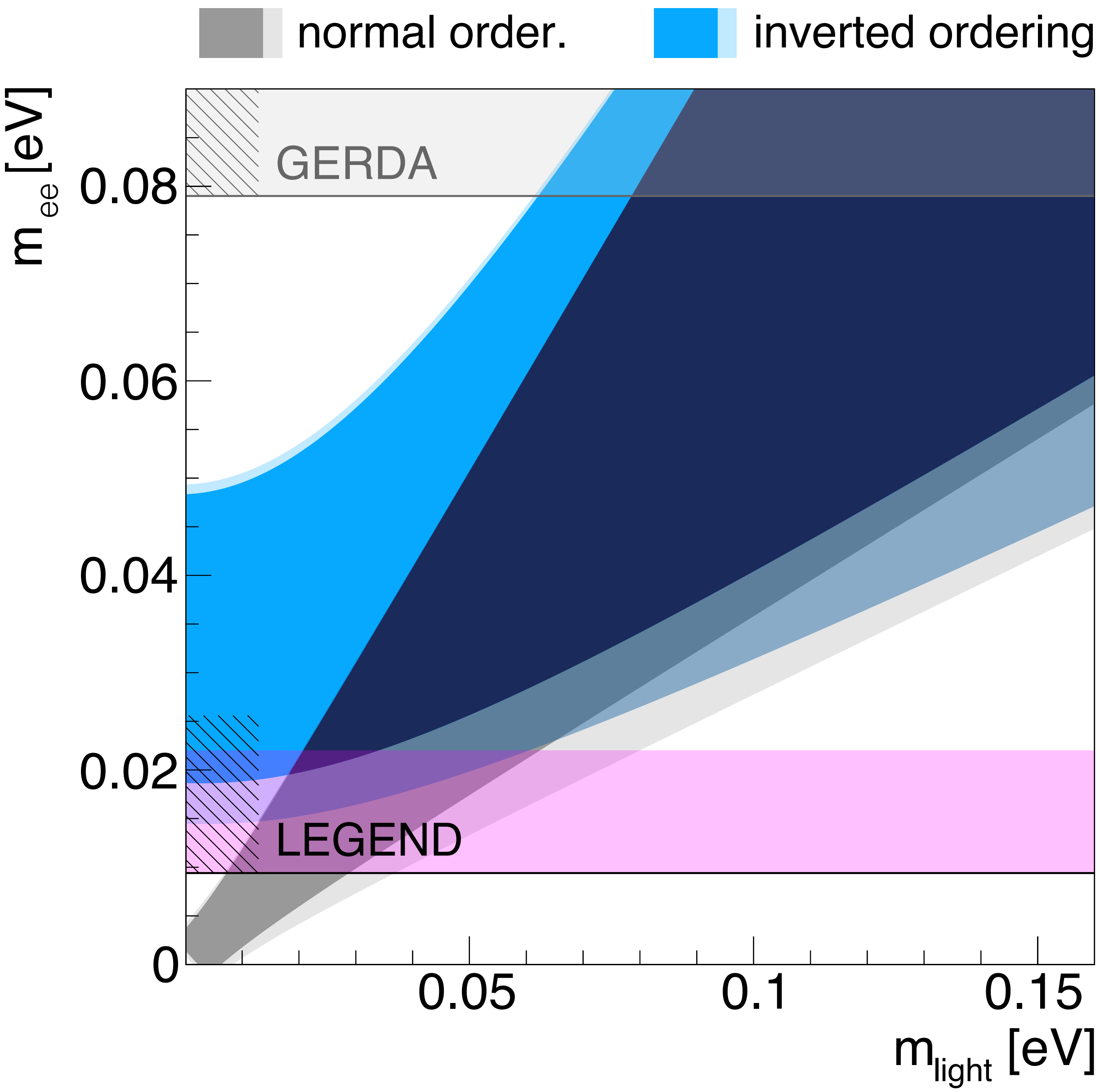

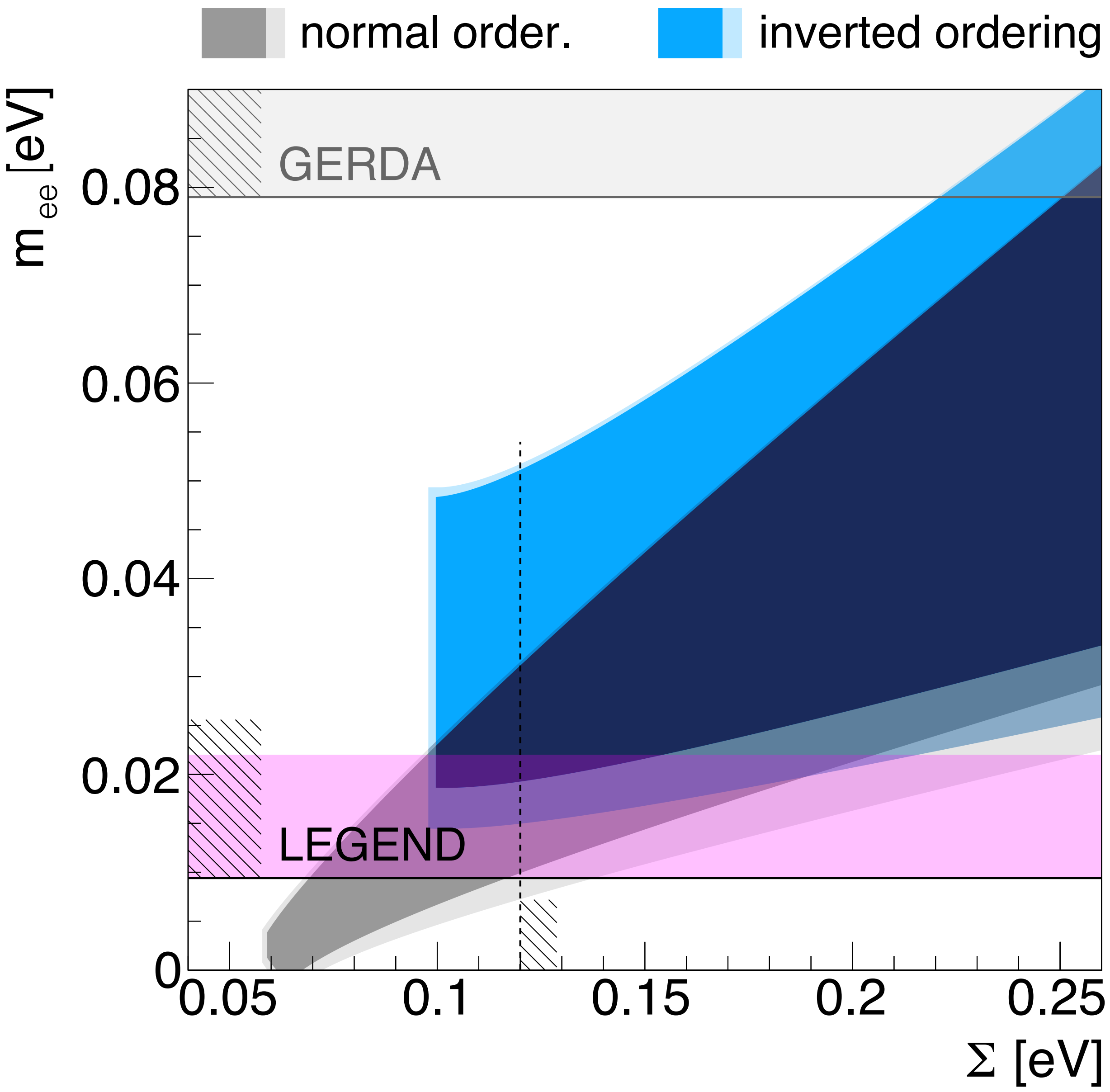

$$\left(T^{0\nu}_{1/2}\right)^{-1} = \underset{\substack{\uparrow \\ \textit{phase space factor}}}{G^{0\nu}}(Q_{\beta\beta}, Z)\ \underset{\substack{\uparrow \\ \textit{nuclear matrix element}}}{|M^{0\nu}|^2} \left(\frac{\langle m_{ee} \rangle}{m_e} \right)^2 \qquad \langle m_{ee} \rangle = \left| \sum_i U^2_{ei} m_i \right|$$

effective Majorana neutrino mass

$$\langle m_{ee} \rangle = \left| U^2_{e1} m_1 + U^2_{e2} m_2 e^{i\alpha} + U^2_{e3} m_3 e^{i\beta} \right|$$

- Limits on m_{ee} from above, can try to rule out IH
  - mix of mass eigenstates, entering $<m_{ee}>$ differently for the two MO

Connection with mass ordering

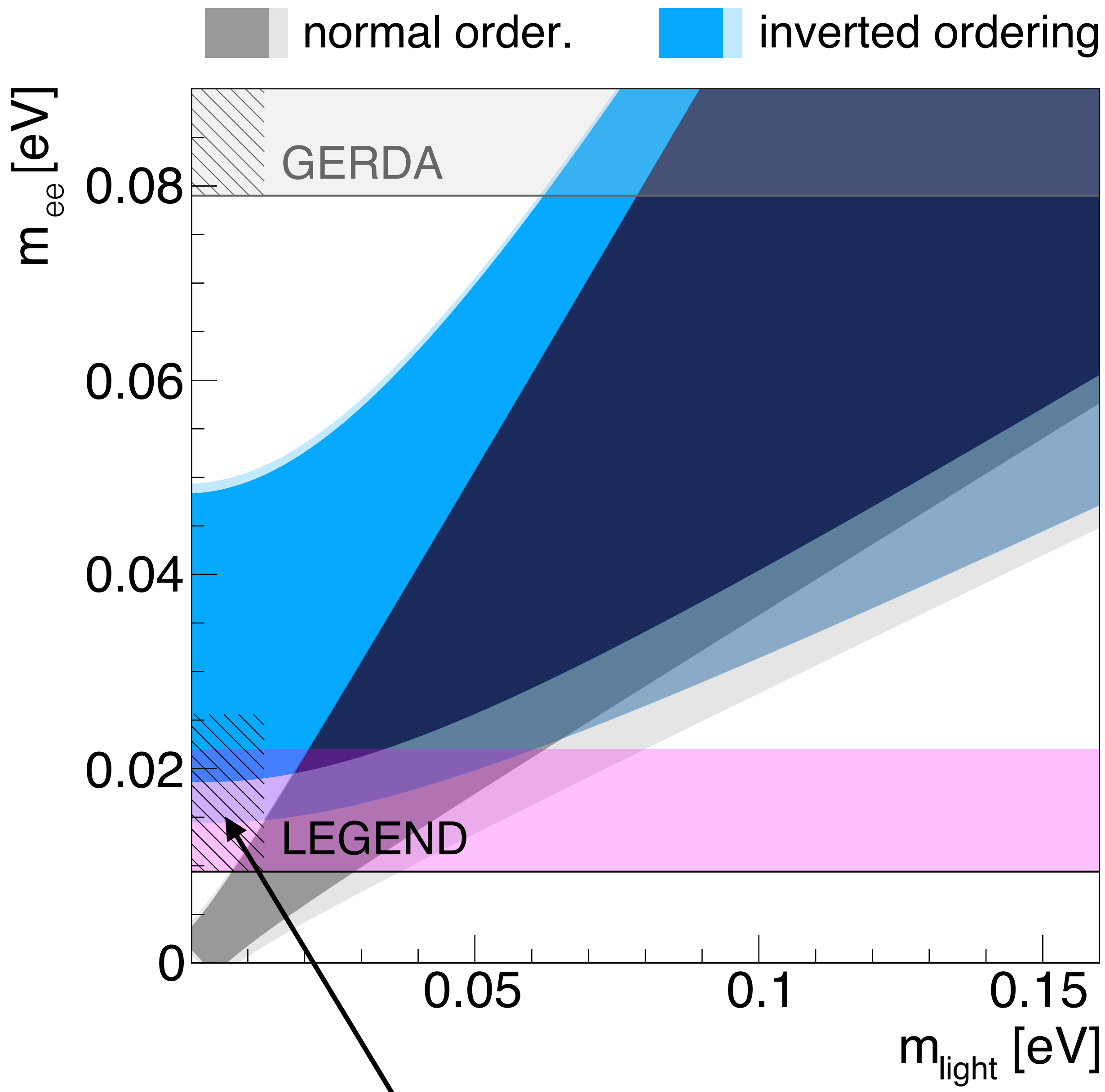

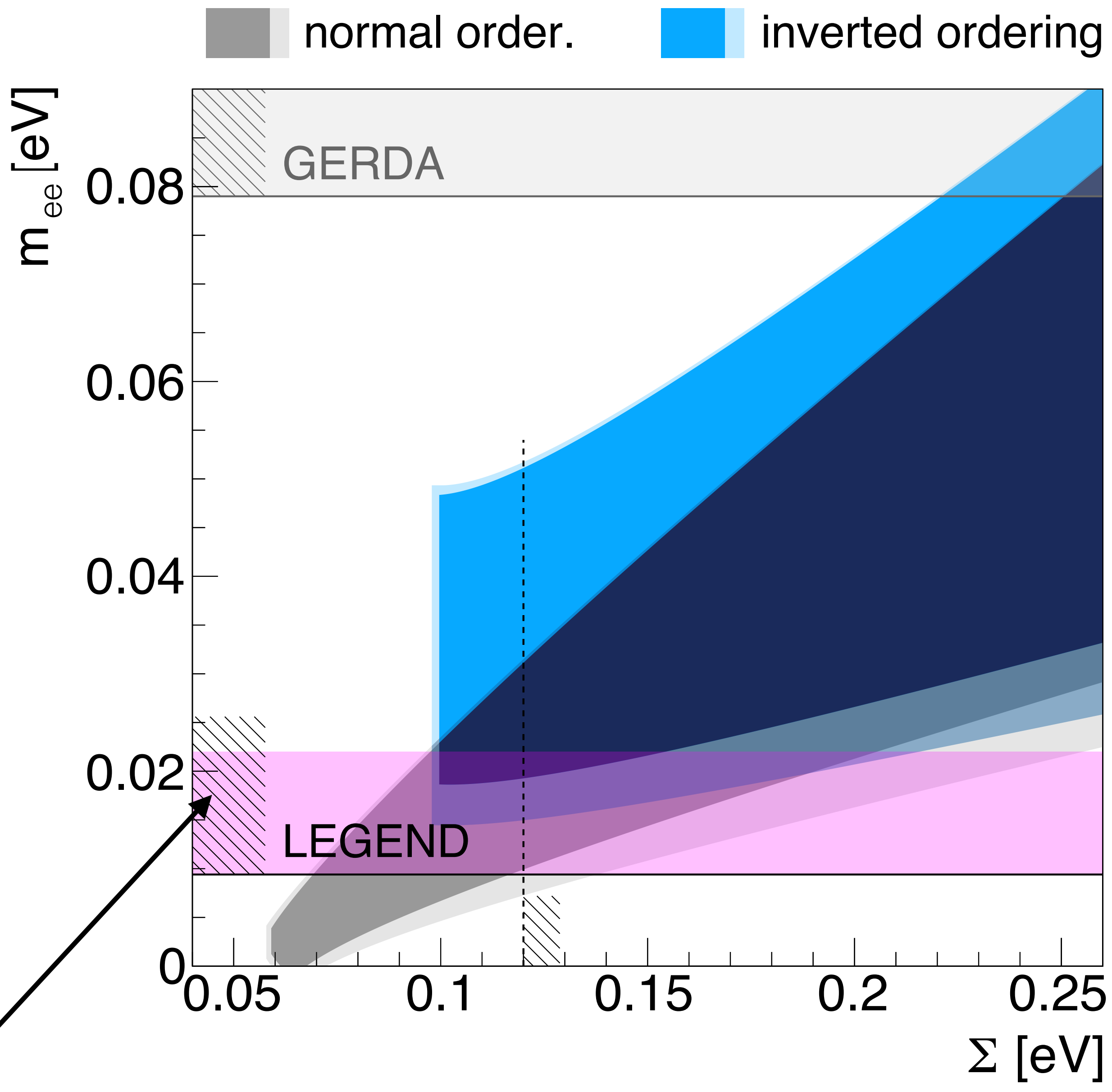

$$\left(T^{0\nu}_{1/2}\right)^{-1} = \underset{\substack{\uparrow\\ \textit{phase space factor}}}{G^{0\nu}(Q_{\beta\beta}, Z)} \; \underset{\substack{\uparrow\\ \textit{nuclear matrix element}}}{\left|M^{0\nu}\right|^2} \left(\frac{\langle m_{ee}\rangle}{m_e}\right)^2$$

$$\underset{\substack{\textit{effective Majorana}\\ \textit{neutrino mass}}}{\langle m_{ee}\rangle = \left|\sum_i U^2_{ei} m_i\right|}$$

$$\langle m_{ee}\rangle = \left|U^2_{e1} m_1 + U^2_{e2} m_2 e^{i\alpha} + U^2_{e3} m_3 e^{i\beta}\right|$$

- Limits on m_{ee} from above, can try to rule out IH
  - nuclear matrix element uncertainties: biggest spoiler in the conversion (next slide)

Nuclear Matrix Element values from various nuclear models

$$\left(T_{1/2}^{0\nu}\right)^{-1} = \underset{\substack{\uparrow \\ \textit{phase space factor}}}{G^{0\nu}(Q_{\beta\beta},Z)}\ \underset{\substack{\uparrow \\ \textit{nuclear matrix element}}}{|M^{0\nu}|^2} \left(\frac{\langle m_{ee}\rangle}{m_e}\right)^2 \qquad \underset{\substack{\textit{effective Majorana} \\ \textit{neutrino mass}}}{\langle m_{ee}\rangle = \left|\sum_i U_{ei}^2 m_i\right|}$$

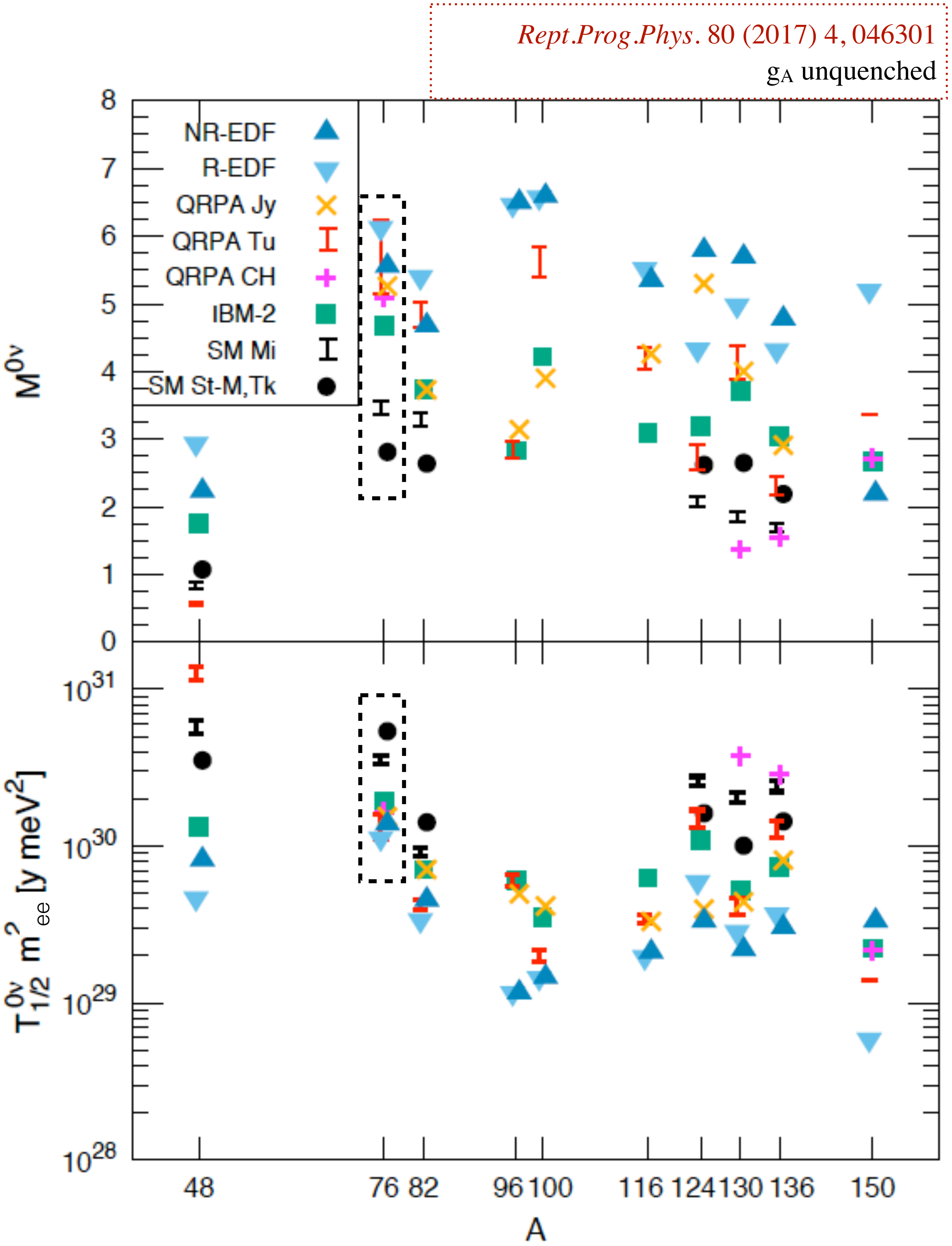

Rept.Prog.Phys. 80 (2017) 4, 046301
g_A unquenched

- Various models predict quite different values, throughout the isotope A range
- Affects the conversion from $T_{1/2}$ to m_{ee}

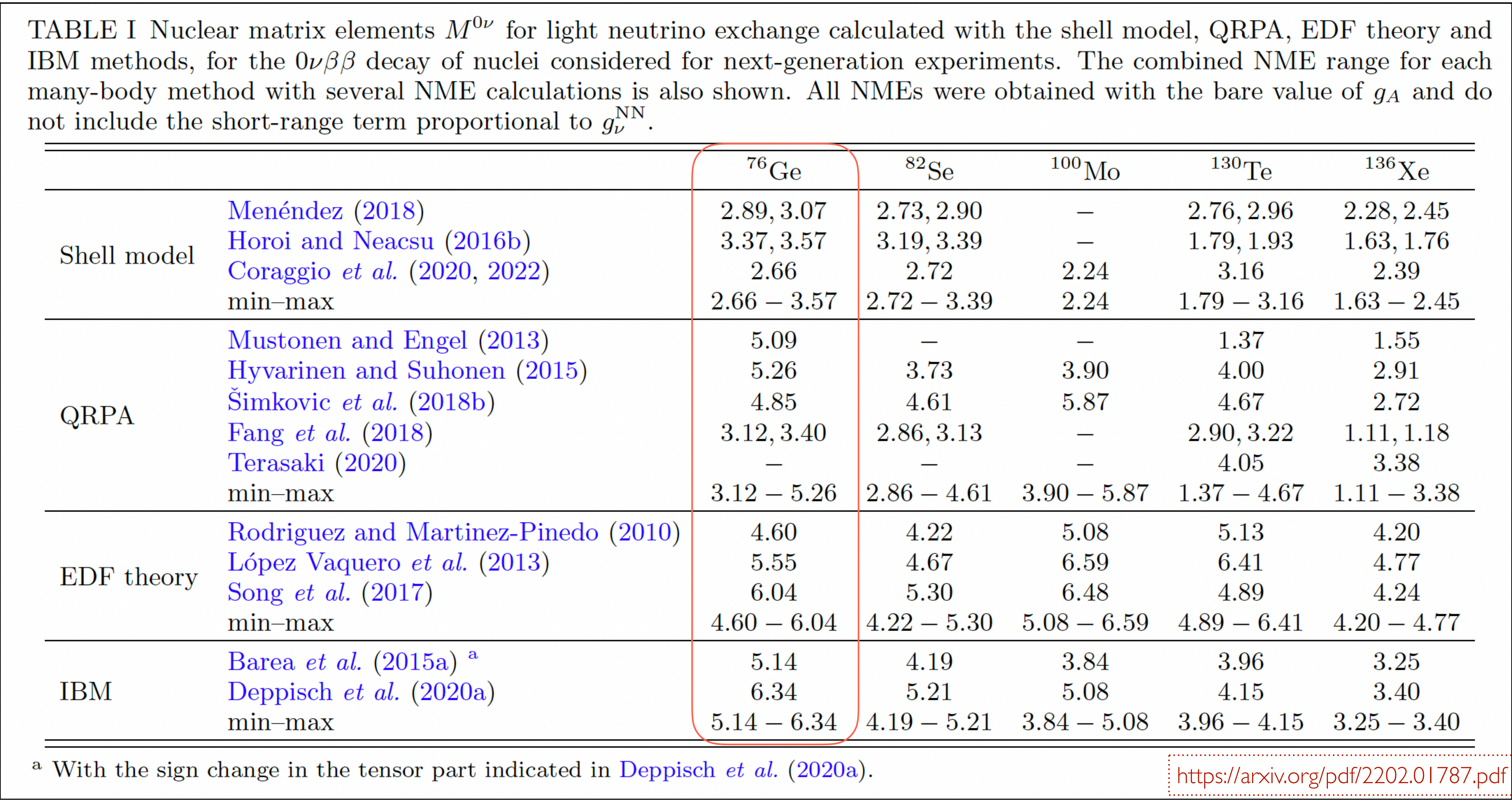

TABLE I Nuclear matrix elements $M^{0\nu}$ for light neutrino exchange calculated with the shell model, QRPA, EDF theory and IBM methods, for the $0\nu\beta\beta$ decay of nuclei considered for next-generation experiments. The combined NME range for each many-body method with several NME calculations is also shown. All NMEs were obtained with the bare value of g_A and do not include the short-range term proportional to $g_\nu^{\rm NN}$.

		^{76}Ge	^{82}Se	^{100}Mo	^{130}Te	^{136}Xe
Shell model	Menéndez (2018)	2.89, 3.07	2.73, 2.90	–	2.76, 2.96	2.28, 2.45
	Horoi and Neacsu (2016b)	3.37, 3.57	3.19, 3.39	–	1.79, 1.93	1.63, 1.76
	Coraggio *et al.* (2020, 2022)	2.66	2.72	2.24	3.16	2.39
	min–max	2.66 – 3.57	2.72 – 3.39	2.24	1.79 – 3.16	1.63 – 2.45
QRPA	Mustonen and Engel (2013)	5.09	–	–	1.37	1.55
	Hyvarinen and Suhonen (2015)	5.26	3.73	3.90	4.00	2.91
	Šimkovic *et al.* (2018b)	4.85	4.61	5.87	4.67	2.72
	Fang *et al.* (2018)	3.12, 3.40	2.86, 3.13	–	2.90, 3.22	1.11, 1.18
	Terasaki (2020)	–	–	–	4.05	3.38
	min–max	3.12 – 5.26	2.86 – 4.61	3.90 – 5.87	1.37 – 4.67	1.11 – 3.38
EDF theory	Rodriguez and Martinez-Pinedo (2010)	4.60	4.22	5.08	5.13	4.20
	López Vaquero *et al.* (2013)	5.55	4.67	6.59	6.41	4.77
	Song *et al.* (2017)	6.04	5.30	6.48	4.89	4.24
	min–max	4.60 – 6.04	4.22 – 5.30	5.08 – 6.59	4.89 – 6.41	4.20 – 4.77
IBM	Barea *et al.* (2015a) [a]	5.14	4.19	3.84	3.96	3.25
	Deppisch *et al.* (2020a)	6.34	5.21	5.08	4.15	3.40
	min–max	5.14 – 6.34	4.19 – 5.21	3.84 – 5.08	3.96 – 4.15	3.25 – 3.40

[a] With the sign change in the tensor part indicated in Deppisch *et al.* (2020a).

https://arxiv.org/pdf/2202.01787.pdf

The observable

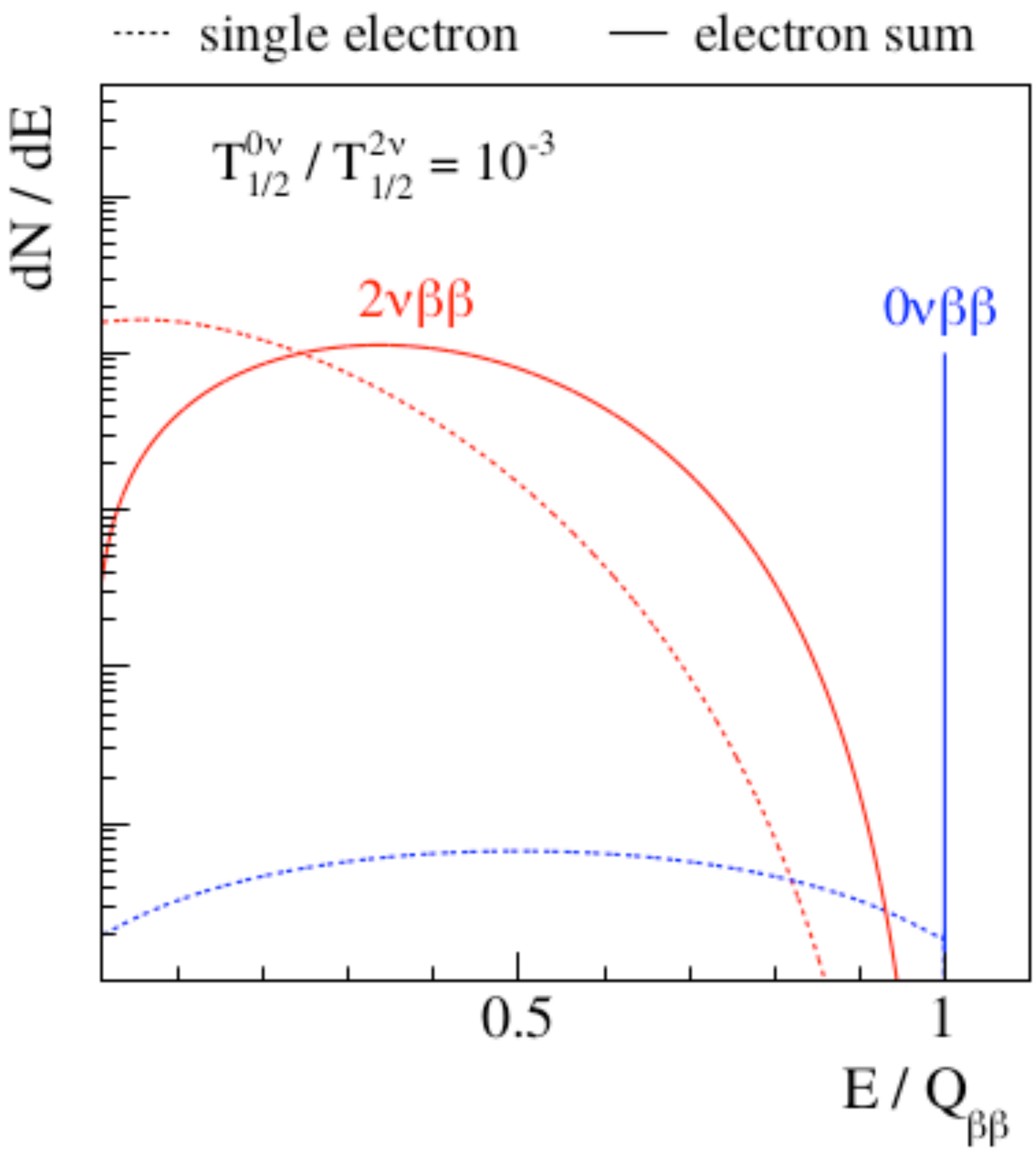

$2\nu\beta\beta : (A, Z) \rightarrow (A, Z{+}2) + 2e^{-} + 2\nu_e$

$0\nu\beta\beta : (A, Z) \rightarrow (A, Z{+}2) + \boxed{2e^{-}}$

Measure overall energy of "2e" considered as "one body" in a 2-body decay → with no neutrinos it's a line at E = $Q_{\beta\beta}$

Comparing different isotopes

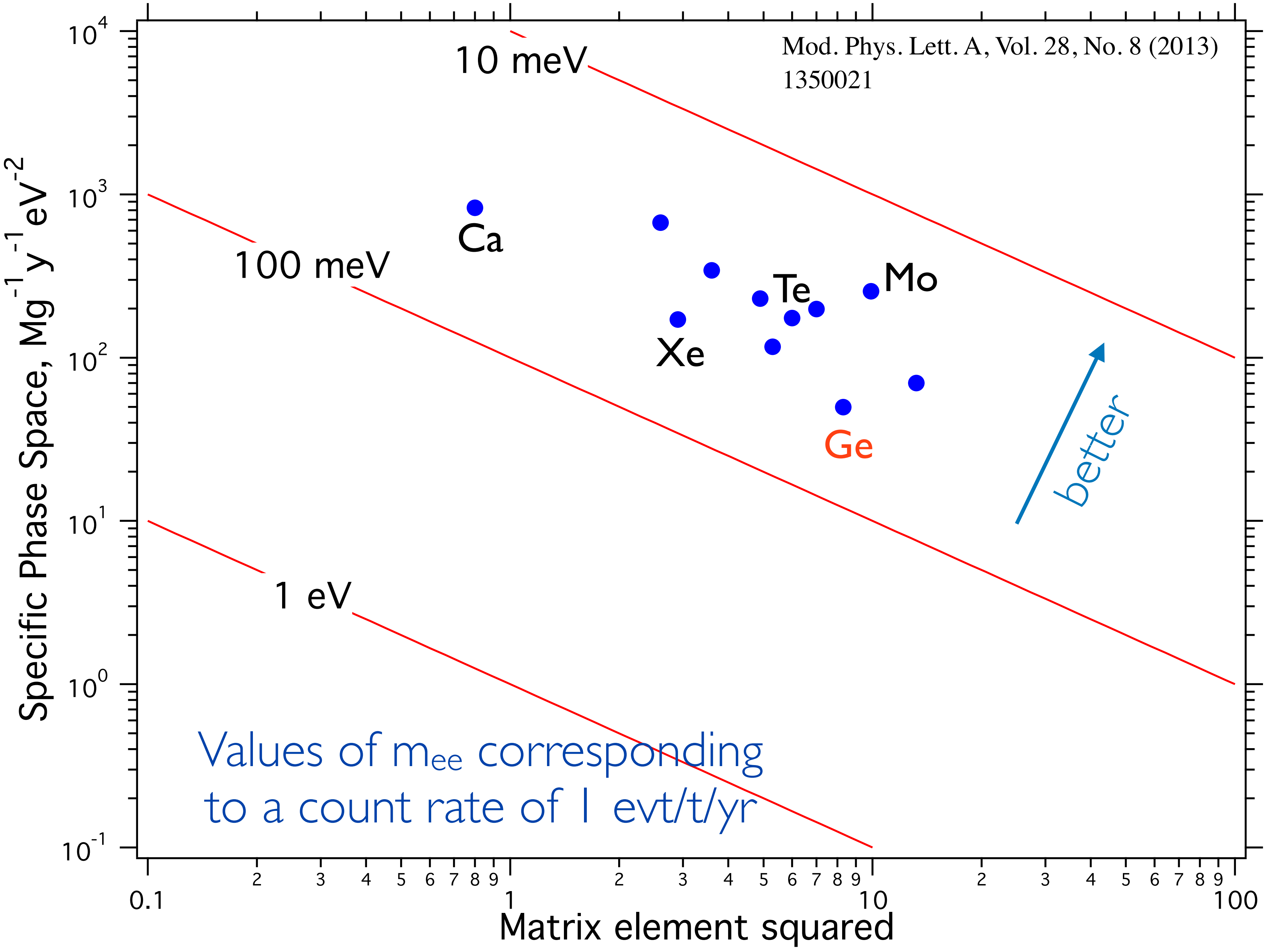

Mod. Phys. Lett. A, Vol. 28, No. 8 (2013) 1350021

Values of m_{ee} corresponding to a count rate of 1 evt/t/yr

- Phase Space and NME inversely correlated.
- Tend to compensate in rate
  - ^{100}Mo best from this point of view

Choice informed mostly by experimental/practical criteria

- Enrichment cost
- Energy resolution
- Background levels of related material and design at Q-value
- Scalability

$$\left(T^{0\nu}_{1/2}\right)^{-1} = G^{0\nu}(Q_{\beta\beta}, Z)\ \left|M^{0\nu}\right|^2 \left(\frac{\langle m_{ee}\rangle}{m_e}\right)^2 \qquad \langle m_{ee}\rangle = \left|\sum_i U^2_{ei} m_i\right|$$

nuclear matrix element

phase space factor

effective Majorana neutrino mass

Alas, it's more like this...

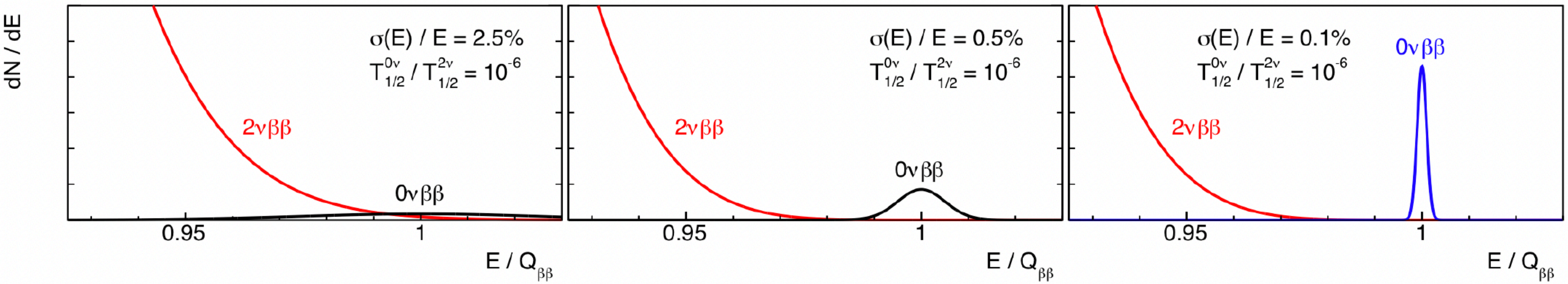

An excellent energy resolution crucial to separate SM from BSM process around Q-value

Experimental sensitivity

- This is essentially a counting exercise in the presence of background
- Sensitivity is dominated by Poisson counting around the Q-value (ROI)

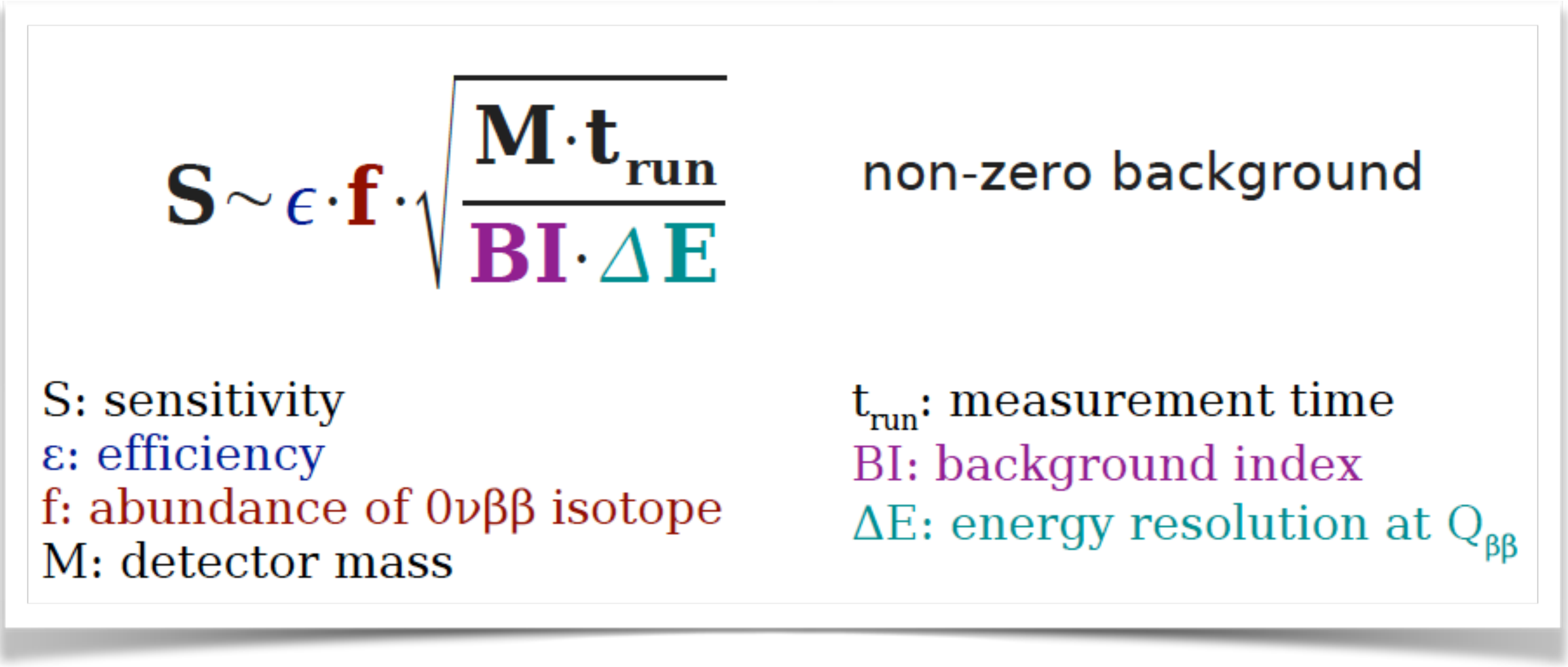

$$\mathbf{S} \sim \epsilon \cdot \mathbf{f} \cdot \sqrt{\frac{\mathbf{M} \cdot \mathbf{t}_{\mathbf{run}}}{\mathbf{BI} \cdot \Delta\mathbf{E}}}$$

non-zero background

S: sensitivity
ε: efficiency
f: abundance of 0νββ isotope
M: detector mass

t_{run}: measurement time
BI: background index
ΔE: energy resolution at $Q_{\beta\beta}$

The pros and cons of Germanium

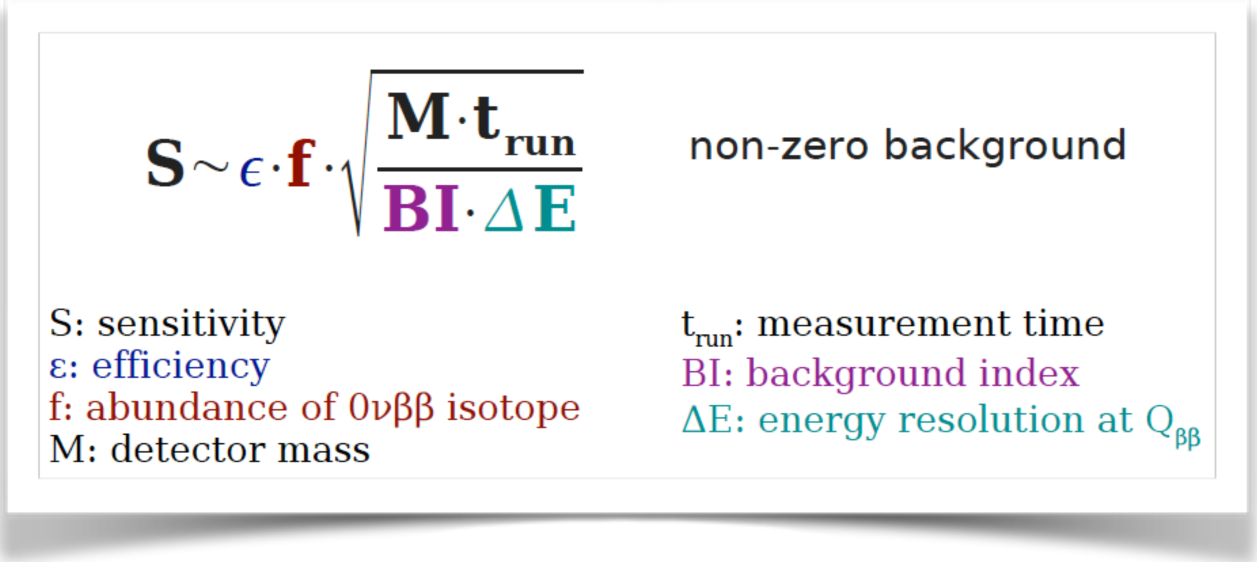

$$S \sim \epsilon \cdot f \cdot \sqrt{\frac{M \cdot t_{run}}{BI \cdot \Delta E}}$$

non-zero background

S: sensitivity

ε: efficiency

f: abundance of 0νββ isotope

M: detector mass

t_{run}: measurement time

BI: background index

ΔE: energy resolution at $Q_{\beta\beta}$

- Source ≡ detector
- semiconductor detectors provide excellent E_{reso} (2.5 keV FWHM @ 2039 keV)
- low intrinsic BI in HPGe
- Bkg rejection capabilities from solid state detectors organized in arrays
- scalable thanks to high demand of HPGe for various applications

- Low isotopic abundance in natural Ge means higher cost to enrich it
- Small phase space

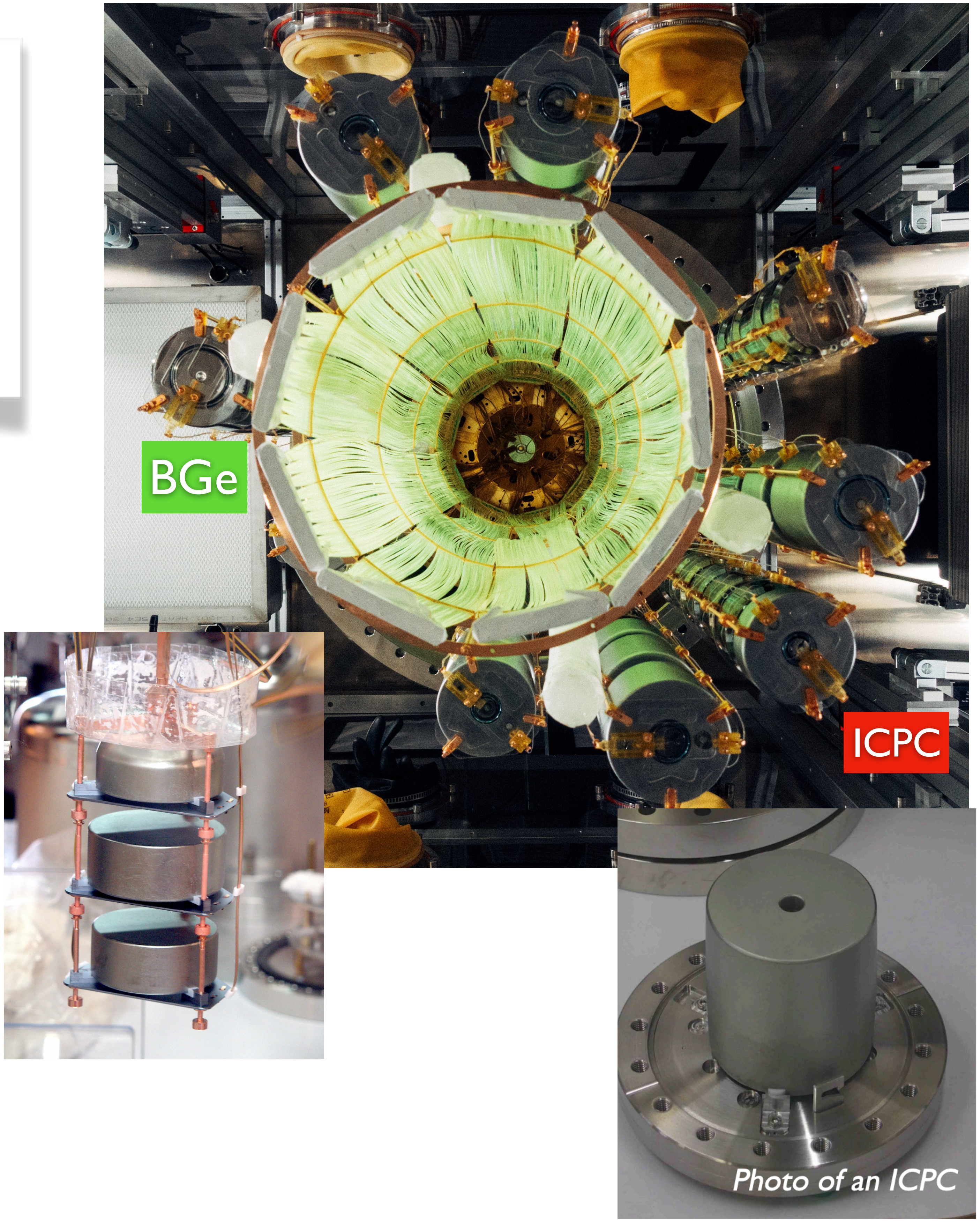

A plot can tell a story...

Y.Kermaidic, Neutrino '20

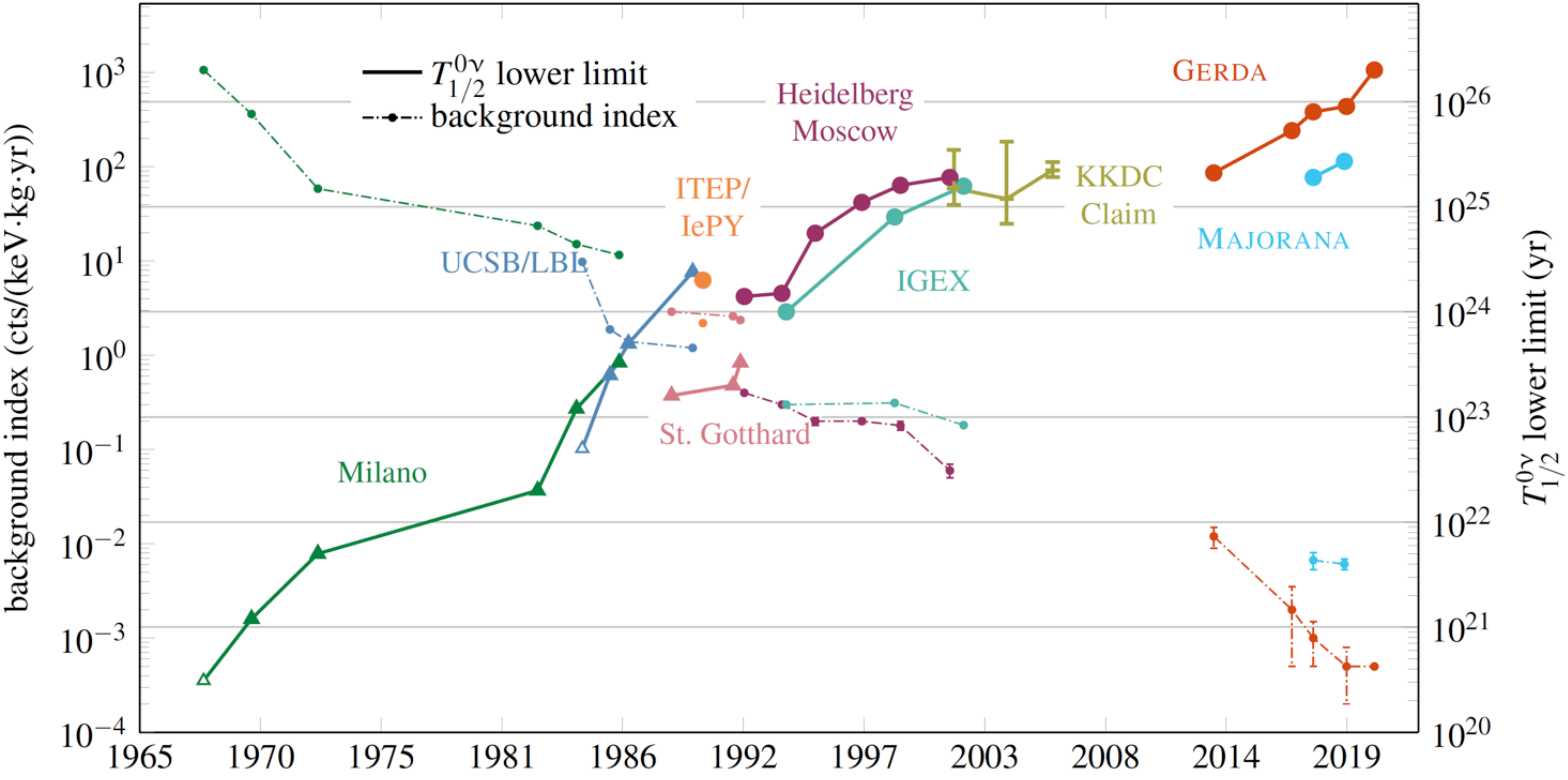

- Searches with Ge have a long tradition and established technique
- GERDA+Majorana Demonstrator=LEGEND

LEGEND's pa and ma

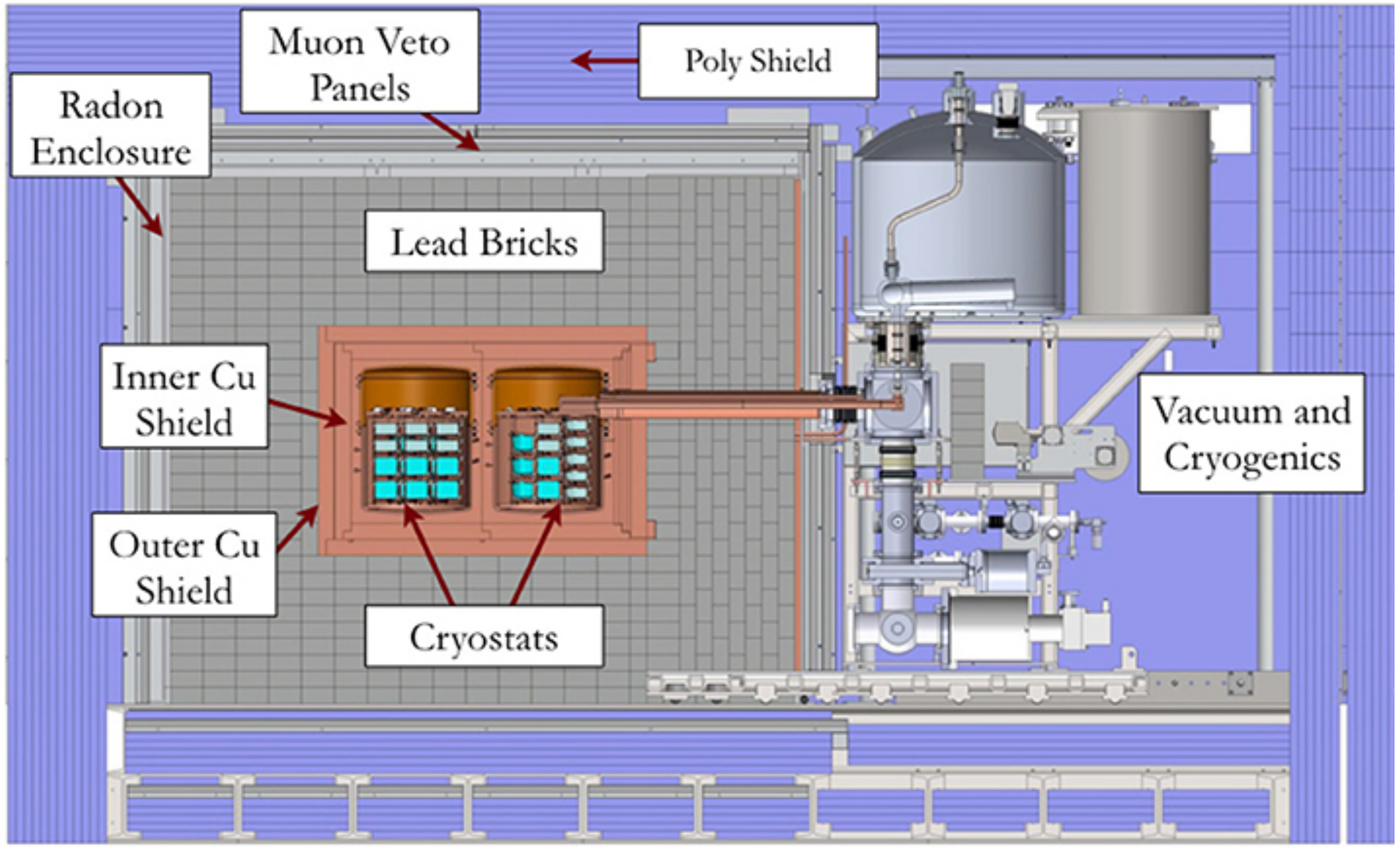

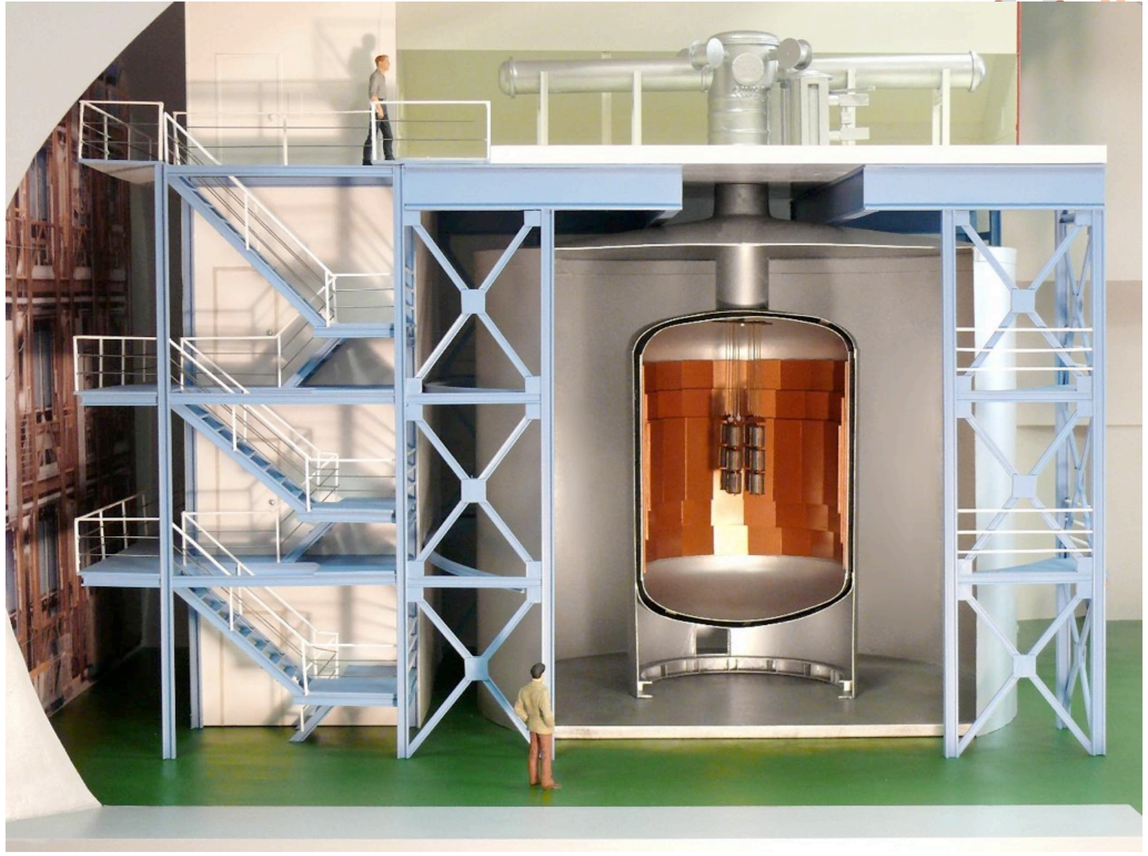

Majorana demonstrator (SURF)

- Conventional screening with passive material (Pb)
- Low noise electronics for better PSD and energy resolution (2.5 keV FWHM @ $Q_{\beta\beta}$)
- Lower threshold for more physics searches
- 29.7 kg of 88% enriched ^{76}Ge crystals (PPC detectors)

GERDA (LNGS)

- New idea implying active LAr-based screening →exploit bkg topologies to detect scintillation and apply coincidences btw LAr and Ge dipped within
- E reso: 2.6-2.9 keV FWHM @ $Q_{\beta\beta}$
- 44.2 kg of 88% enriched ^{76}Ge crystals (coax+BEGe+ICPC detectors)

<u>In common</u>: careful control of radioactive bkg at material fabrication and specialized analysis techniques (material+ambient)

⇒ Lowest bkg rate and best E reso for any 0ν2β expt

LEGEND’s pa and ma

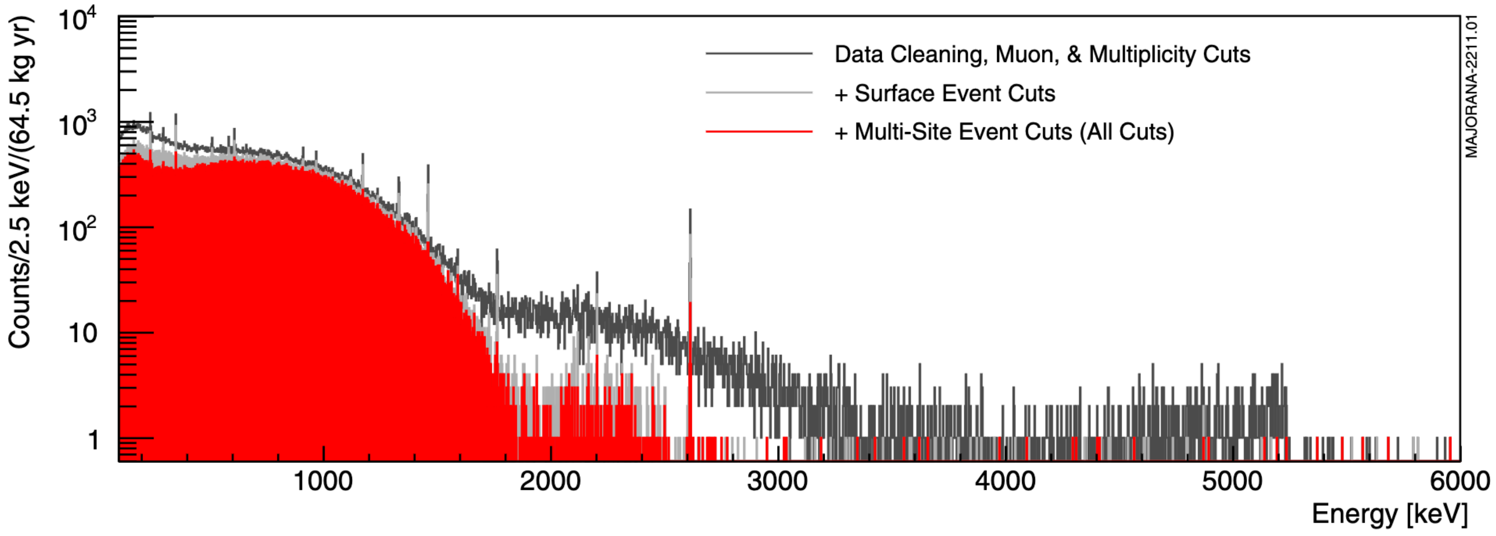

Majorana demonstrator (SURF)

- Exposure: 64.3 kg yr
- BI@Q: 15.7×10^{-3} counts/(FWHM kg yr)
- Median $T_{1/2}$ Sensitivity: 8.1 10^{25} yr
- Full Exposure Limit: $T_{1/2} > 8.3$ 10^{25} yr (90% CL)
- Phys. Rev. Lett. 130, 062501

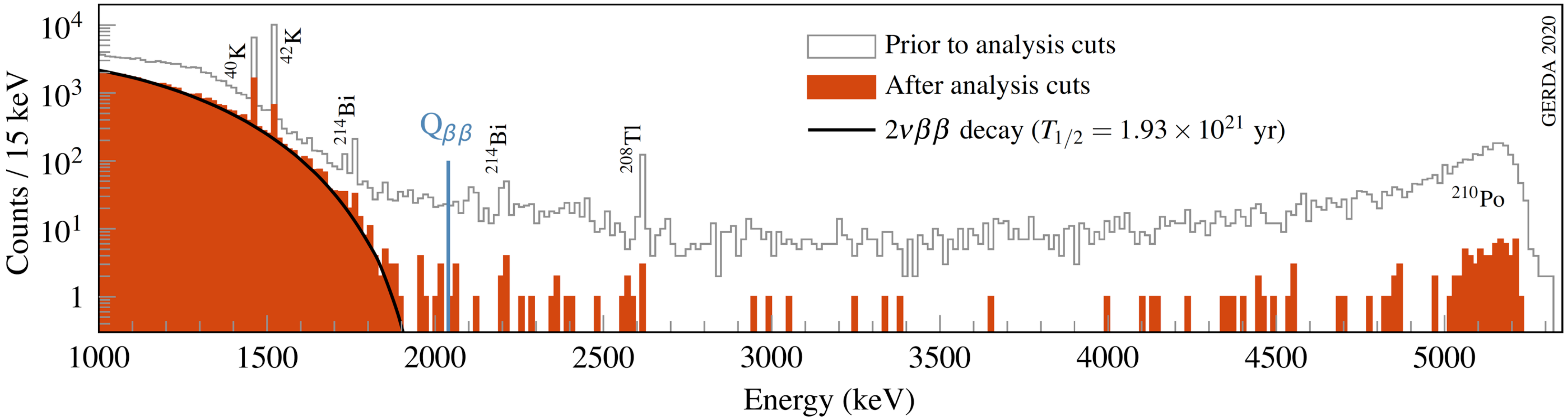

GERDA (LNGS)

- Exposure: 104 kg yr
- BI@Q: 5.2×10^{-4} counts/(keV kg yr)
- Median $T_{1/2}$ Sensitivity: 1.8 10^{26} yr
- Full Exposure Limit: $T_{1/2} > 1.8$ 10^{26} yr (90% CL)
- Phys. Rev. Lett. 125, 252502 (2020)

- Two-staged approach with a "demonstrator" of ~200 kg (**Legend-200**) towards the full-fledged experiment with 1 ton scale (**Legend-1000**)
- What's to "*demonstrate*"? Development of large Point-contact detectors, layout can be scaled up, bkg reduction can be taken even farther aggressively (incl. cosmogenic activation)

Collaboration Meeting, Roma Tre, May 2023

What sensitivity looks like

(FWHM: Full Width at Half Maximum; 2.355 σ for a Gaussian peak)

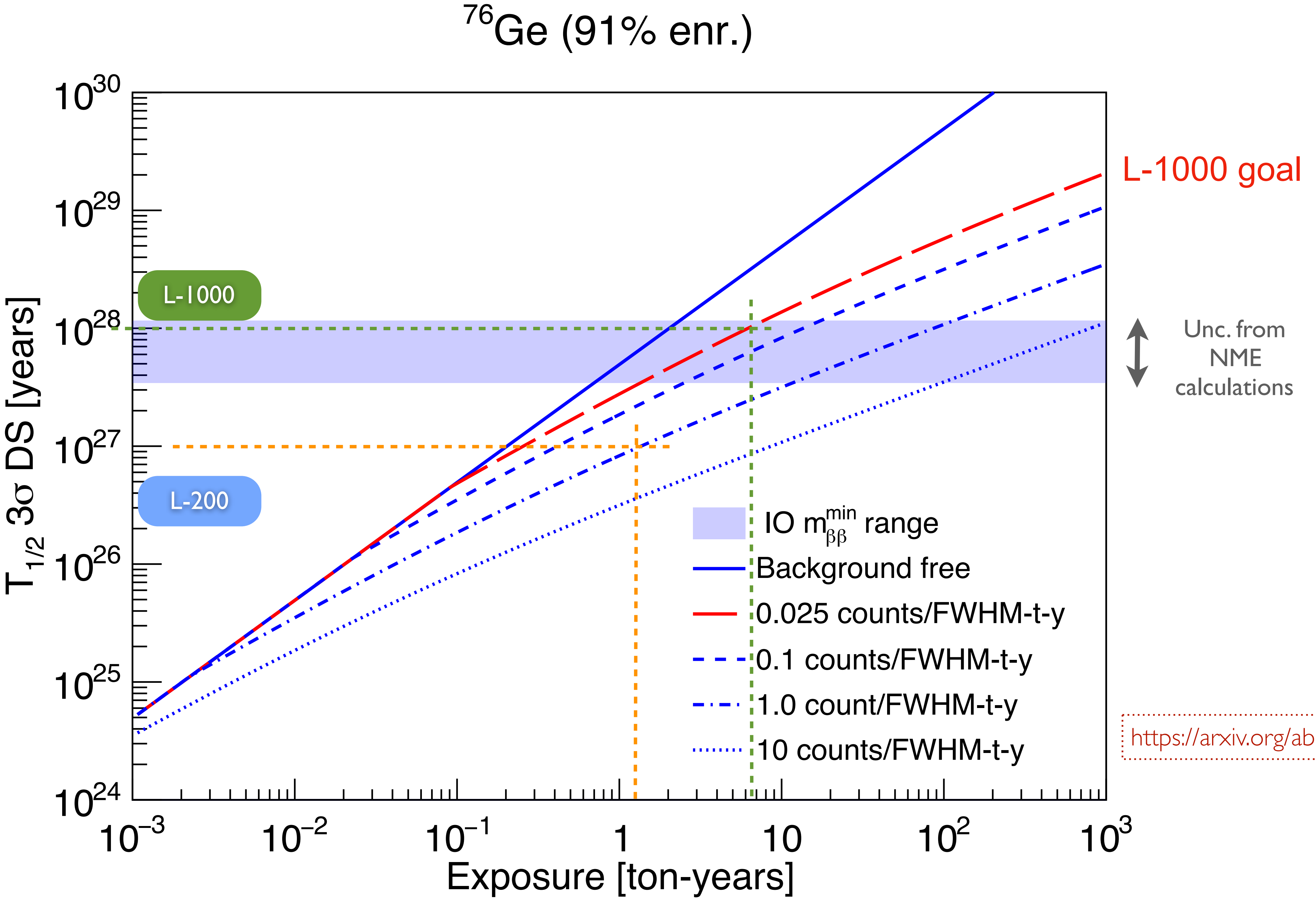

https://arxiv.org/abs/2107.11462

- Value of $T_{1/2}$ for which a ^{76}Ge-enriched experiment has a **50%** chance to observe a signal above background with **3σ** significance
- *Less than one background count* expected in a 4σ Region of Interest (ROI) with 10 t y exposure

LEGEND-200 site: LNGS

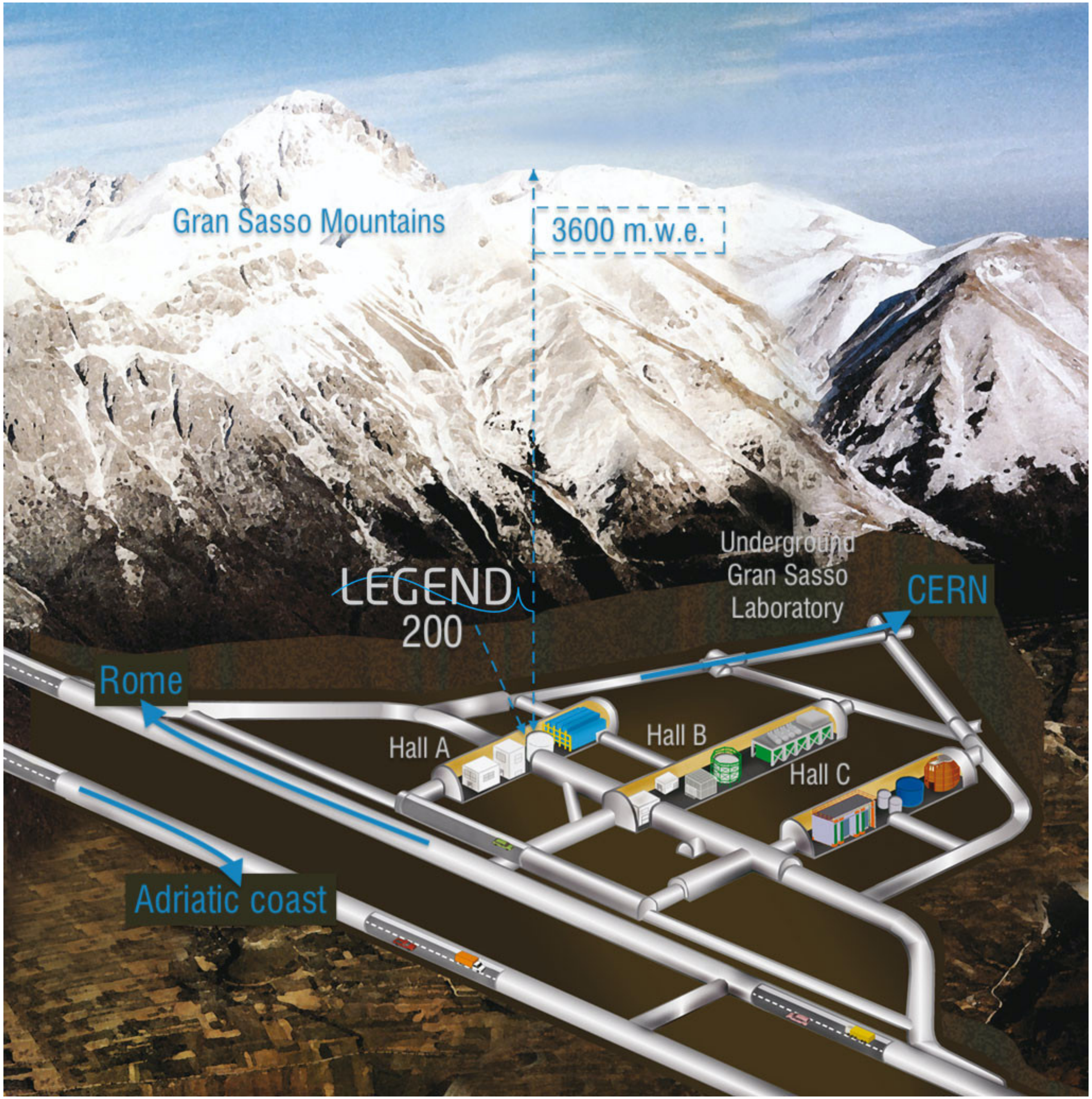

- L-200 is now hosted in what was GERDA's infrastructure at LNGS
- Same concept of Ge detectors dipped within LAr in pre-existing cryostat
- Mountain provides screening against cosmic rays

- Expected sources of external bkg include γ from U/Th decays, neutrons, remaining cosmic rays (prompt and delayed)
- Intrinsic: radioactive surface contamination, ^{39}Ar decays, cosmogenic activation of isotopes

Read also:
Universe **2021**, *7*, 386.

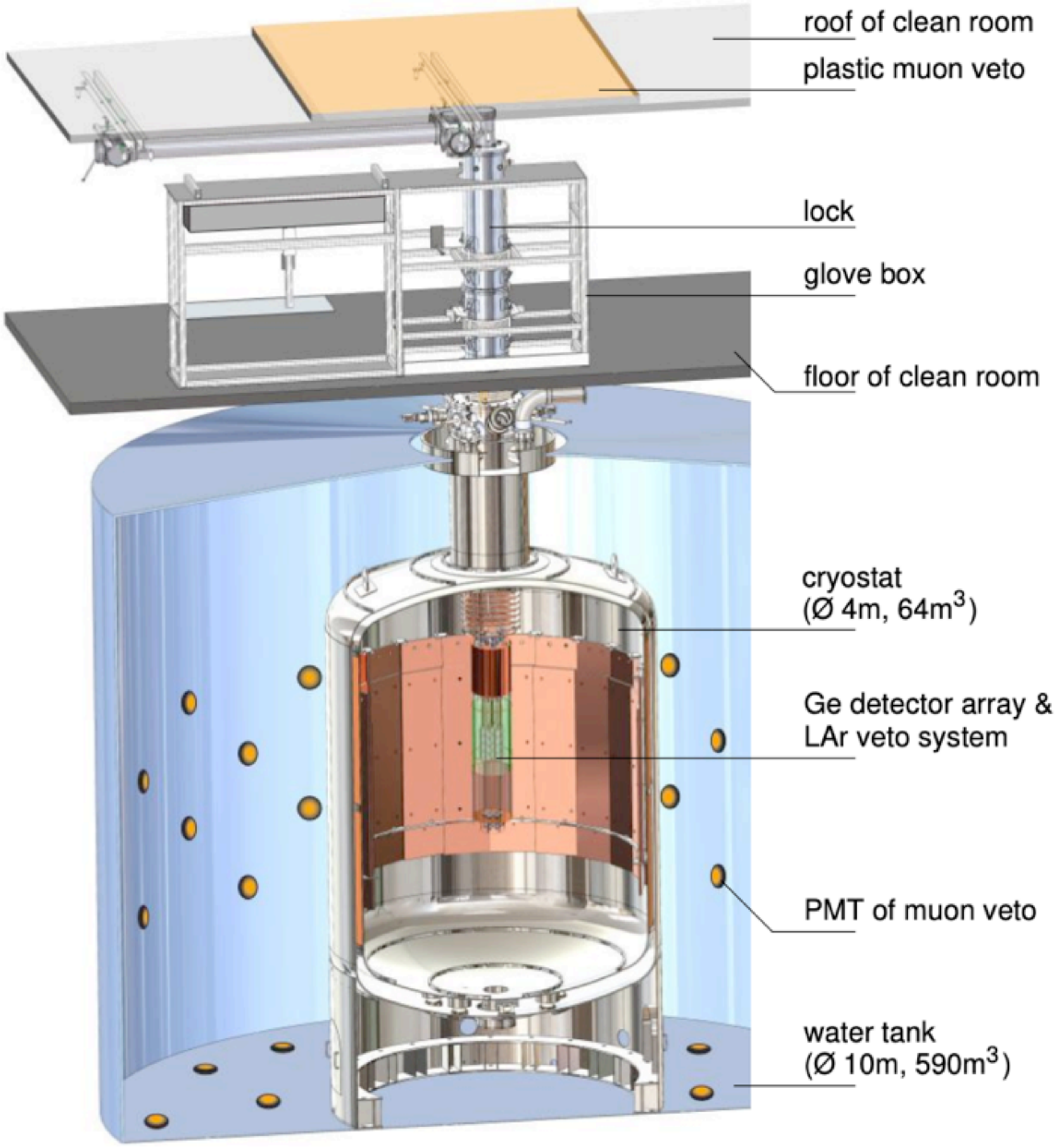

- high-purity germanium (HPGe) detectors enriched in ^{76}Ge up to 92%: source + detector
- detectors mounted on low-mass holders (to minimize radioactive bkg)
- embedded in liquid argon (LAr): cryogenic coolant and absorber against external radiation
- ultrapure water tank: buffer around cryostat as additional absorber + Cherenkov veto

A heart of (High Purity) Germanium

- p-type diodes with point-contact (vs extended contact, *see next slides*)
- Charge collection at p^+ electrode (Boron-implanted), polarization potential applied at n^+ electrode (diffused Li)

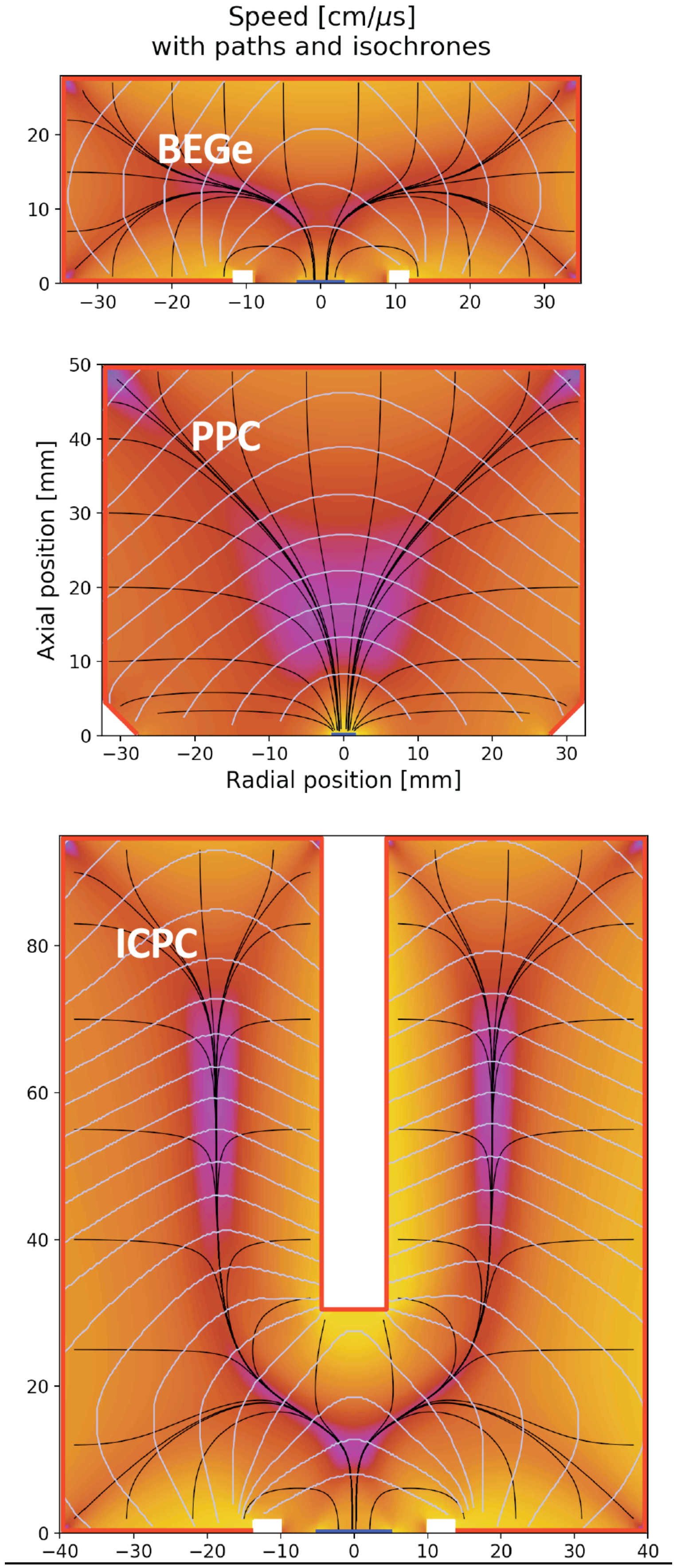

Speed [cm/μs]
with paths and isochrones

BEGe (from GERDA) and PPC (from MJD)

- A part of the original suite of diodes from the past are retained in L-200: about 50 kg
- Very good E resolution
- Well established PSD technique exploiting stable field configuration across volume to reject bkg
- but small mass: ≤1 kg each

ICPC (new)

R. Cooper et al., NIM A665, 25 (2011)]

- Remaining 140 kg are of this type
- Larger mass (>1.5 kg, up to <2.5> kg for L-1000)
- but retaining similar charge drift times across volume
- Reduced surface-to-volume ratio (α and β), less dirty cables, pre-amps
- Lower cost per kg, higher efficiency

ICPC: response uniformity

NIM A665, 25 (2011)

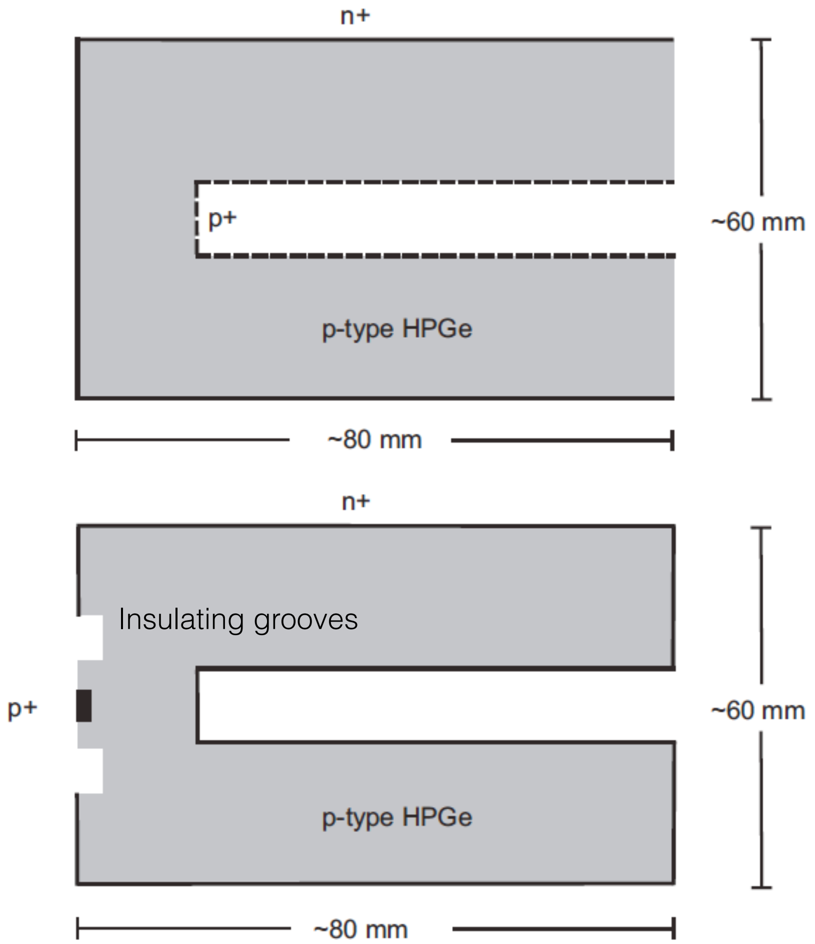

Fig. 1. Schematic diagrams of a closed-end coaxial p-type HPGe detector (top) and the new geometry Inverted Coaxial detector (bottom).

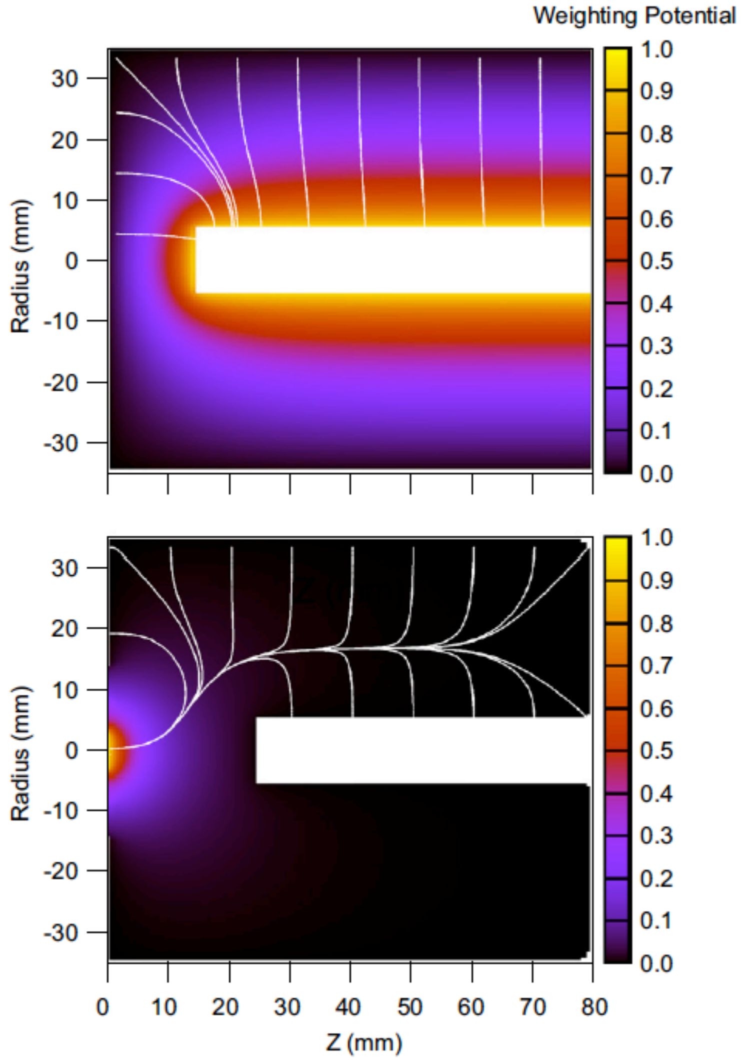

Notice more uniform weighting potential across volume = more uniform response to diverse classes of bkg happening at various sites = better PSD

PC diodes also offer better E_{reso} than extended contact (coaxial)

- thanks to reduced electrode size (smaller capacitance, ~pF)

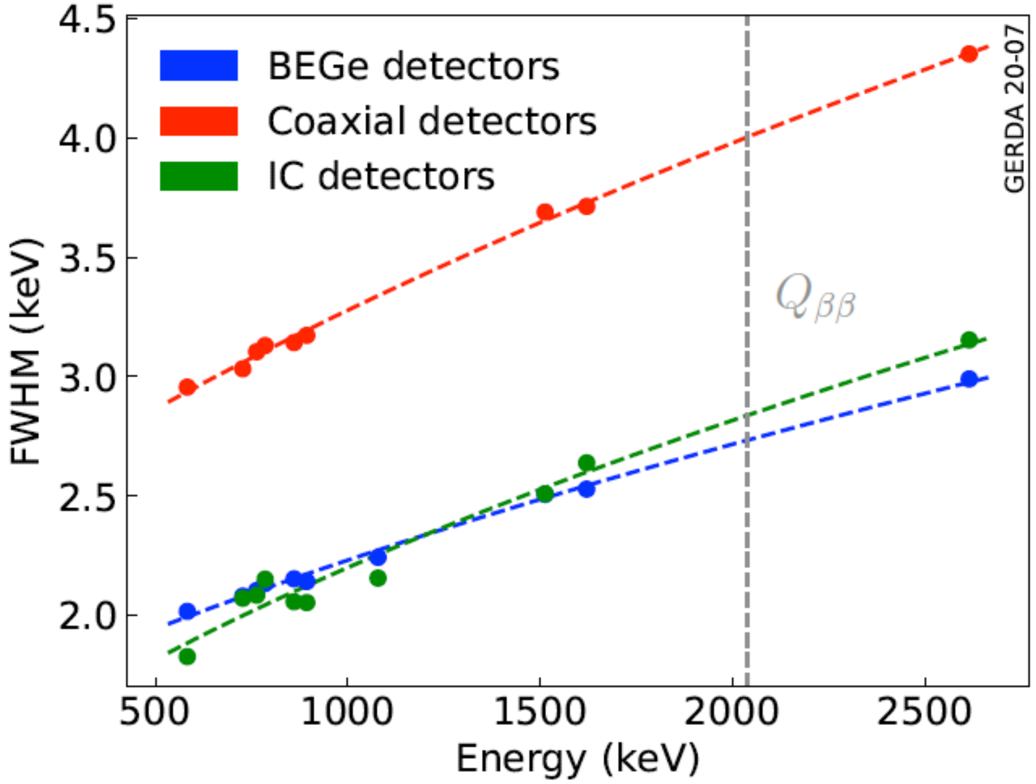

LEGEND-200 Ge diode cocktail

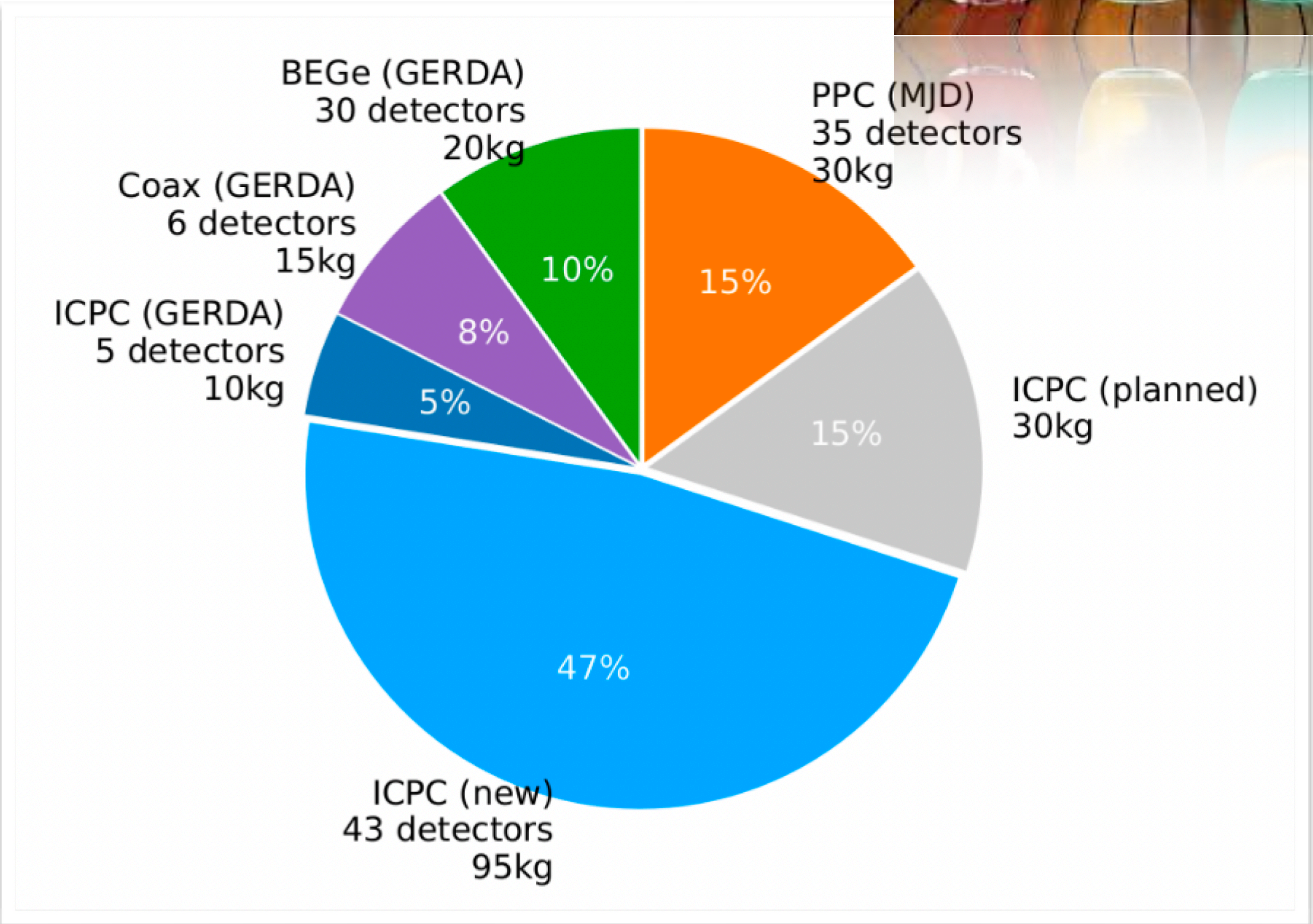

PSD in Ge: concept

Read also: NIM A 891 (2018) 106-110

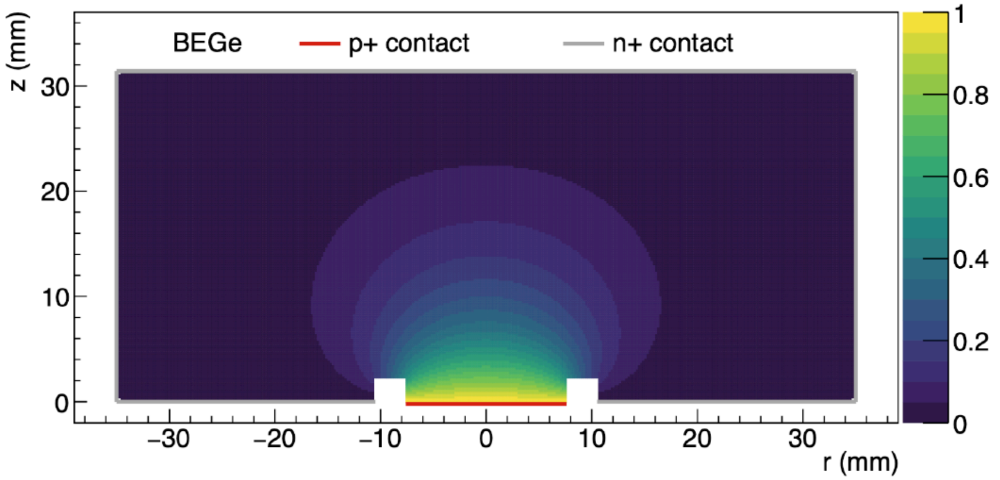

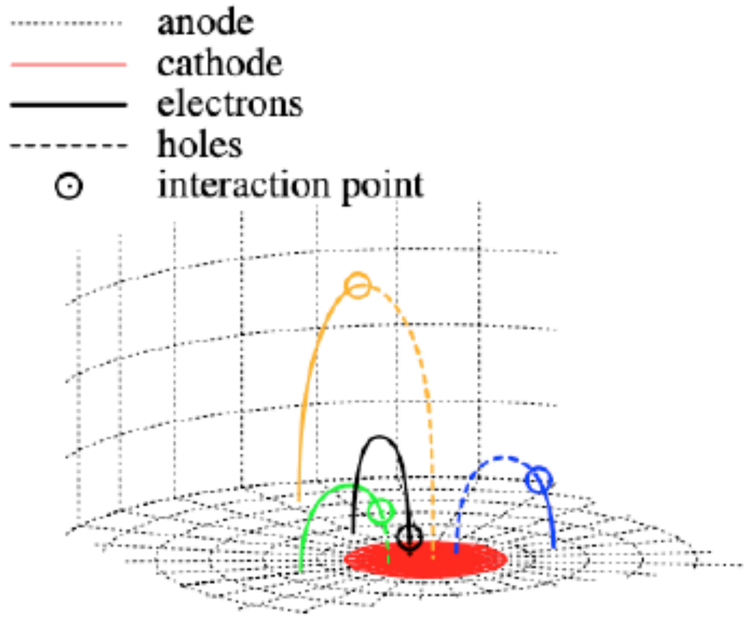

- Q and A spectra allow to differentiate events according to where energy deposition occurs in crystal

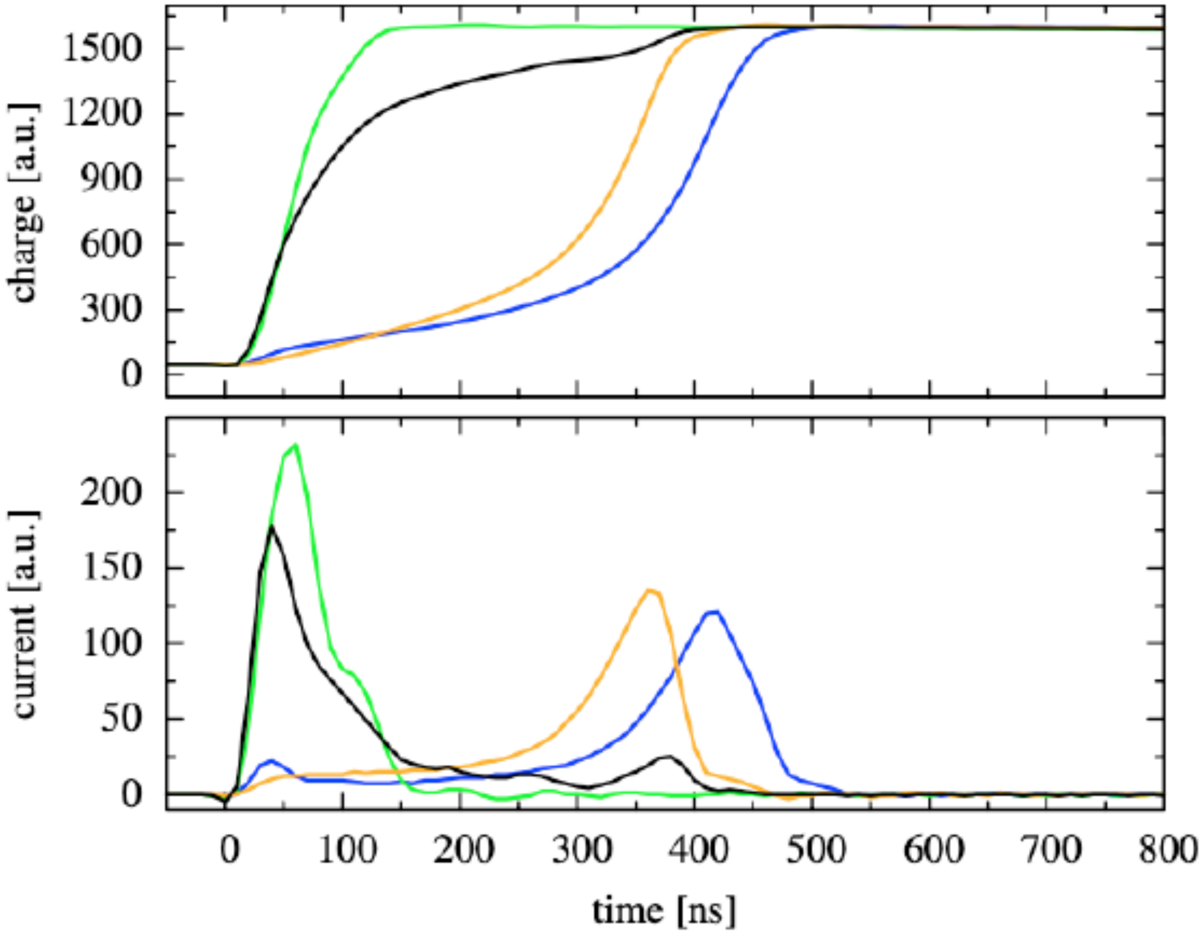

- If all ionization happens in single site (SSE), Q and A proportional and compatible with single cluster
- If ionization is diffused (Bethe-Bloch or Compton, MSE), total Q is split in smaller peaks of A

Why is PSD important?

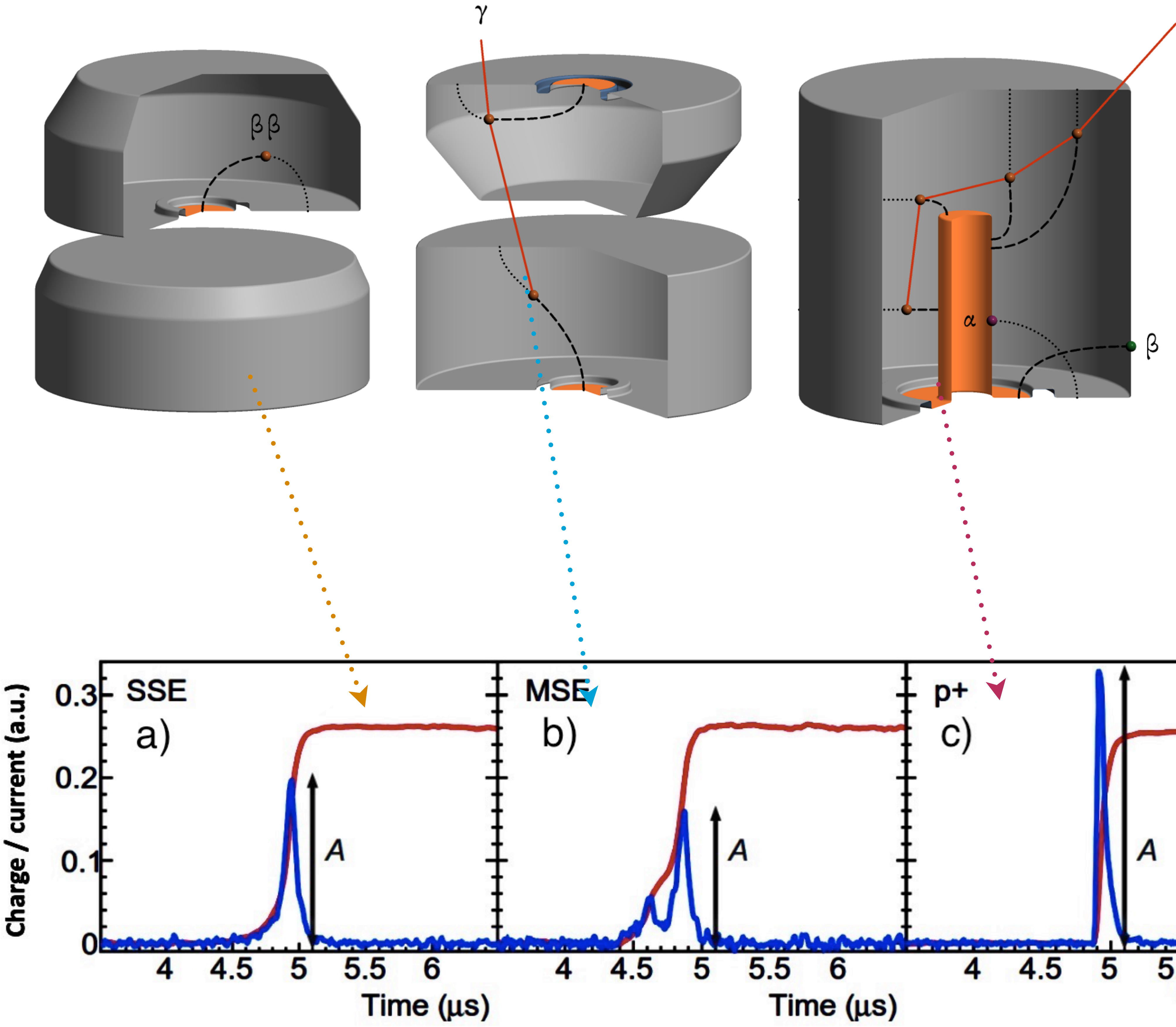

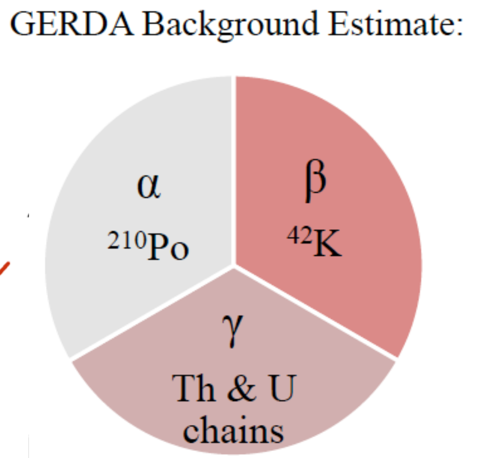

Why is PSD important?

GERDA Background Estimate:

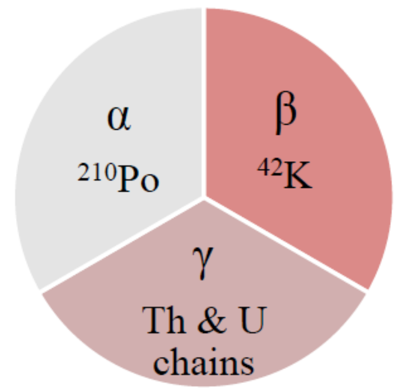

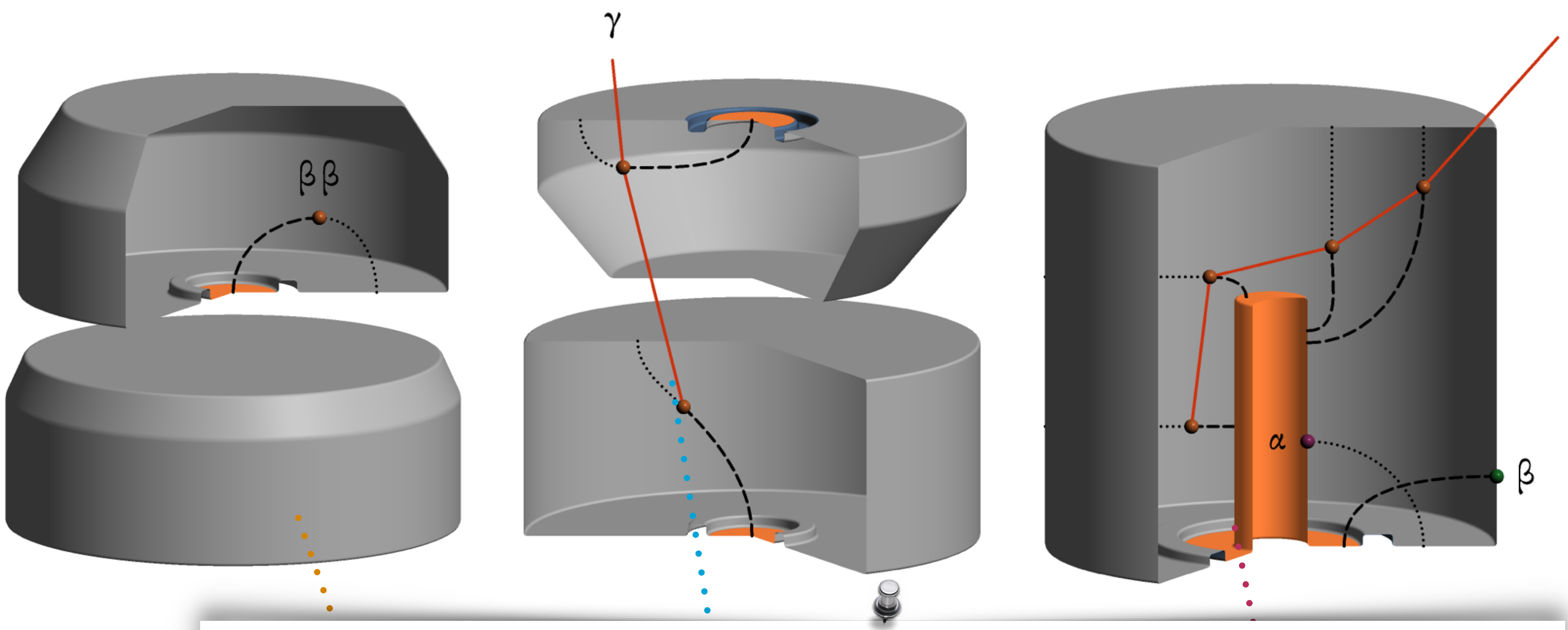

See later for L-200 PSD performance preliminary figures

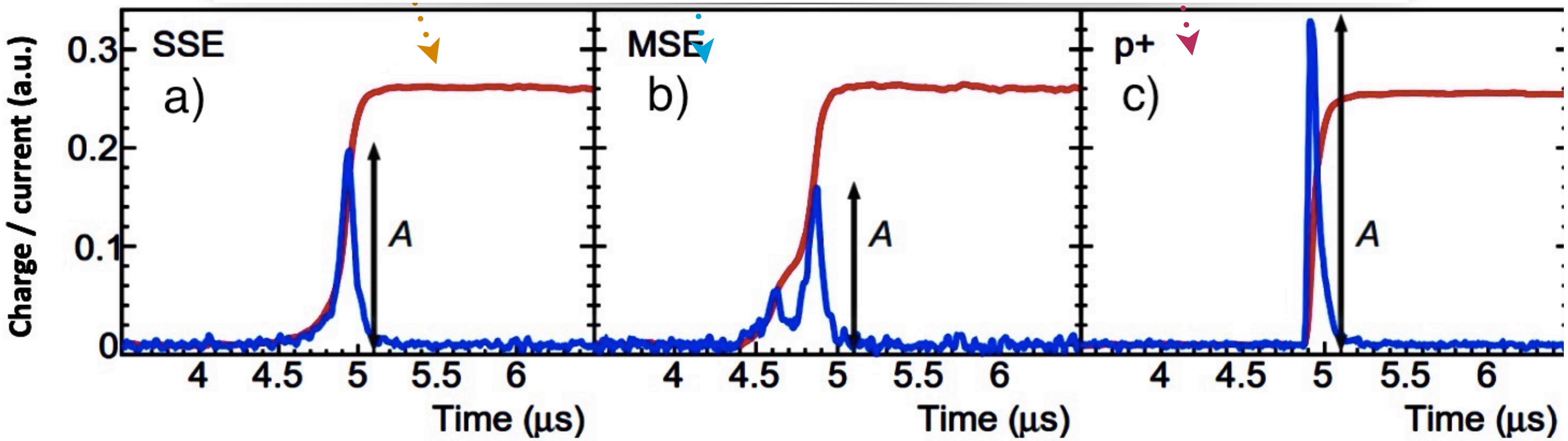

Origin of radioactive bkgs

- α comes from ^{210}Po (τ=138 days) coming from ^{238}U chain on diode surface and attracted to migrate towards p$^+$ electrode by its strong field
- γ comes from
  - various branches of U and Th chain on materials (FETs, cables, Cu mounts);
  - and from $^{40/42}$Ar → $^{40/42}$K → $^{40/42}$Ca* decays (K ion drifted by LAr convective motion and electric field lines towards n$^+$ dead layer = SSE)
- β mainly from $^{40/42}$K decays close to diodes, same as above

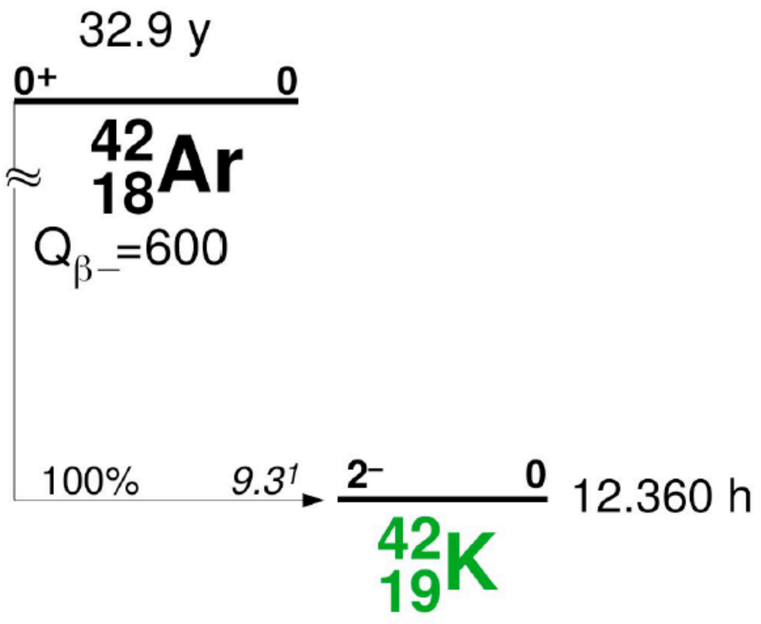

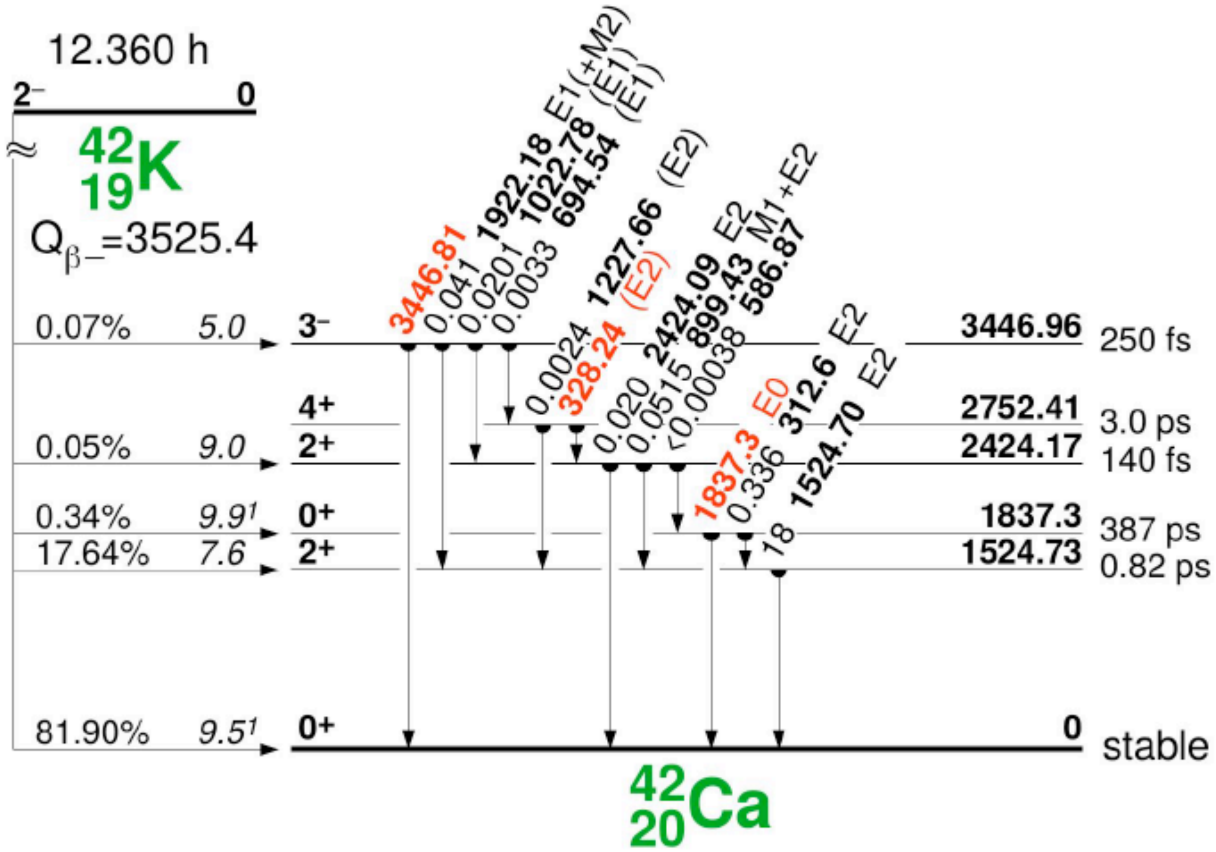

MITIGATION measures of radioactive bkgs

- α comes from ^{210}Po (τ=138 days) coming from ^{238}U chain on diode surface and attracted to migrate towards p^{+} electrode by its strong field
- γ comes from
  - various branches of U and Th chain on materials (FETs, cables, Cu mounts);
  - and from $^{40/42}$Ar → $^{40/42}$K → $^{40/42}$Ca* decays (K ion drifted by LAr convective motion and electric field lines towards n^{+} dead layer = SSE)
- β mainly from $^{40/42}$K decays close to diodes, same as above

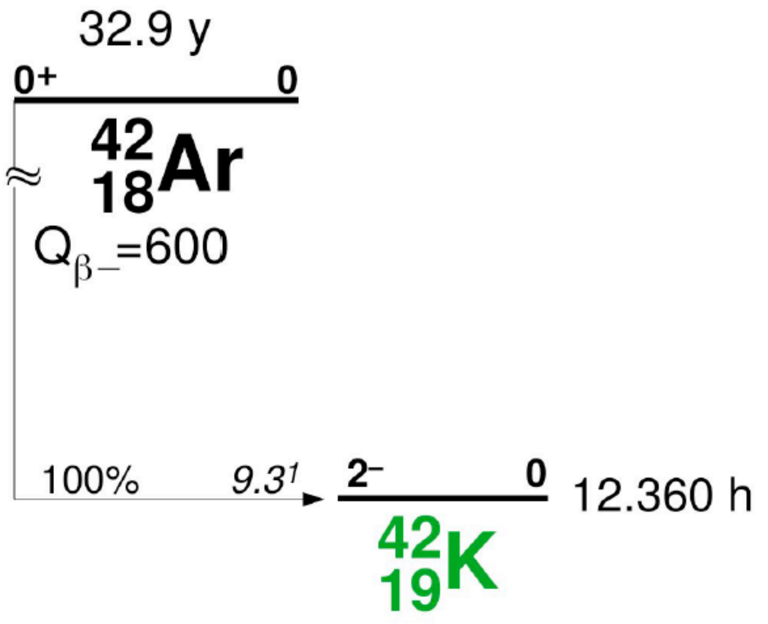

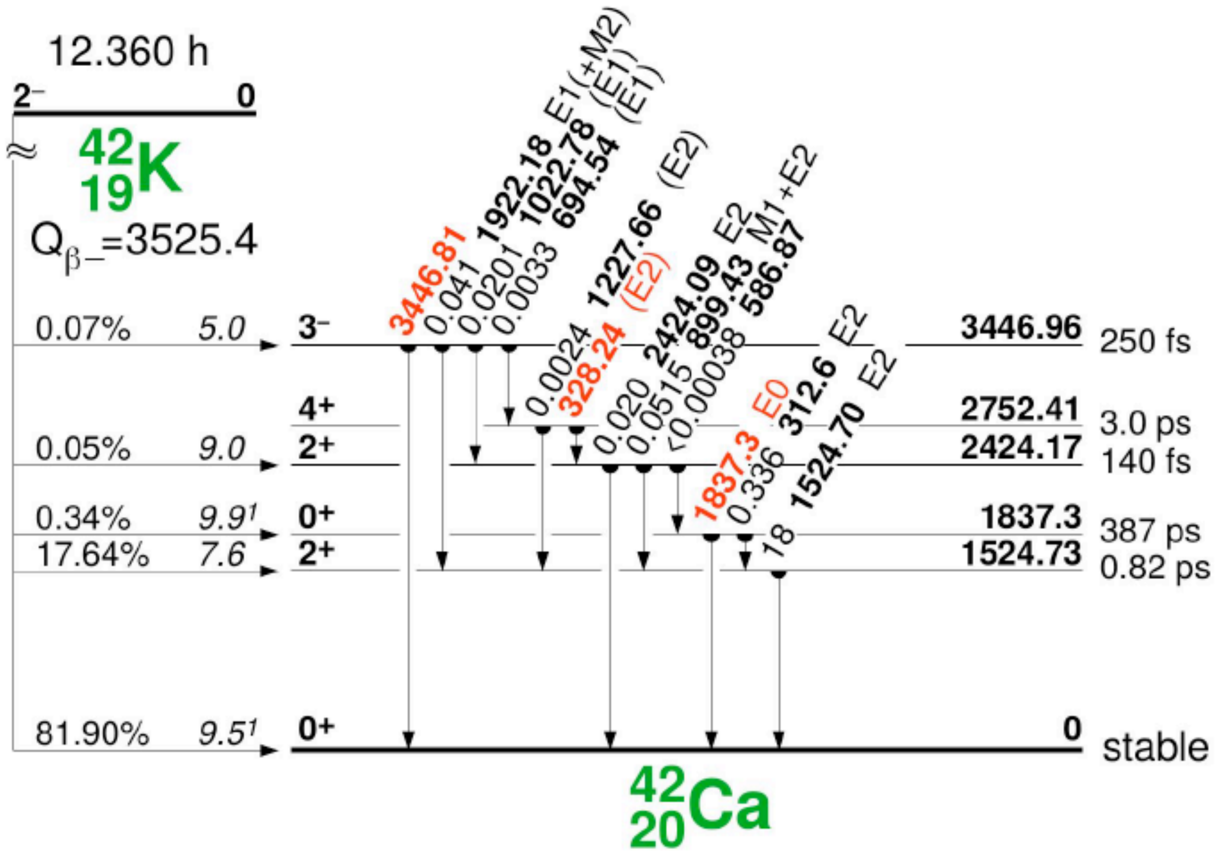

UG electro-formed copper

- Applies experience of MJD, which used 1.2 tons of UGEFCu because of its radio-purity (≤ 0.1 μBq/kg Th/U chains, very low in cosmogenic ^{60}Co)
- 3 new EF baths were constructed at SURF to supply clean Cu for detector housing components
- Advancements in the understanding of post machining contamination of plastics and metals will feed into L-1000 effort

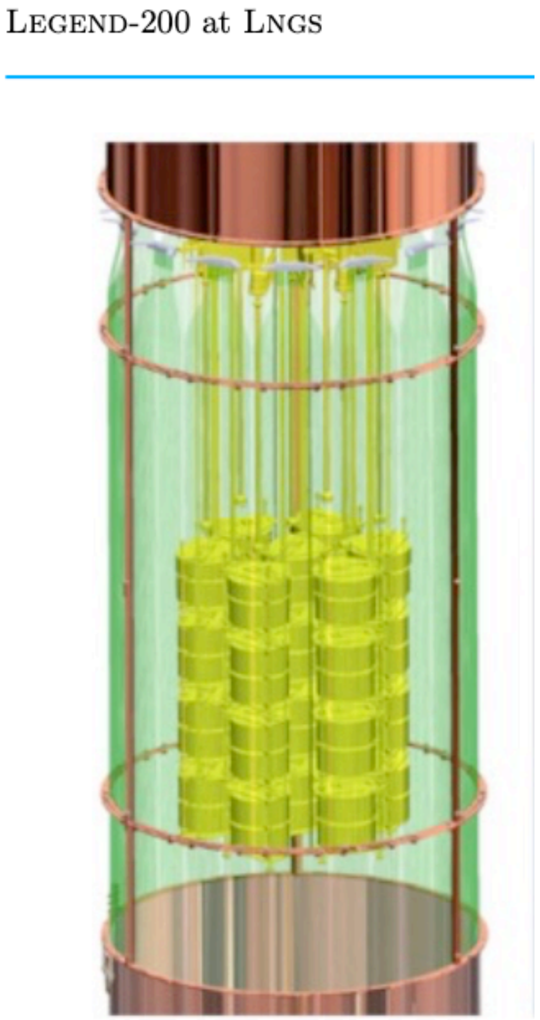

LEGEND-200 at LNGS

EFCu can be placed next to detectors, in LAr: improves signal/ noise and, consequently, PSD

PEN plates: veto yourself

- PEN — Poly(ethylene 2,6-naphthalate) is a scintillating plastic (1/3 LY of conventional plastic scintillators)
  - wavelength-shifts to ~450 nm the 128 nm photons from LAr
- Mechanically stronger than silicon, stronger than Cu at cryogenic temperatures (T=87 K)
- Meets radio-purity req. ≤ 1 μBq/piece for Ra/Th

Low (5-7 g) mass geometry optimized for L-200

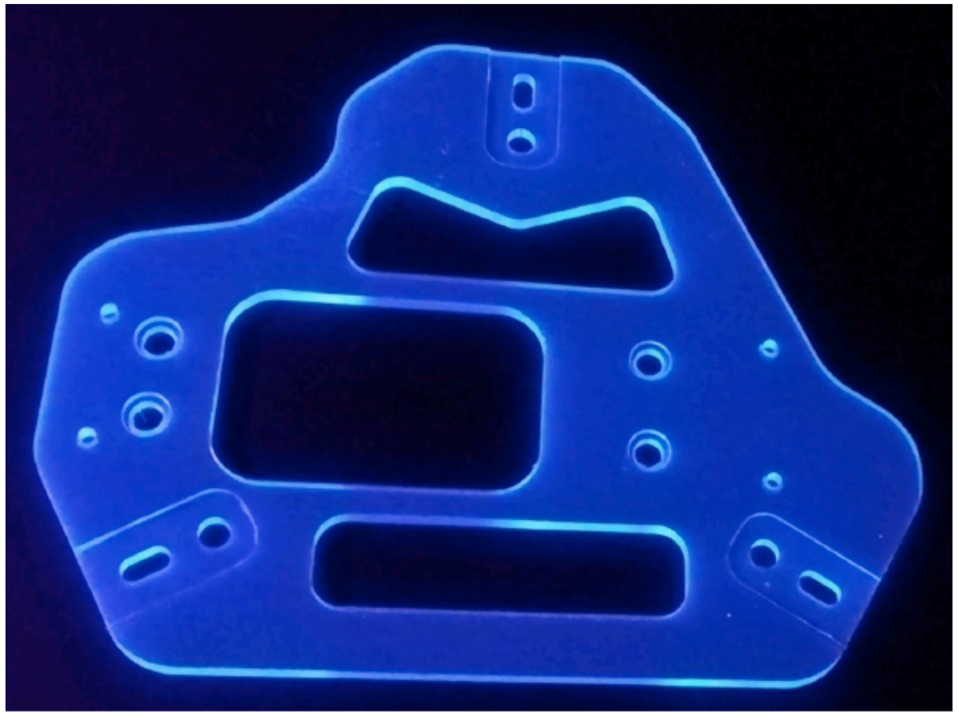

- PEN holders deployed in LEGEND-200
  - Replace Si plates (GERDA)
- On-going further R&D for additional cleanliness and improved optical properties for L-1000

Plates fitting read-out electronics

MITIGATION measures of radioactive bkgs

- α comes from ^{210}Po (τ=138 days) coming from ^{238}U chain on diode surface and attracted to migrate towards p$^+$ electrode by its strong field
- γ comes from
  - various branches of U and Th chain on materials (FETs, cables, Cu mounts);
  - and from $^{40/42}$Ar → $^{40/42}$K → $^{40/42}$Ca* decays (K ion drifted by LAr convective motion and electric field lines towards n$^+$ dead layer = SSE)
- β mainly from $^{40/42}$K decays close to diodes, same as above

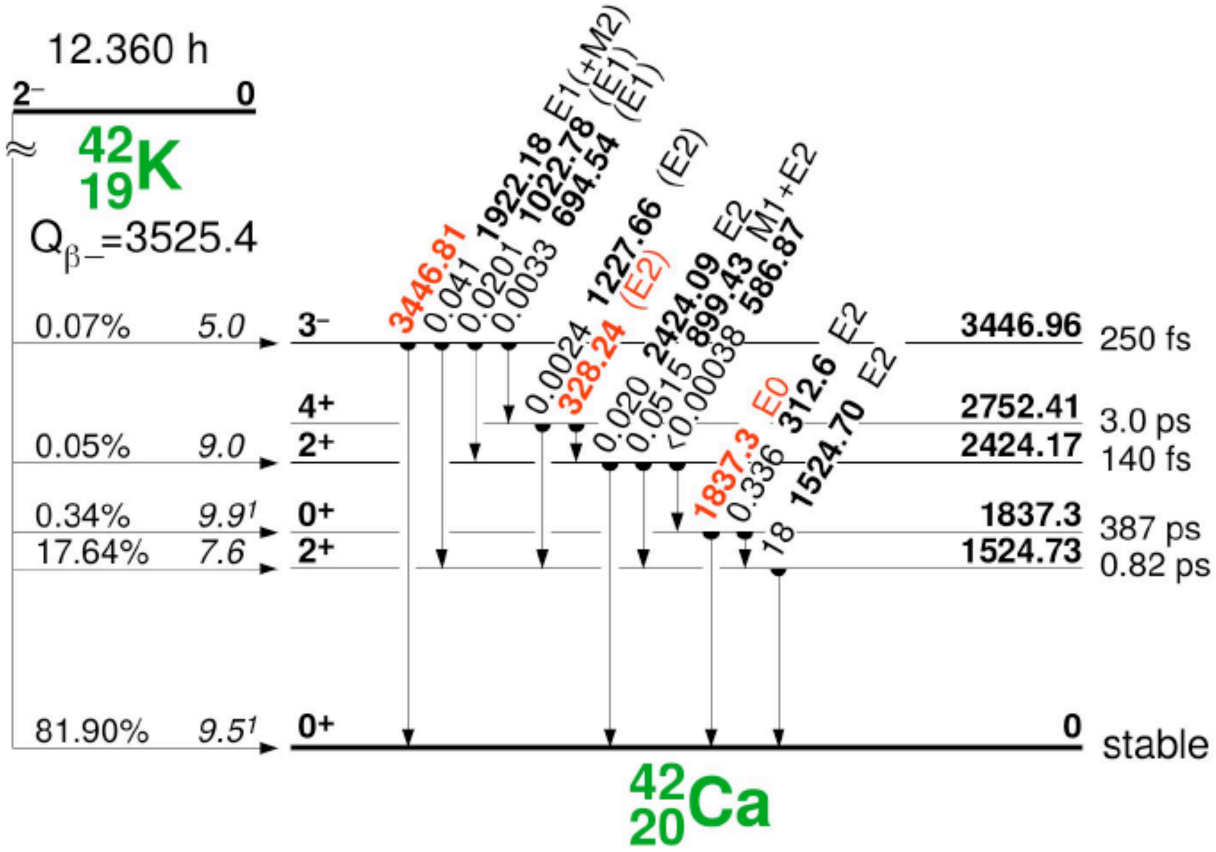

TPB-coated nylon cylinders surrounding each string to limit effect of drifting K-ions

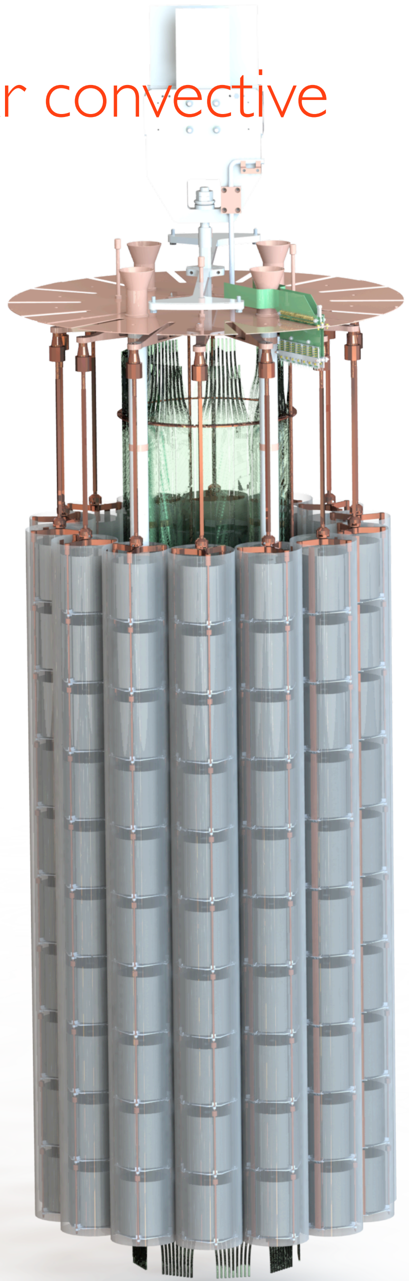

LAr instrumentation

- Retain a crucial element of GERDA: instrument LAr volume to read out light from scintillation
  - 2 shrouds of optical fibres for enhanced coverage coated in TBP as WLS
  - connected SiPM with new FE electronics ⇛ enhanced SPE resolution *(https://arxiv.org/abs/2211.03069v1)*
  - Reflective foil around outer shroud to increase light collection ⇛ about ×3 <N(PE)> wrt Gerda *(EPJ C 82, 442 (2022))*
- Actively vetoes incoming radiation from U/Th/K in coincidence with diodes
  - 2 software chains for optimized energy reco + resilience against noise *(DPLMS, see also EPJ C (2023) 83:149)*
- But introduces bkg itself:
  - radioactivity from fibers, SiPM
  - high-activity from β decays of sub-dominant isotope ^{39}Ar *[1.41 Bq/l (NIM A 574 83)]*

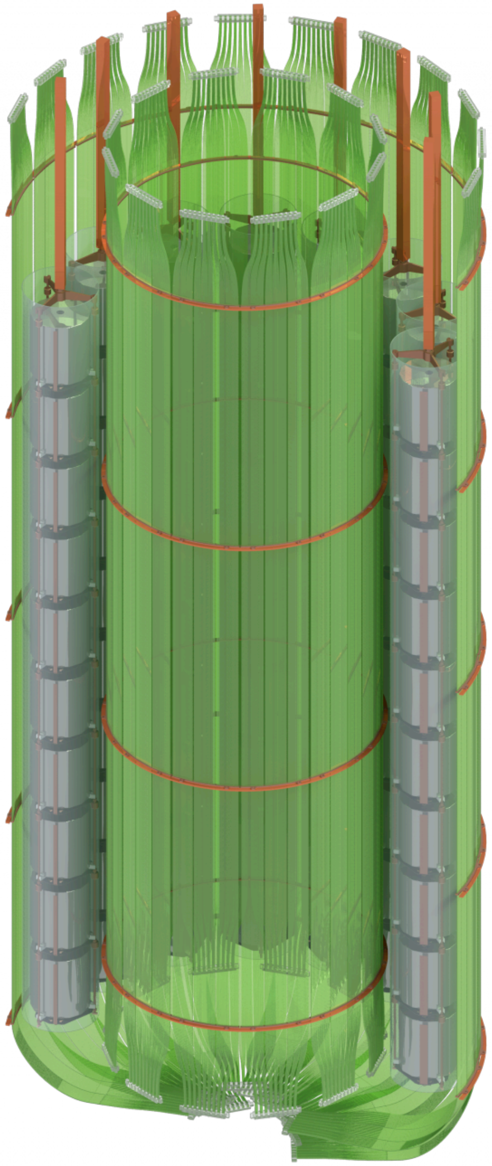

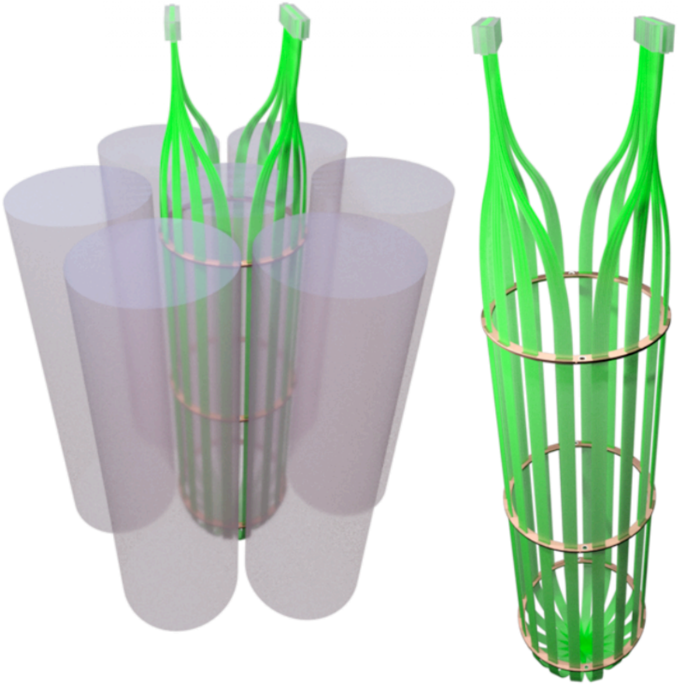

Read also: NIM A 1048 (2023)

LAr instrumentation - preliminary performance

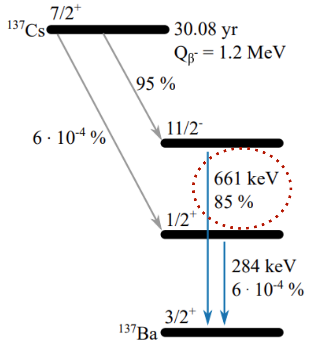

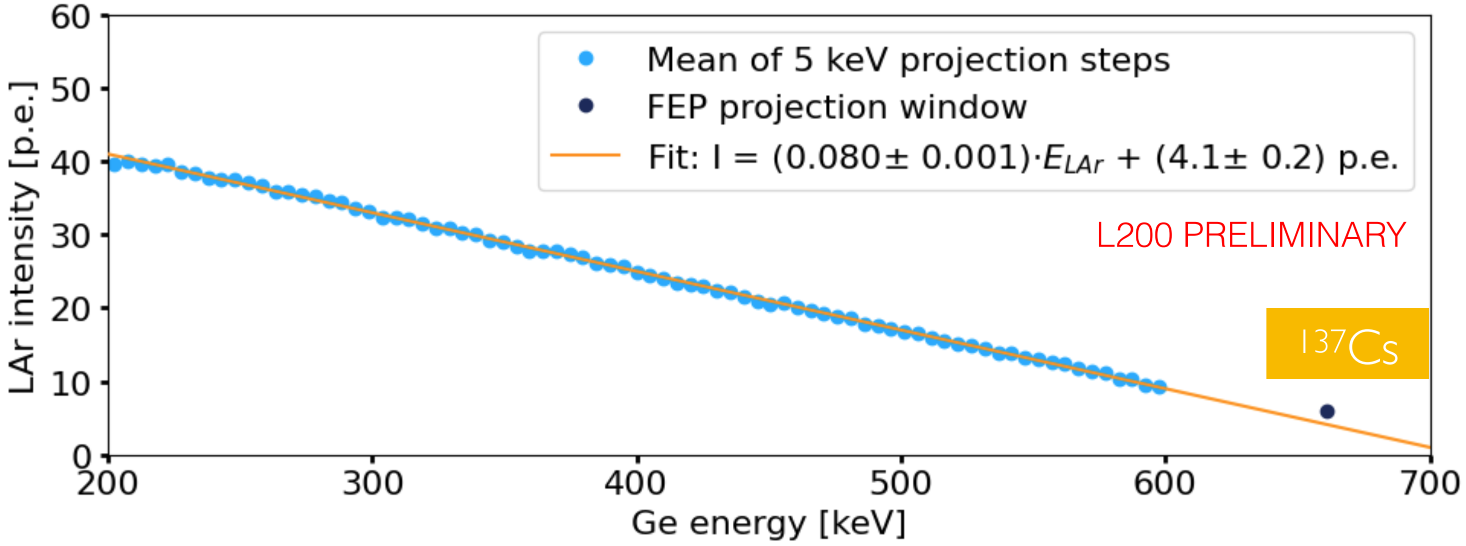

^{137}Cs

- Very low electronics noise (few tens of μV)
- only few % rate of random coincidences created by noise fluctuations
- Good linearity of E response

^{226}Ra

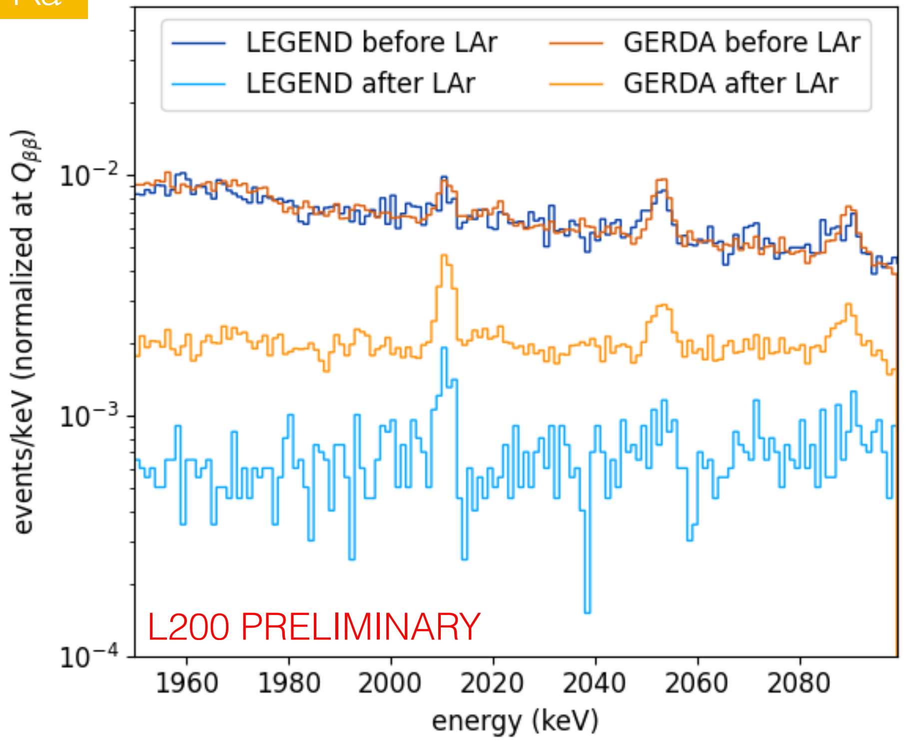

Approx ×3 improvement in bkg suppression wrt to GERDA

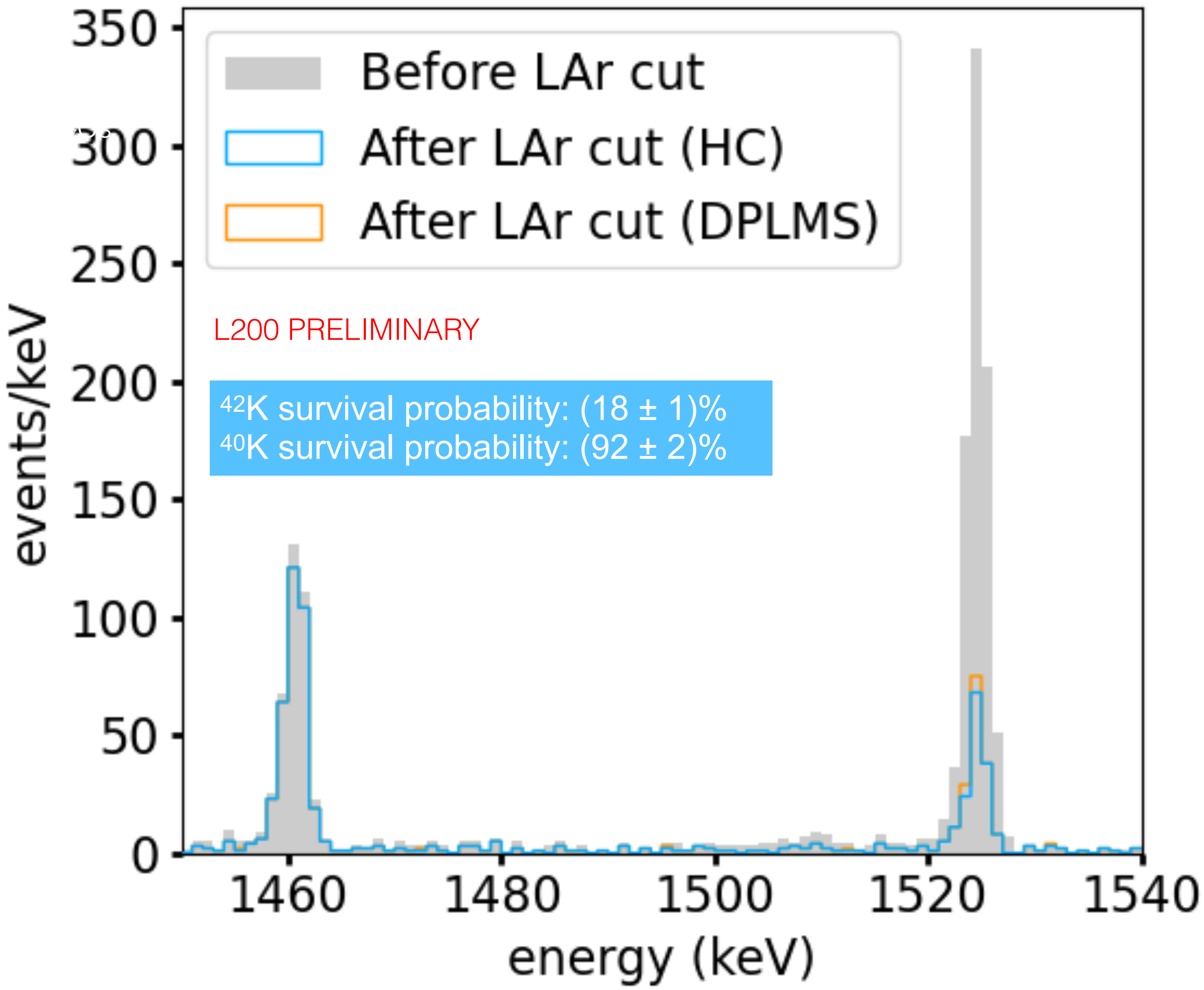

^{42}K survival probability: (18 ± 1)%
^{40}K survival probability: (92 ± 2)%

Active Background rejection

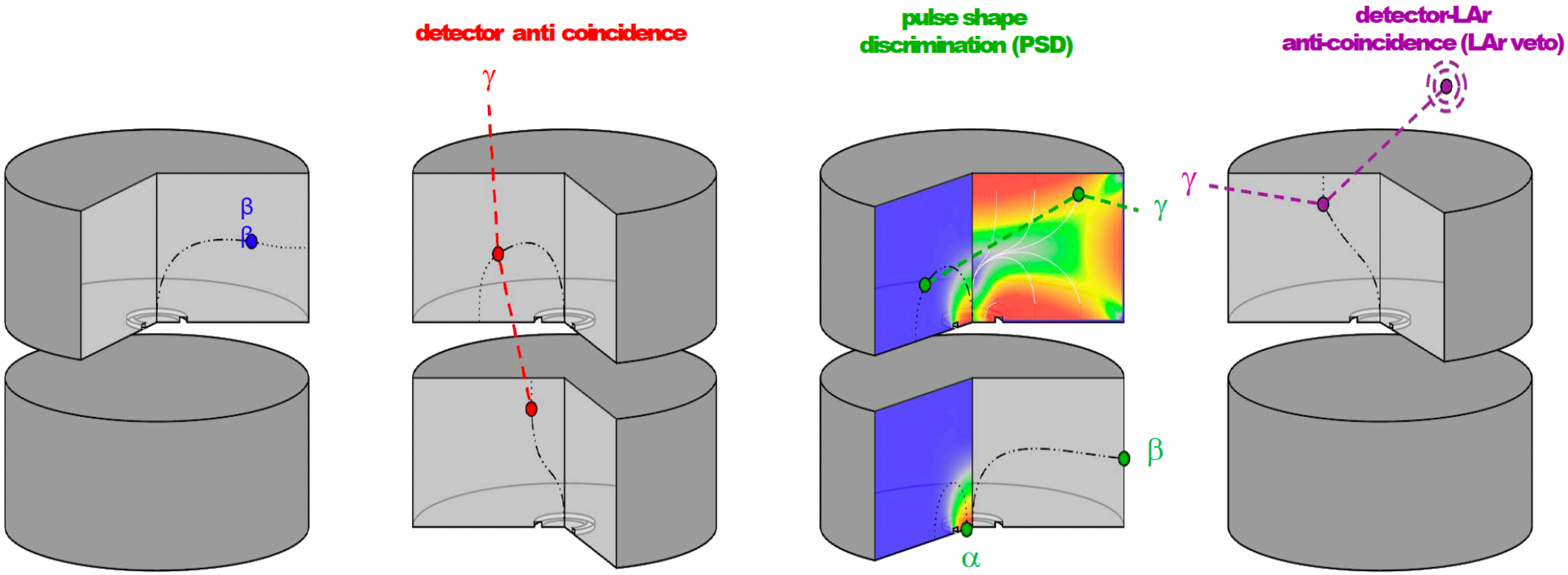

Synopsis

Expected background budget L-200

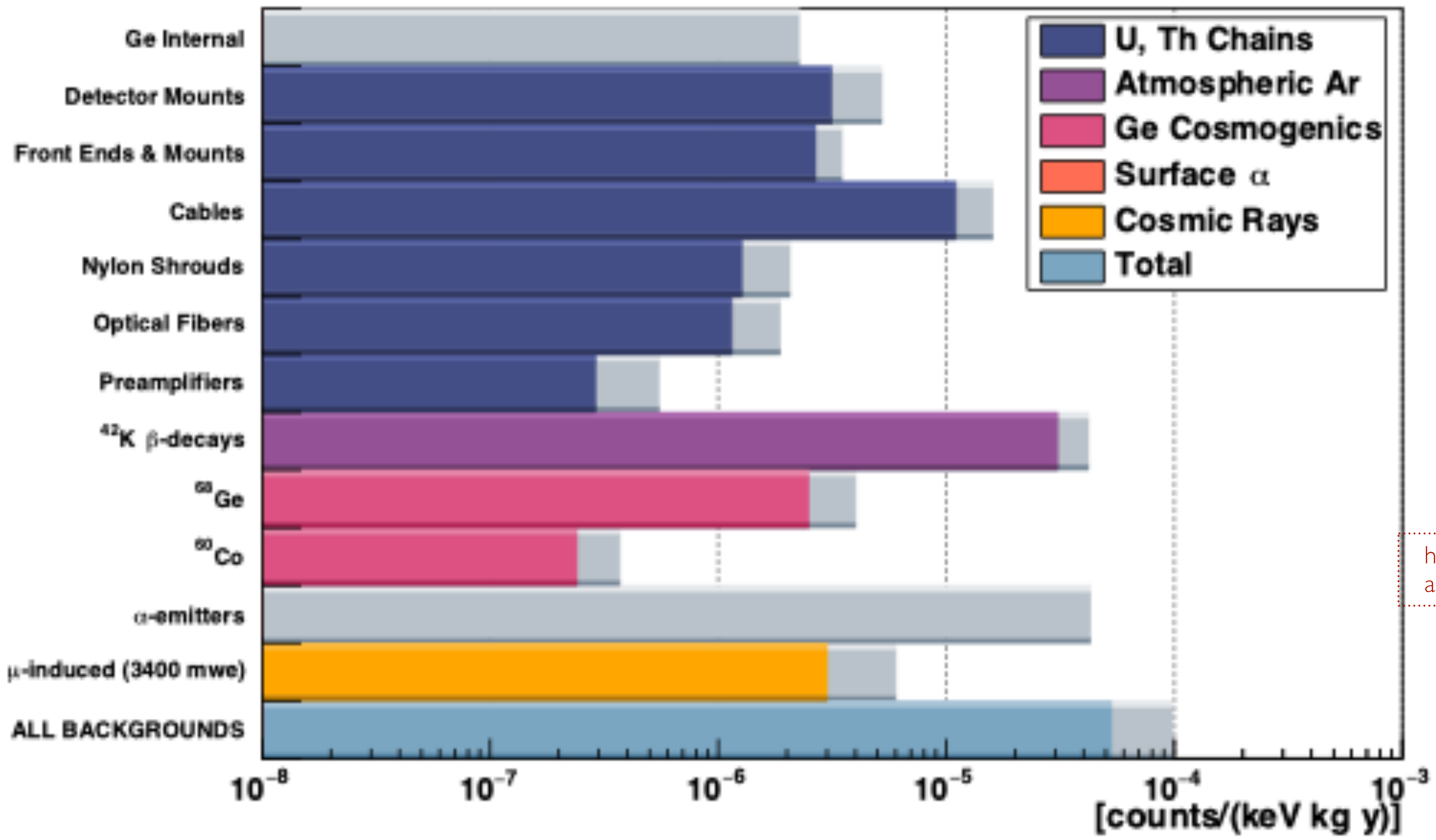

https://arxiv.org/abs/2107.11462

~ 2-3 times lower BI than GERDA

Energy calibration

- 16 ^{228}Th sources ($T_{1/2}$=1.9 yr, A~5 kBq/source) for use in cold
- Away during data-taking and inserted by 4 dedicated motorized units
- Response checked at various energies periodically

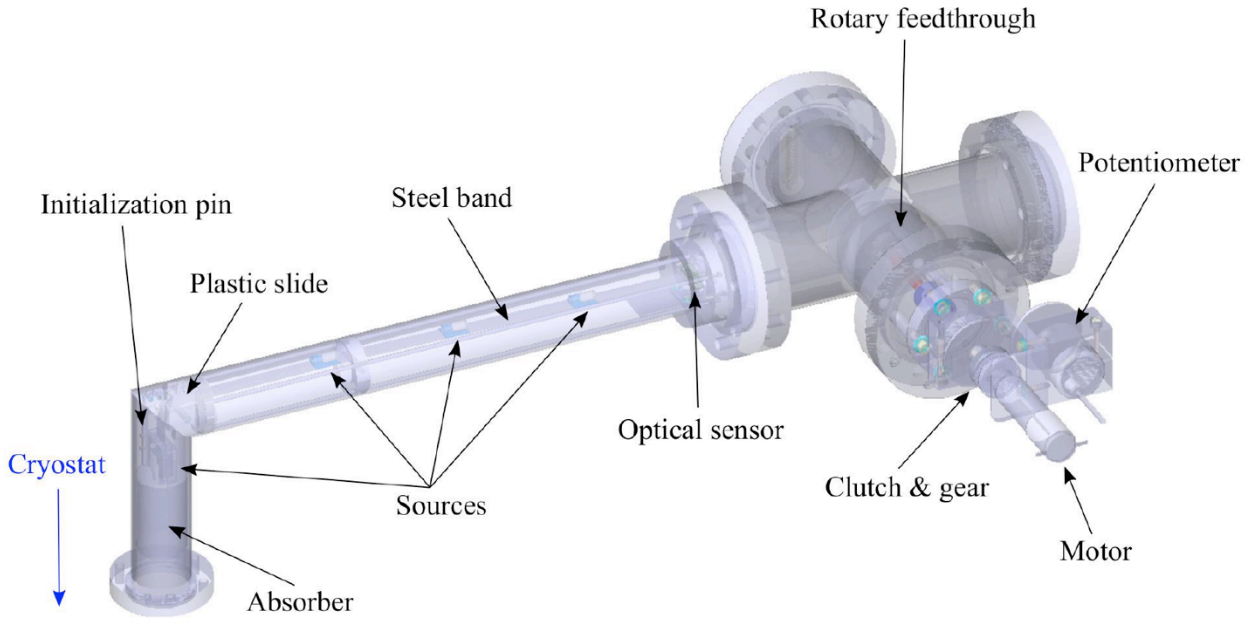

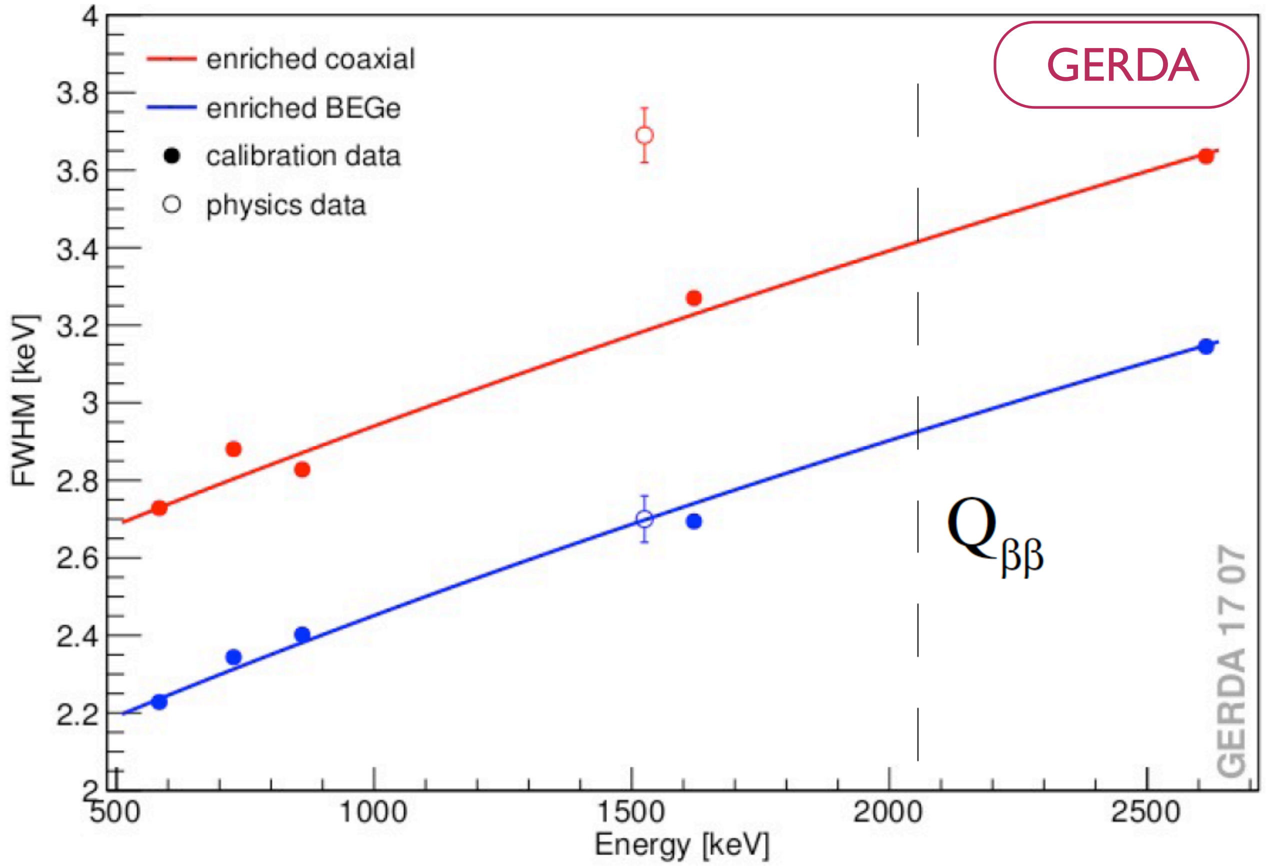

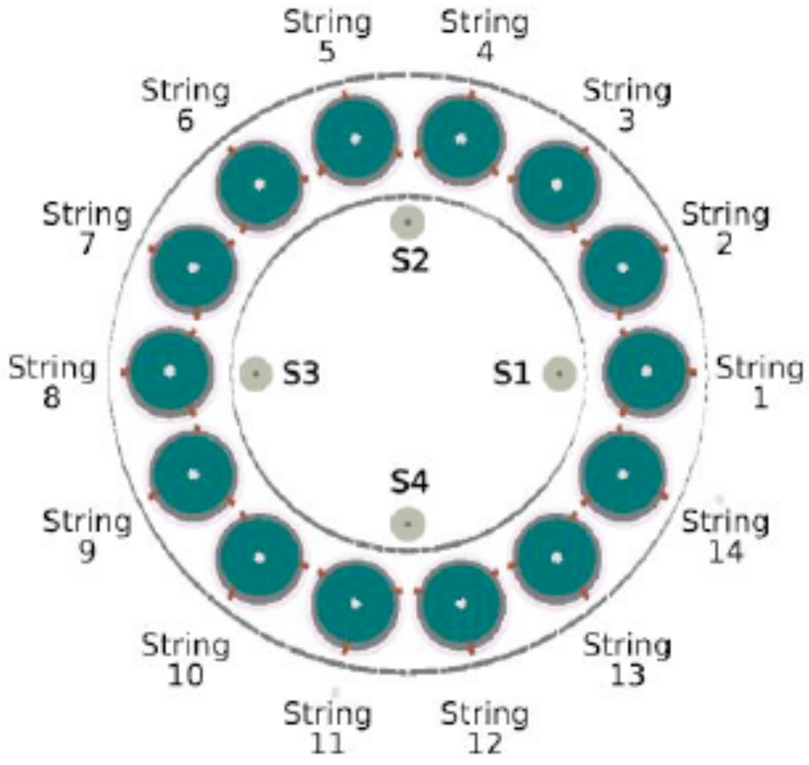

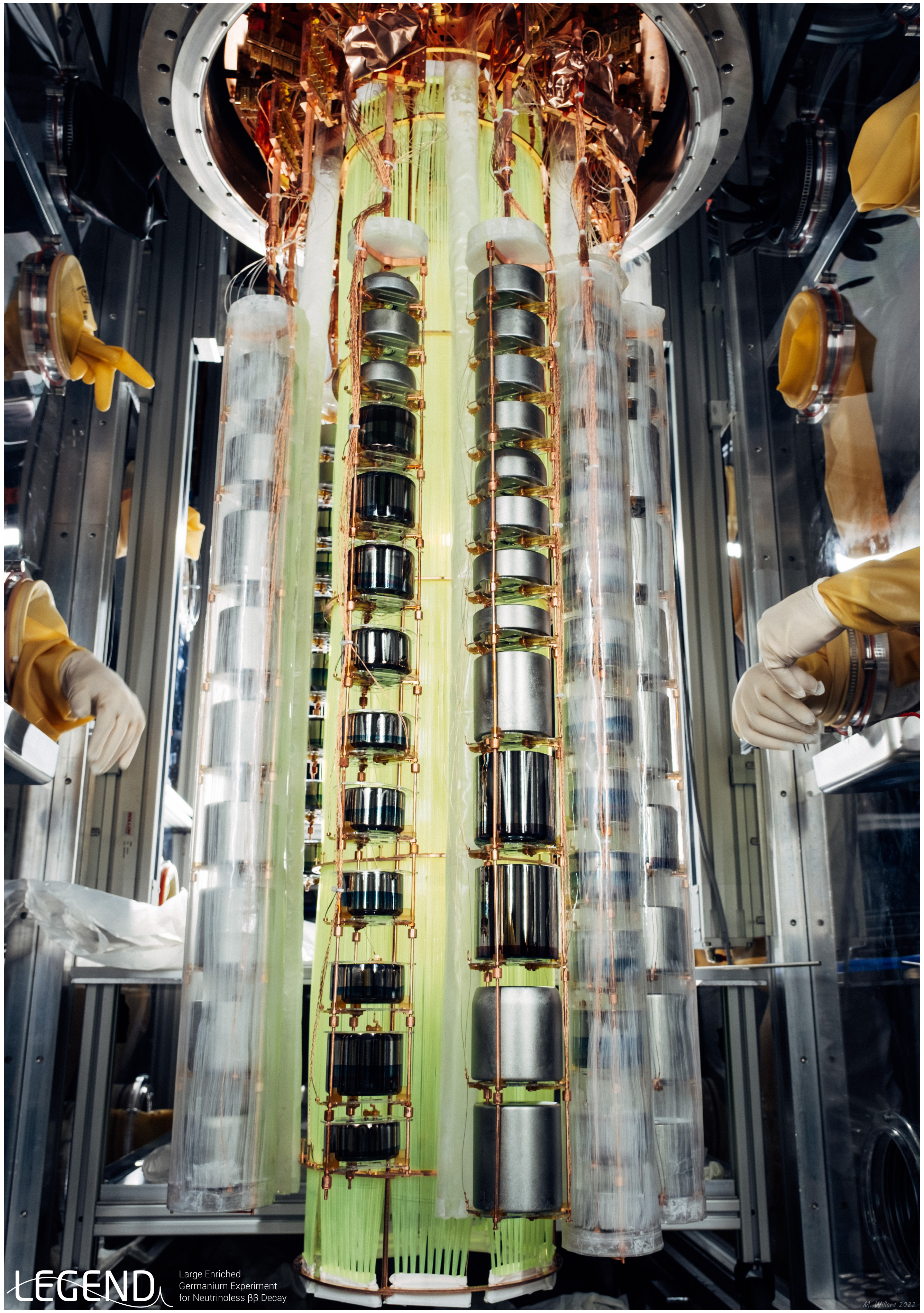

Current status…

☑ 140 kg taking data since March '23

- Start of stable physics data taking
- 122 kg usable for analysis
- 100 kg yr by the end of the year

☑ 140 kg taking data since October '22

- Commissioning and performance evaluation with larger scale

☑ First 60 kg: taken data over summer 2022

- set-up, start of DAQ, electronics noise, early performance evaluation

Ge diodes - preliminary performance

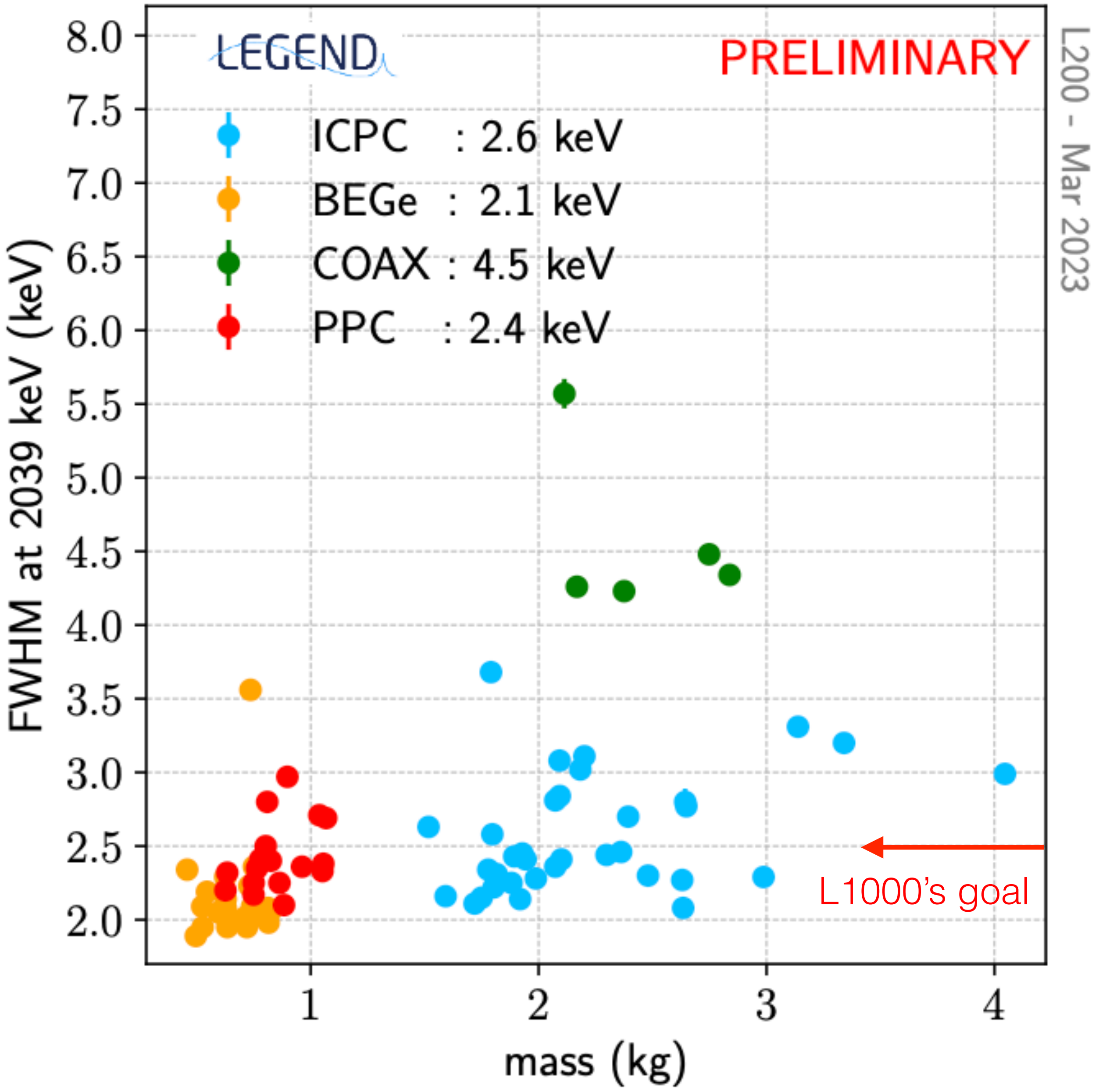

L1000's goal

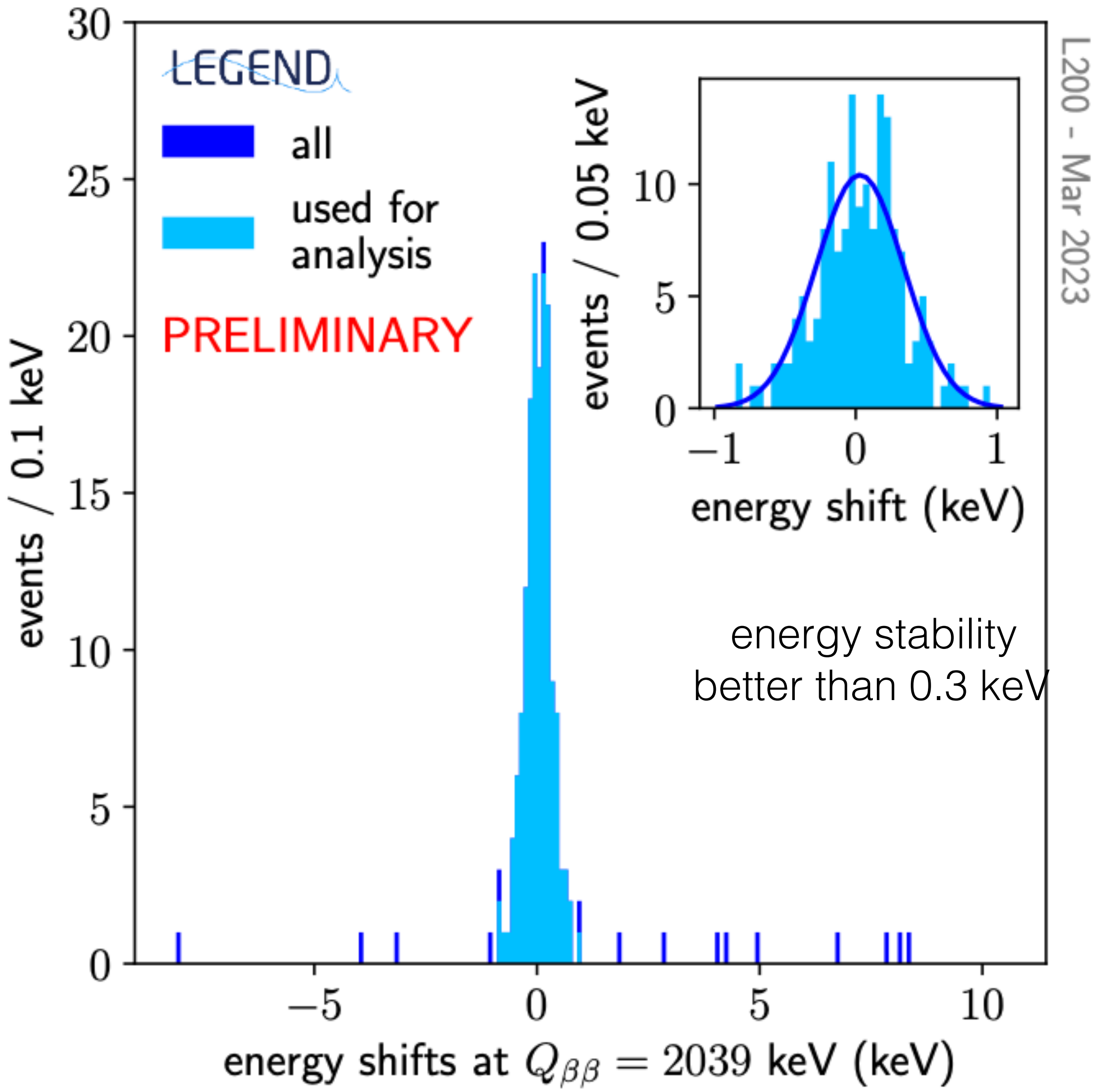

energy stability better than 0.3 keV

- Preliminary energy resolution in first L-200 physics period with full set-up very satisfying
- Stable to 0.3 keV for all "good" detectors
- Resolution of ICPC does not depend on its mass
  - heavier detectors also show excellent E_{res}
  - Allows to scale up mass in view of L1000

PSD - preliminary performance

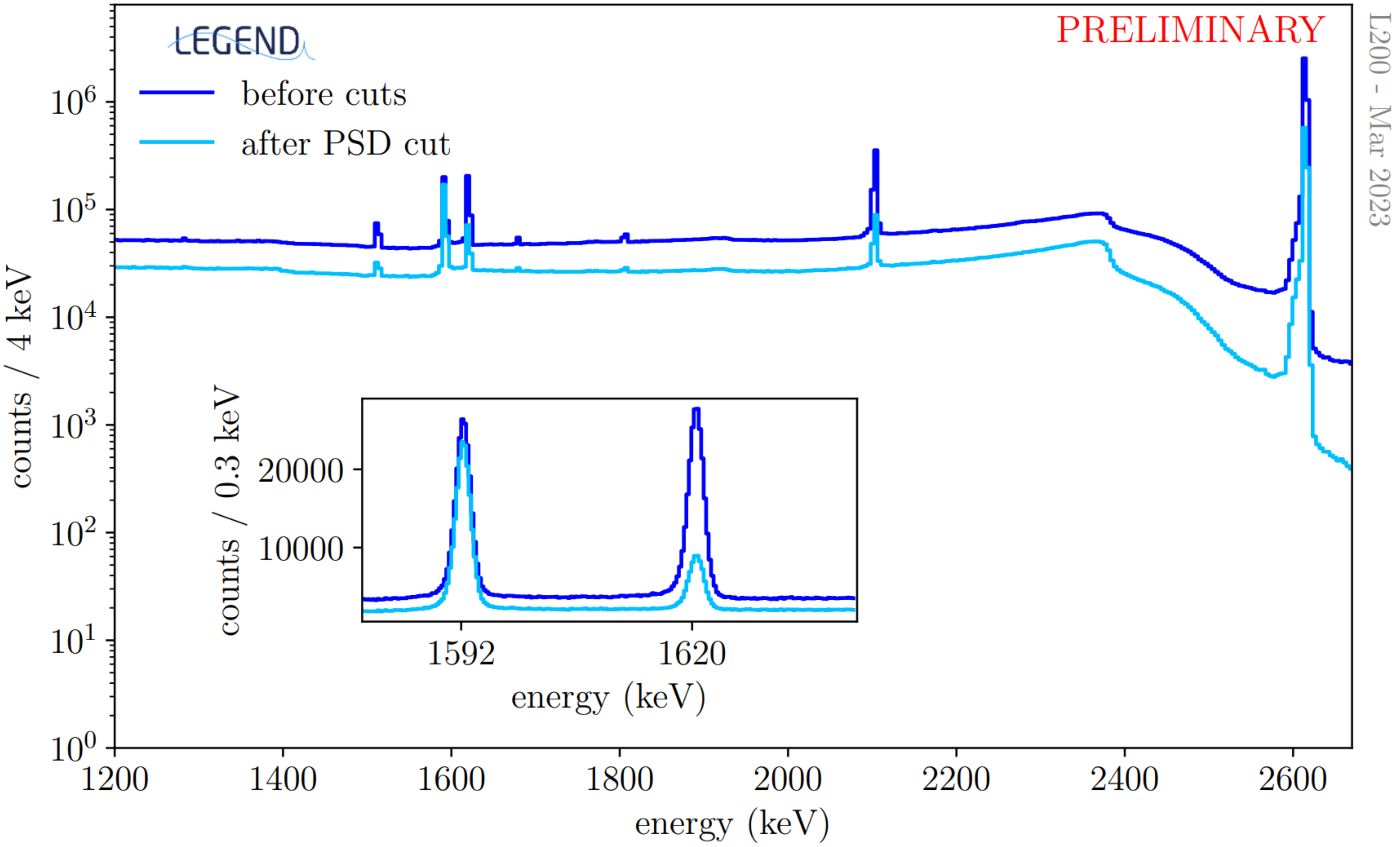

- Weekly calibration used also to extract benchmark performance of PSD on radiogenic bkgs
  - E=1592.5 keV from DEP of ^{208}Tl is <u>proxy for 0ν2β</u> topology: PSD retains 90% of them
  - E=1621 keV from FEP of ^{212}Bi is proxy for multi-site event: PSD rejects ~90%
- Consistent with expectations (remember GERDA/slide 32?)

See also EPJC **82**, 284 (2022)

L-200 → L-1000

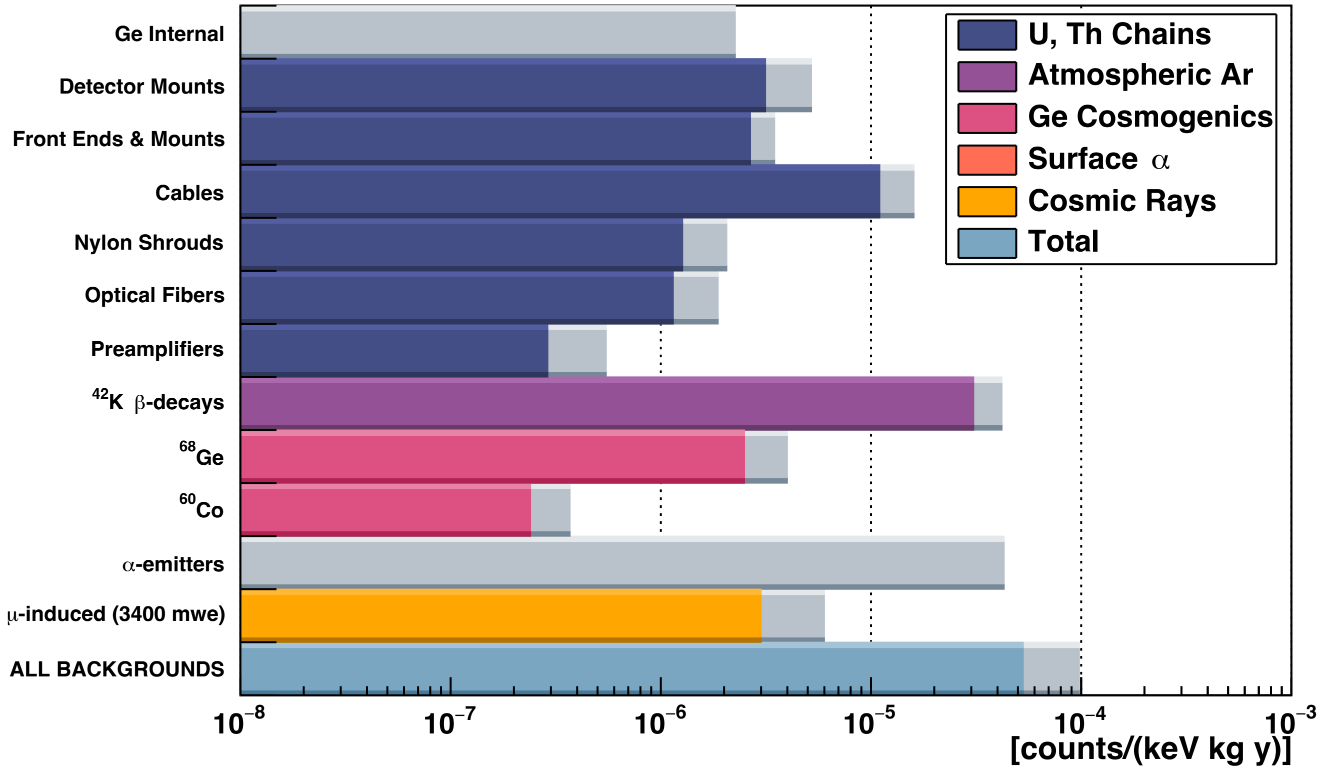

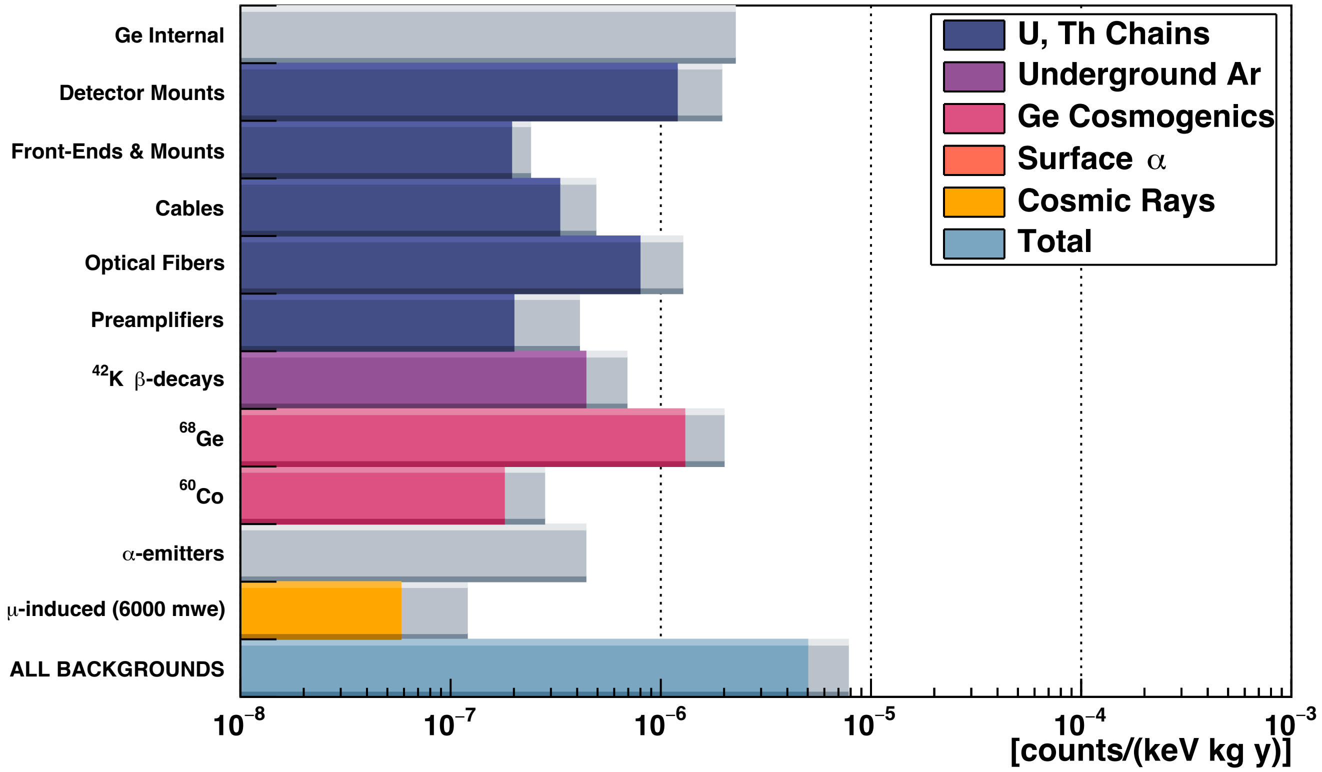

- Largest reductions are on ^{42}K, α, μ

- + “trimming” here and there on radio-purity of materials, esp. cables

- Need specialised work to stop cosmogenic bkg, esp. if at LNGS

~ 50 times lower BI than GERDA

L-1000 design

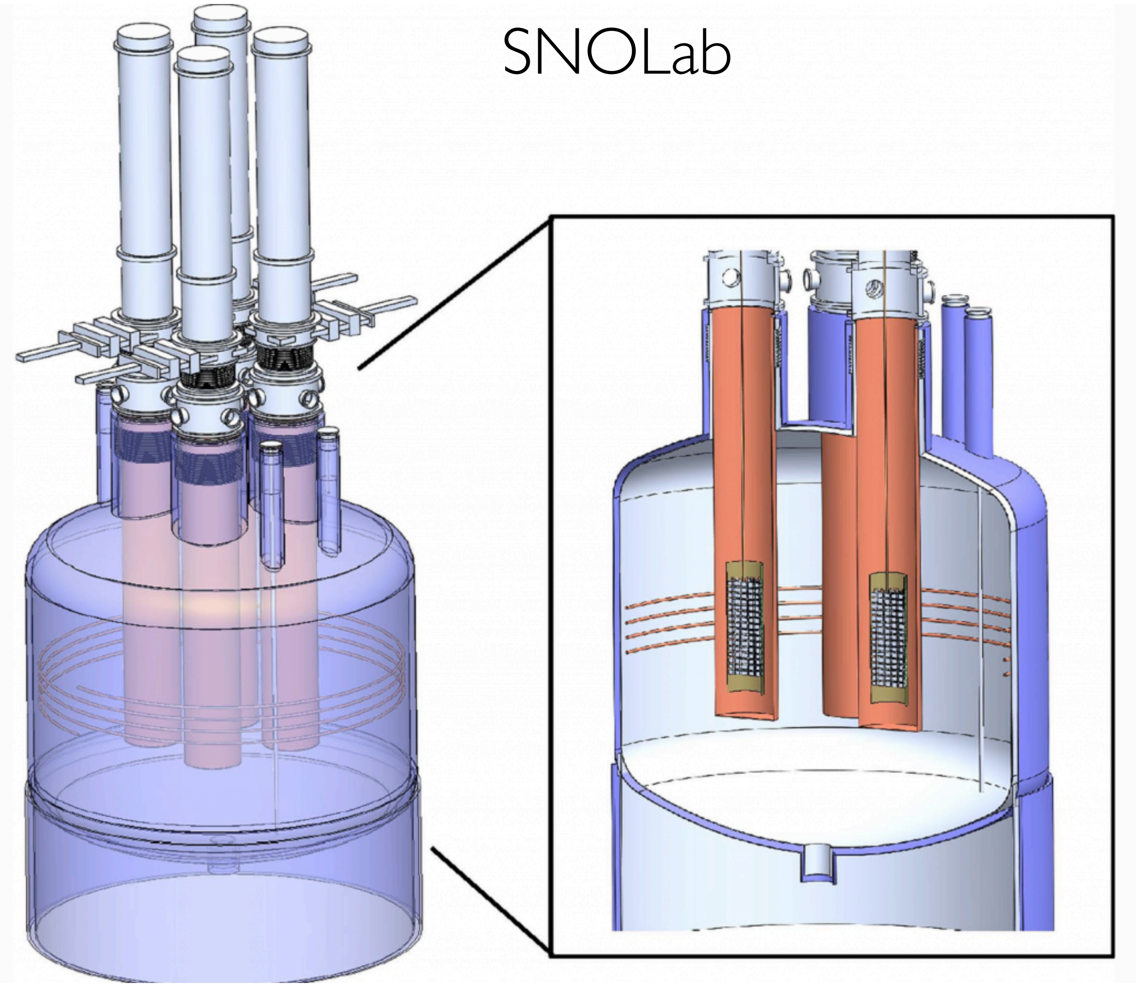
SNOLab

LNGS
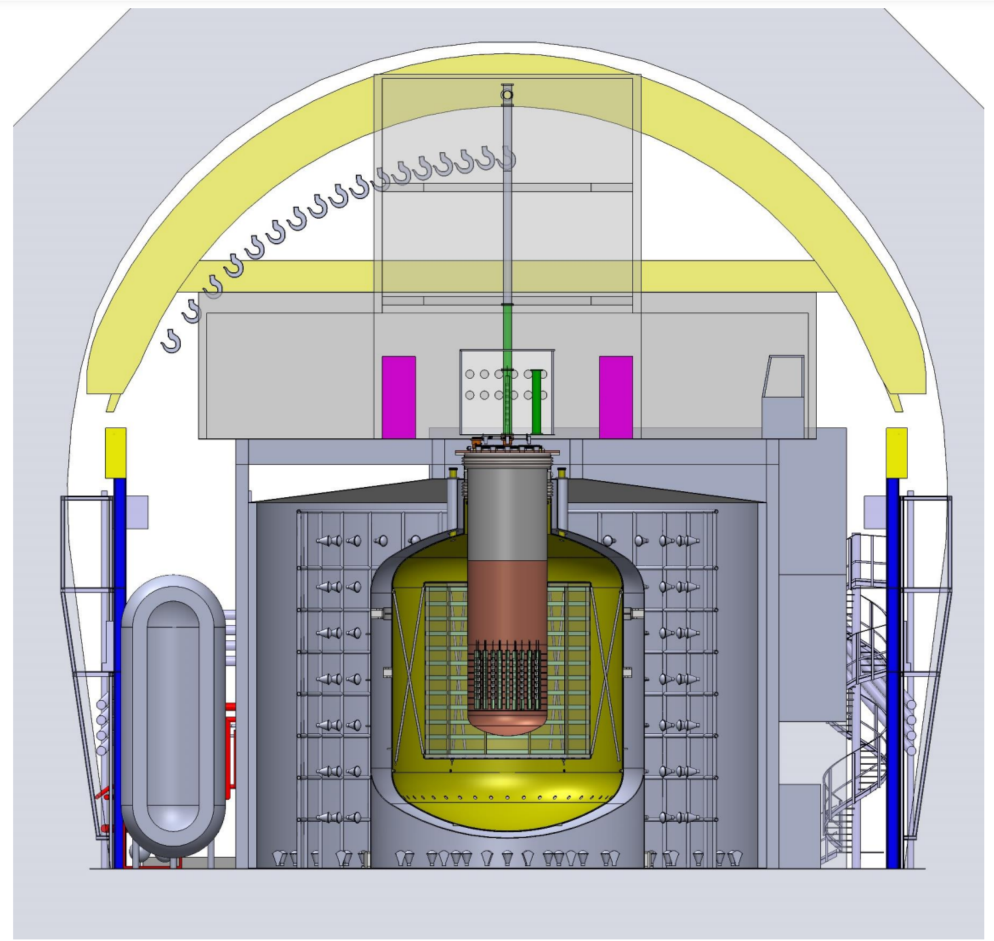

- Host lab yet TBD: SNOLab or LNGS, based on several arguments/criteria
- String concept replicated in payloads, in total ~400 detectors
- Re-entrant tubes (UGEFCu) modular with different arrangements for SNOLab or LNGS
- E.g. at LNGS: LAr cryostat in “water tank” (5.5 m Ø LAr, 2-2.5 m layer of water)

UGAr to reduce ^{42}Ar/^{42}K

- ^{42}K from β decay of ^{42}Ar resulting from cosmogenic activation in various processes (e.g. *PRD 100, 072009 (2019)*)
  - low fraction in atmospheric Ar, but high enough activity
- Underground Ar significantly less subject to cosmic ray activation → highly depleted in such isotopes (down by factors ~10^4)
- Proposed to use part of the combined production (*extraction at URANIA, US + chemical purification at ARIA, Italy*), estimated need 25 tons: use only in payload cryostat, standard "atmospheric" Ar in outer volume
- Ion collection depends on n^+ dead-layer thickness: to be optimized
- Use of nylon cylinders around strings for further screening under discussion
  - shields, but only partially; self-vetoes, but only partially
  - could be good enough (after PSD and LAr veto), several studies done and on-going for GERDA and L-1000 [e.g. *EPJC 75, 506 (2015)*]
  - Else PEN? Encapsulated detectors (no LAr)? Xe-doped LAr for charge-exchanges?

Cosmic muons

- While "prompt" events in time with muon passage can be effectively rejected (95 to 99%) by water or LAr veto, delayed effects can generate disturbance
- Particularly production of Ge isotopes from capture of spallated neutrons (^{77,m}Ge)
- At SNO depth w/o further shielding expect ~10^{-7} cts/kev/kg/yr (1% of desired BI)
  - at LNGS x100

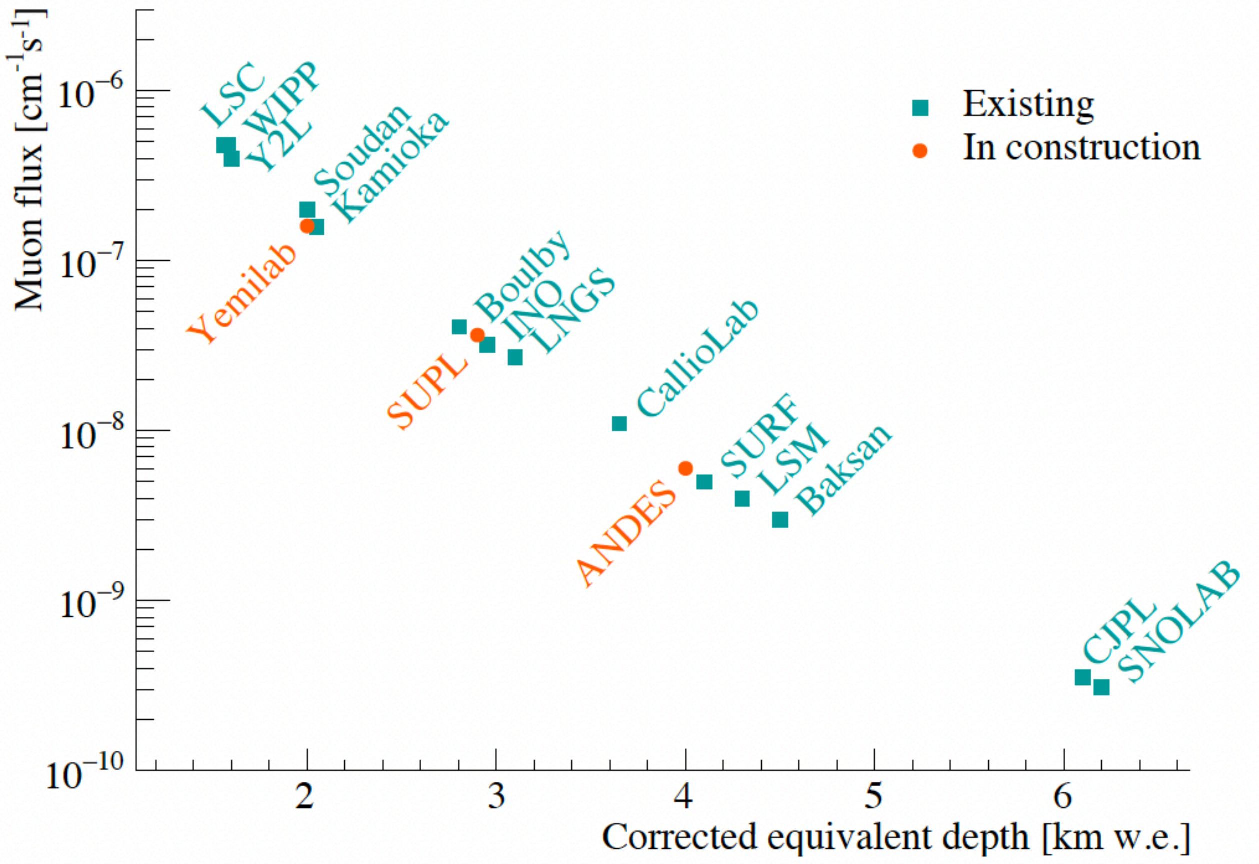

FIG. 15 Muon flux as a function of kilometers of water-equivalent depth (km w.e.) for a selection of deep underground laboratories worldwide. The actual depth is corrected for the overburden shape, if it is not flat. Thus laboratories located under a mountain have a slightly lower equivalent depth than the actual one. Figure adapted from Ianni (2020).

Cosmic muons

- While "prompt" events in time with muon passage can be effectively rejected (95 to 99%) by water or LAr veto, delayed effects can generate disturbance
- Particularly production of Ge isotopes from capture of spallated neutrons (^{77,m}Ge)
- At SNO depth w/o further shielding expect $\sim 10^{-7}$ cts/kev/kg/yr (1% of desired BI)
- at LNGS x100, **but** gain "virtual" depth:
  - By virtue of polymeric, low-radioactive neutron moderators in LAr with high hydrogen content

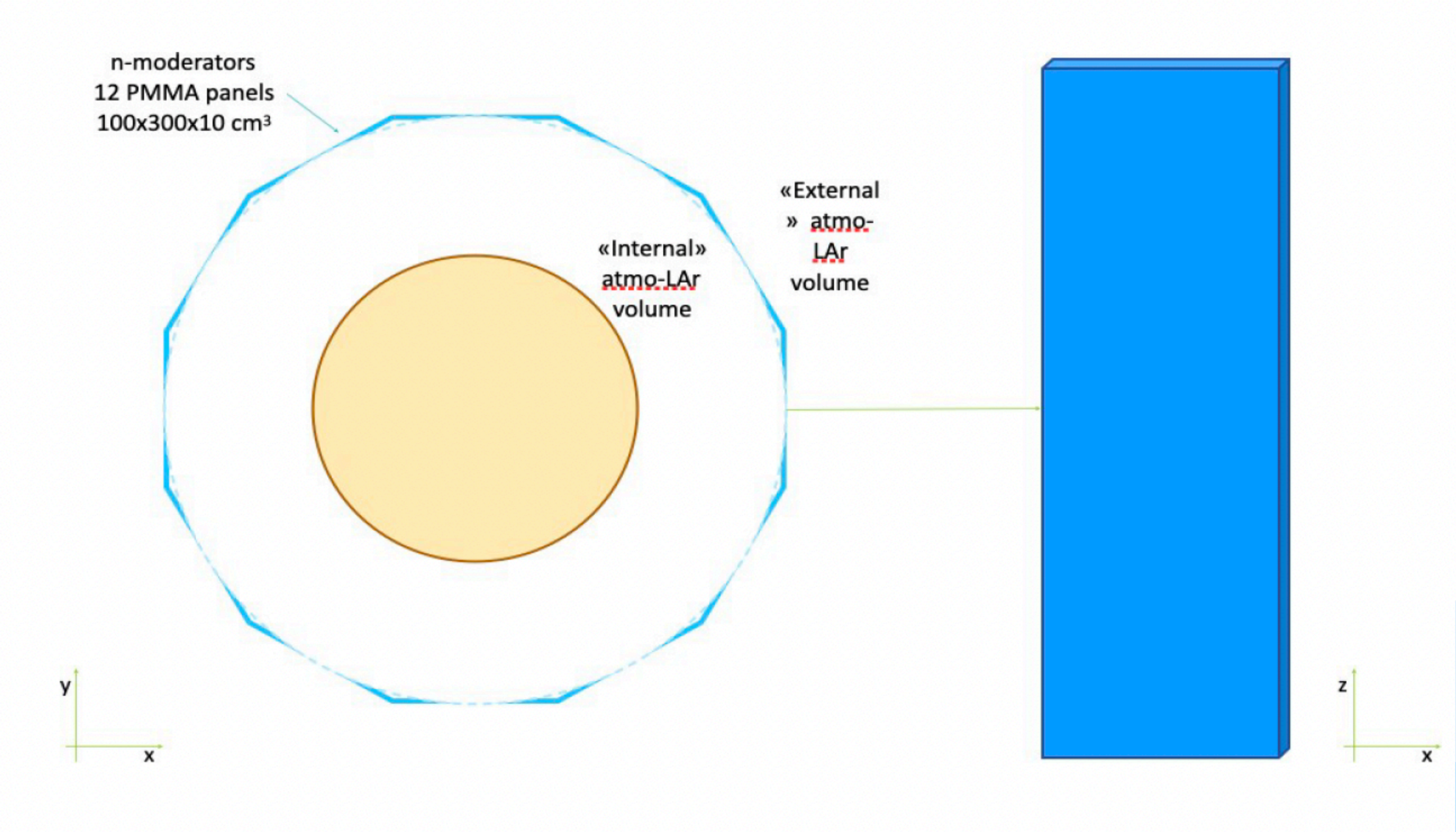

- R&D on-going on plastics, radio-assaying, doping with Gd/B
- expected to reduce neutron captures on Ge by ~half)
- Aim to equip with read-out to tag neutron captures in panel or near-by argon

Cosmic muons

- While "prompt" events in time with muon passage can be effectively rejected (95 to 99%) by water or LAr veto, delayed effects can generate disturbance
- Particularly production of Ge isotopes from capture of spallated neutrons (^{77,m}Ge)
- At SNO depth w/o further shielding expect ~10^{-7} cts/kev/kg/yr (1% of desired BI)
- at LNGS x100, but gain "virtual" depth:
  - By virtue of polymeric, low-radioactive neutron moderators in LAr
  - + panel read-out for independent trigger on delayed detection of n capture on ^{40}Ar (factor of × 10 reduction in μ-induced ^{77,m}Ge decays) *(EPCJ 78 (2018) no.7, 597)*

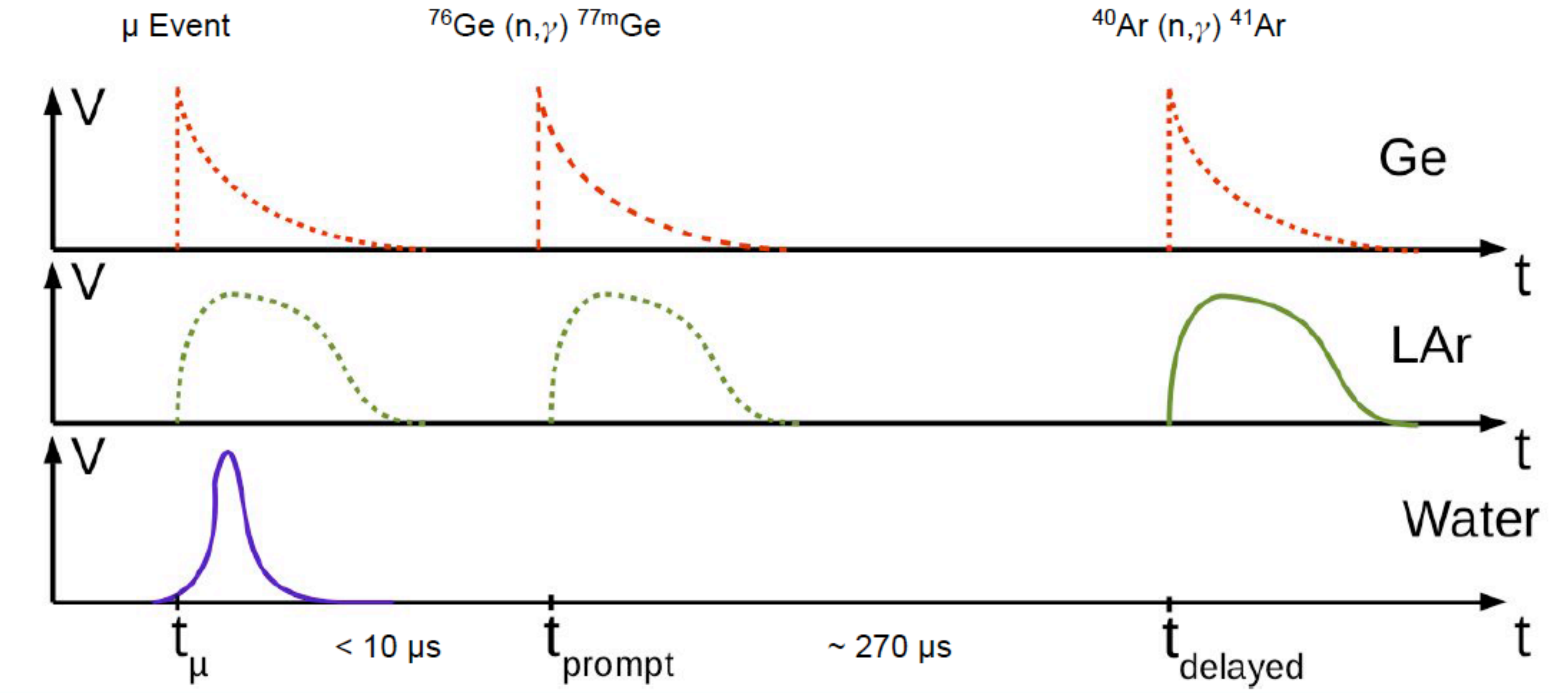

LNGS vs SNOLab

- LNGS infrastructure allows to start earlier
- Expected to fill gap between two labs essentially in toto in terms of discovery sensitivity
- At the price of a ~7% signal inefficiency

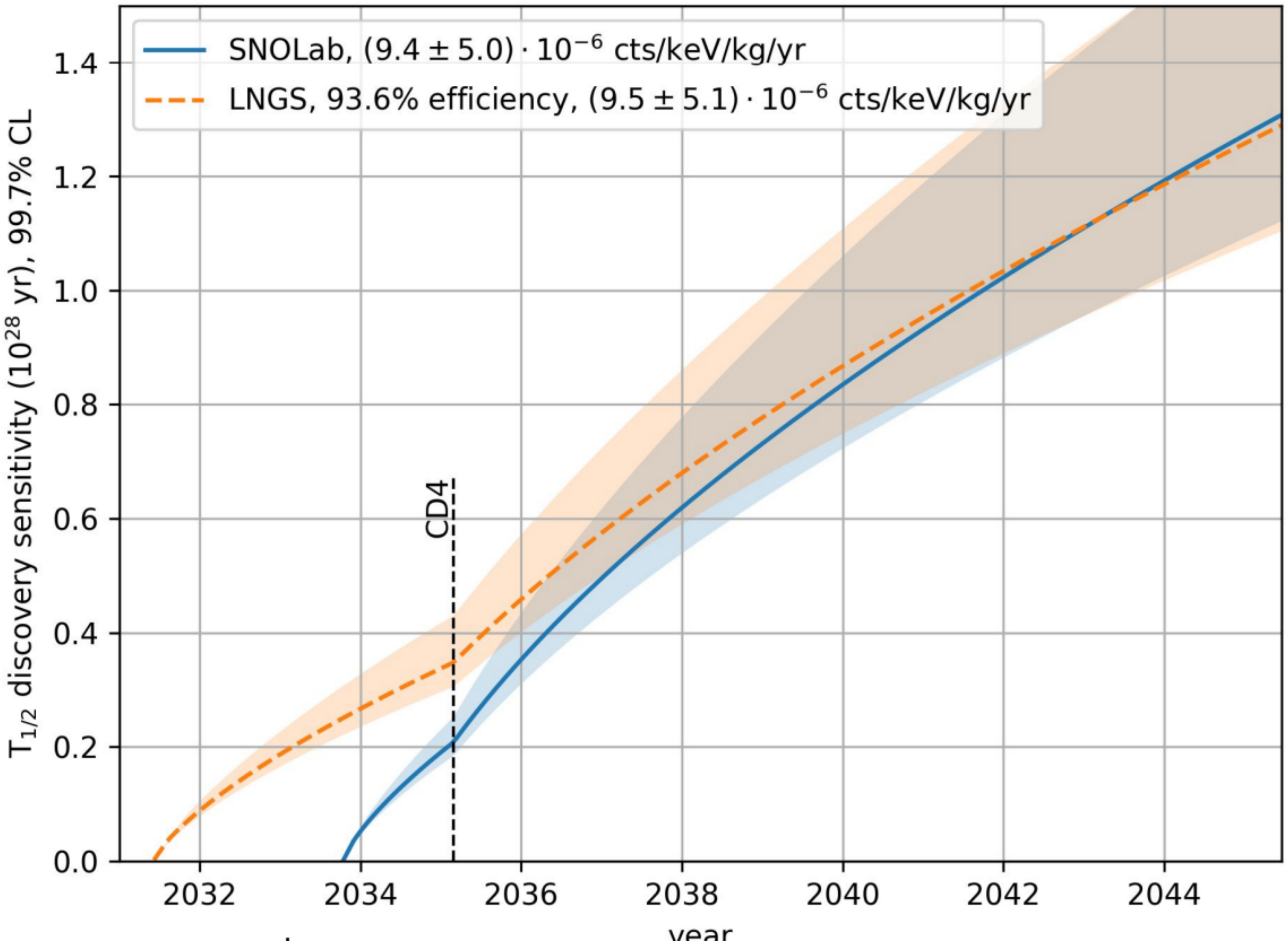

Alpha

- Those α depositing on diode surface making it through the p^+ electrode or the this-surfaced insulating grooves
  - most of the surface is a too-thick n^+
- Hard to estimate a priori (consider upper limits from previous experiments)
- PSD, PSD and yet improved PSD
  - complementary techniques in GERDA and MJD more or less effective depending on charge diffusion in detector geometry (BEGe vs PPC)
  - therefore, design the LEGEND-1000 ICPC detector electrode geometry based on the relative size of the detector's passivated surface

Selection of additional R&D

- Larger mass detectors: different configurations with similar weighting potential being still pursued as alternatives to baseline, but need time
- Material:
  - clean manufacturing of alloys and plastics by laser-excitation additive "3-D printing" (SLA)
  - In-house synthesis of more radio-pure PEN
- FE: Reduced front-end substrate and connector mass, related to new ASIC radio-pure boards (JINST15 P09022)
- All signal cables in re-entrant tube from clean Kapton (incl Diode HV)

LEGEND + rest of the world

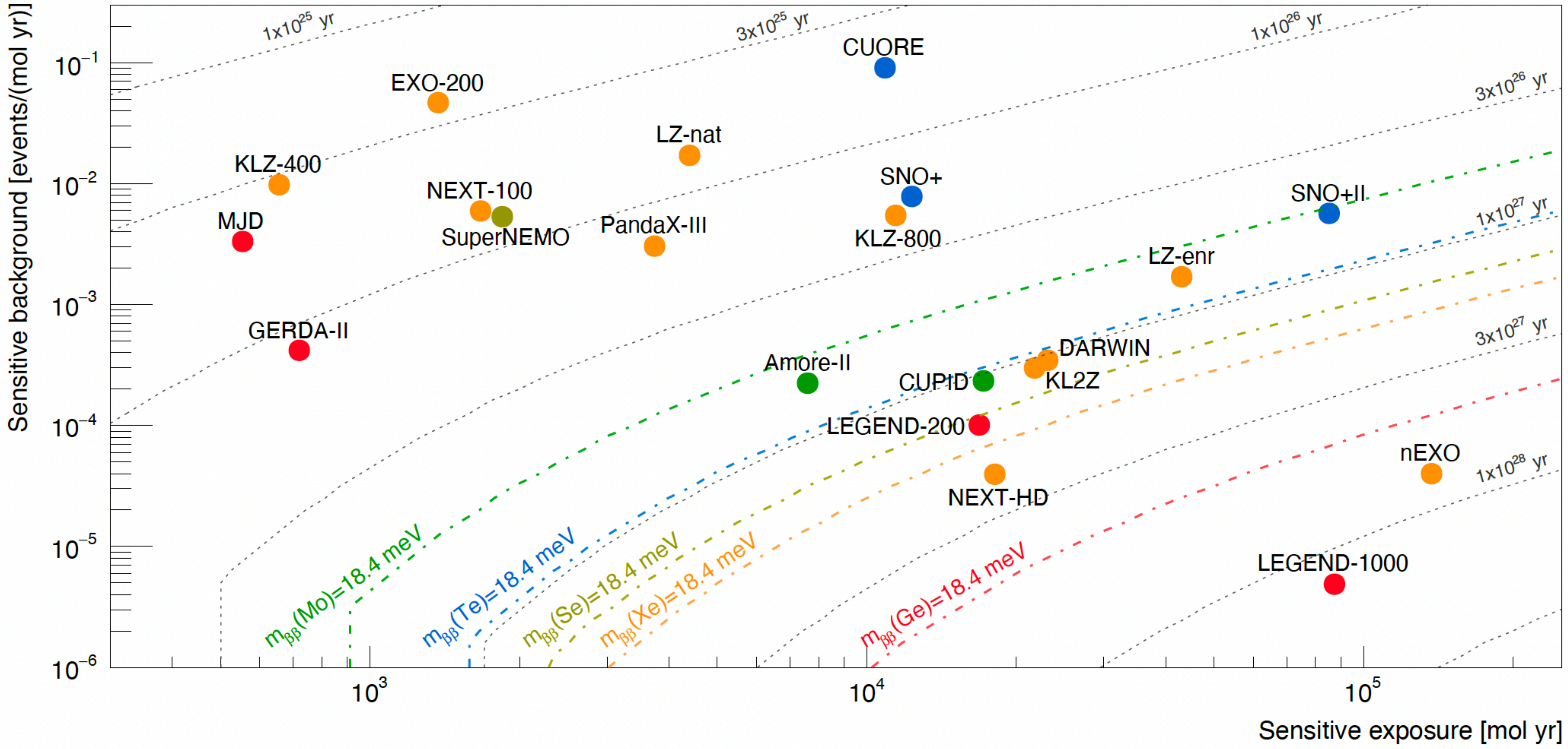

FIG. 21 Sensitive background and exposure for recent and future experiments. The grey dashed lines indicate specific discovery sensitivity values on the $0\nu\beta\beta$-decay half-life. The colored dashed line indicate the half-life sensitivities required to test the bottom of the inverted ordering scenario for ^{76}Ge, ^{136}Xe, ^{130}Te ^{100}Mo, and ^{82}Se, assuming for each isotope the largest NME value among the QRPA calculations listed in Tab. I. A livetime of 10 yr is assumed except for completed experiments, for which the final reported exposure is used.

https://arxiv.org/pdf/2202.01787.pdf

(Approx) timelines

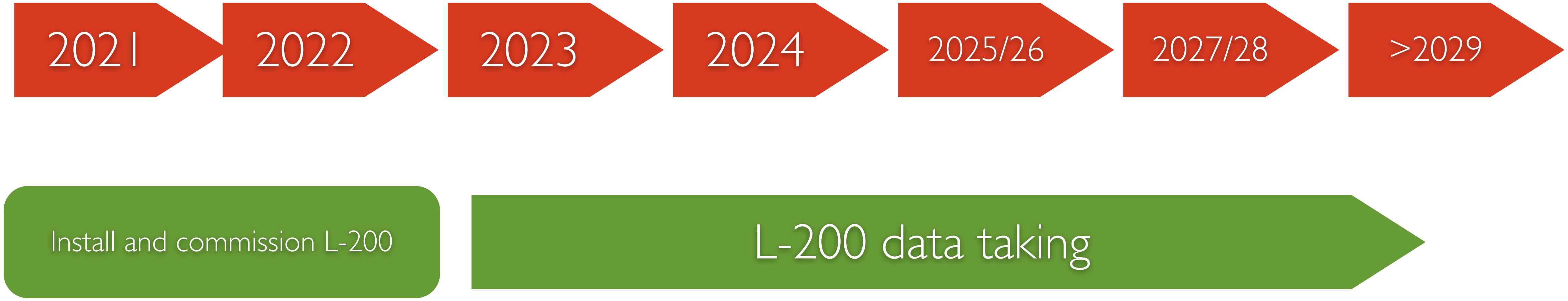

2021

2022

2023

2024

2025/26

2027/28

>2029

Install and commission L-200

L-200 data taking

L-1000 timeline

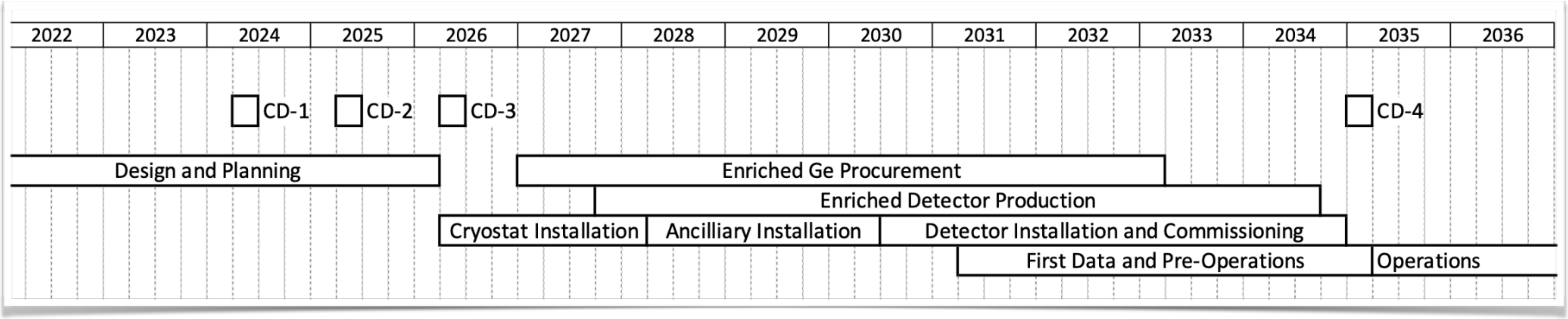

Back-up

MO separation

$$\langle m_{\beta\beta}\rangle = \left|\sum_{i=1}^{3} U_{ei}^2 m_i\right|$$

$$= \left|m_0 c_{12}^2 c_{13}^2 + \sqrt{m_0^2 + \delta m_{\rm sol}^2}\, s_{12}^2 c_{13}^2 e^{2i(\alpha_2-\alpha_1)} + \sqrt{m_0^2 + \delta m_{\rm sol}^2 + \delta m_{\rm atm}^2}\, s_{13}^2 e^{-2i(\delta_{\rm CP}+\alpha_1)}\right| \quad \text{NO}$$

$$= \left|m_0 s_{13}^2 + \sqrt{m_0^2 - \delta m_{\rm atm}^2}\, s_{12}^2 c_{13}^2 e^{2i(\delta_{\rm CP}+\alpha_2)} + \sqrt{m_0^2 - \delta m_{\rm sol}^2 - \delta m_{\rm atm}^2}\, c_{12}^2 c_{13}^2 e^{2i(\delta_{CP}+\alpha_1)}\right| \quad \text{IO.}$$

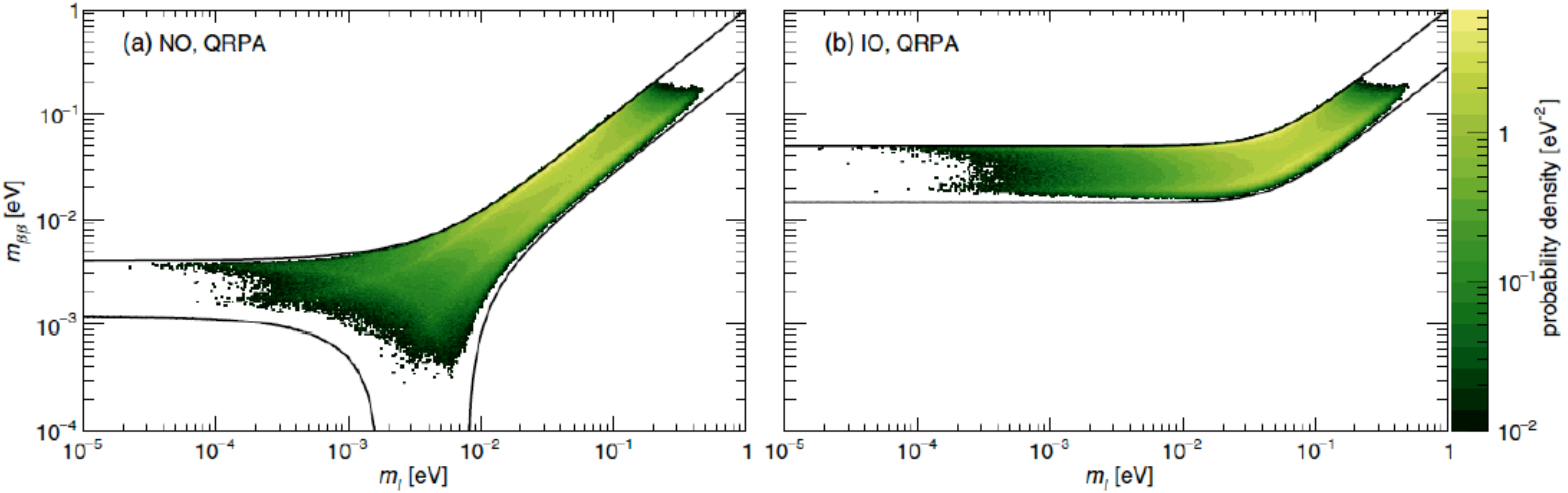

Phys. Rev. D 96, 053001

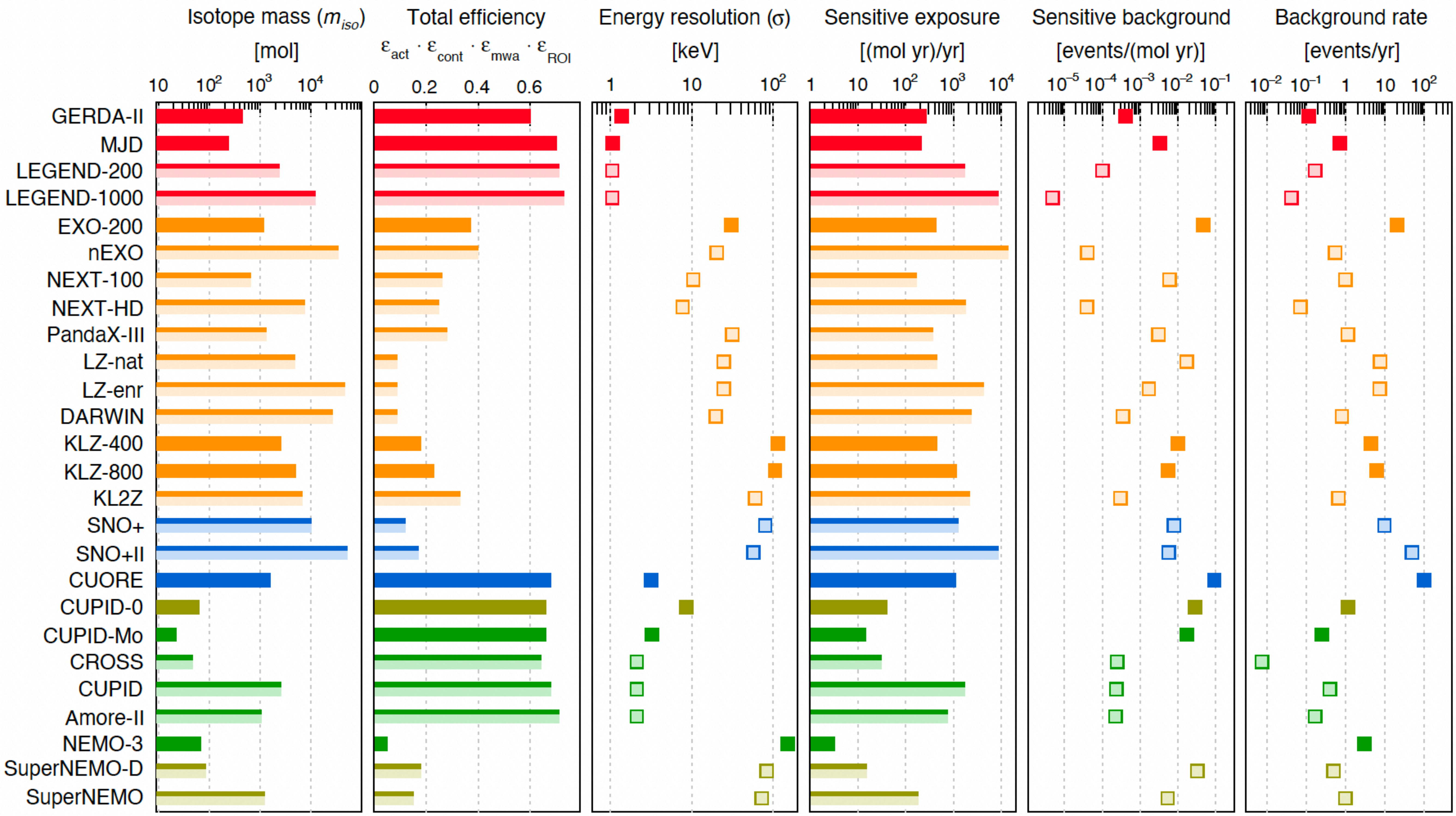

FIG. 20 Fundamental parameters driving the sensitive background and exposure, and consequently the sensitivity, of recent and future phases of existing experiments (see Eq. 47). Red bars are used for ^{76}Ge experiments, orange for ^{136}Xe, blue for ^{130}Te, green for ^{100}Mo, and sepia for ^{82}Se. Similar exposures are achieved with high mass but poorer energy resolution and efficiency by gas and liquid detectors, or with small mass but high resolution and efficiency by solid state detectors. The sensitive exposure is computed for one year of livetime. Ligher shades indicate experiments which are under construction or proposed.

https://arxiv.org/pdf/2202.01787.pdf

Active veto optical parameters

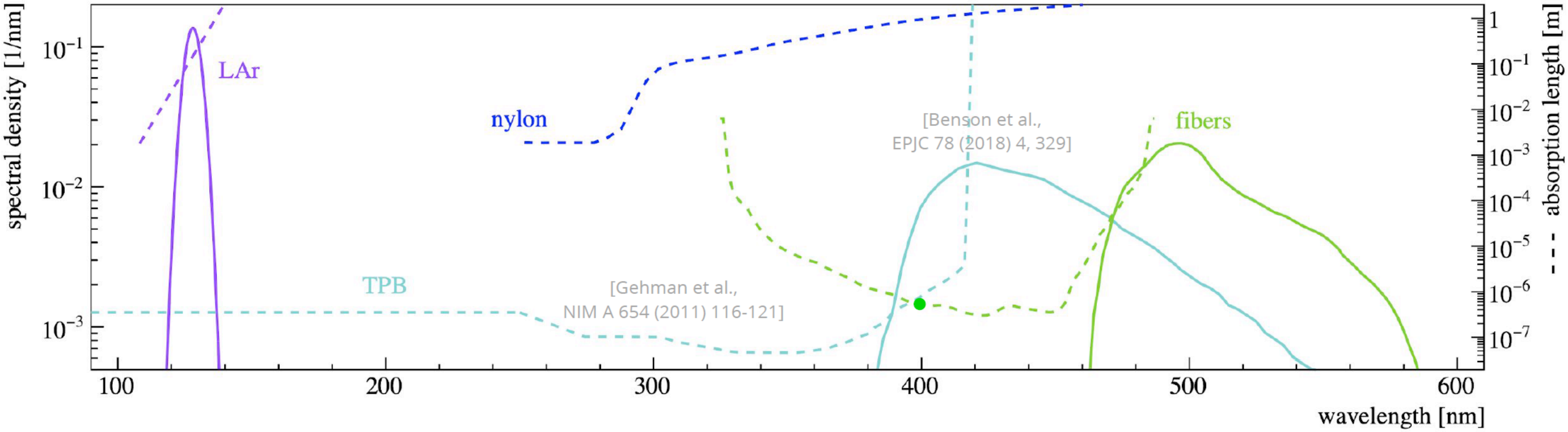

LAr active veto, related specs

- Ar_2 excimer scintillates at 128 nm (VUV), LY O(10k photons/MeV deposited), singlet and triplet states mix in fast (~few ns) and slow (~1.5 μs) components

- triplet attenuation highly depends on recombination with impurities (N, O, Xe ppm-to-ppb) sneaking at Ar distillation
- "class 5.5" LAr from plant + in place at LNGS ad-hoc system to purify LAr as it flows between tank and cryostat
- Expected to result in $\lambda_{att} \lesssim 1$m, small wrt cryostat radius

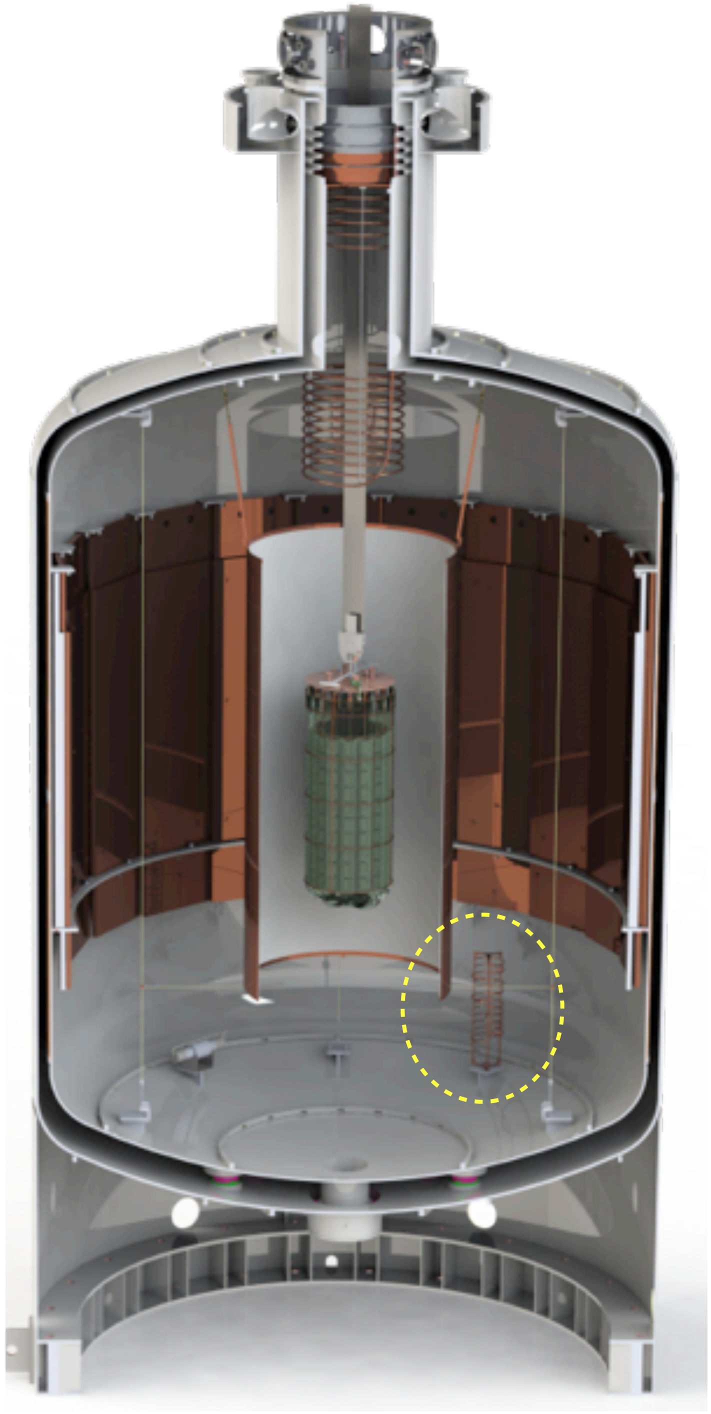

LLAMA device in LAr will monitor in time attenuation and triplet lifetime

TABLE XV. The relevant properties of PEN.

Property	**Value**	
Atomic composition	$[C_{14}H_{10}O_4]_n$	
Density: δ	$1.35\,g/cm^3$	
Melting point	270°C	
Peak emission λ	445±5 nm	
Light yield	≈ 4000 photons/MeV	
Decay constant	34.91 ns	
Attenuation length	≈ 5 cm	
Young's modulus: E [GPa]	1.855±0.011 (296 K)	3.708±0.084 (77 K)
Yield strength: σ_{el} [MPa]	108.6±2.6 (296 K)	209.4±2.8 (77 K)

L200: Front-End electronics

- Low-Mass (radio-pure) FE on ULTEM inert plastic *(a la MJD)* feeding into "CC4" CSA pre-amp *(a la GERDA)*
- Output from CC4: ~2.7 V to flange/air

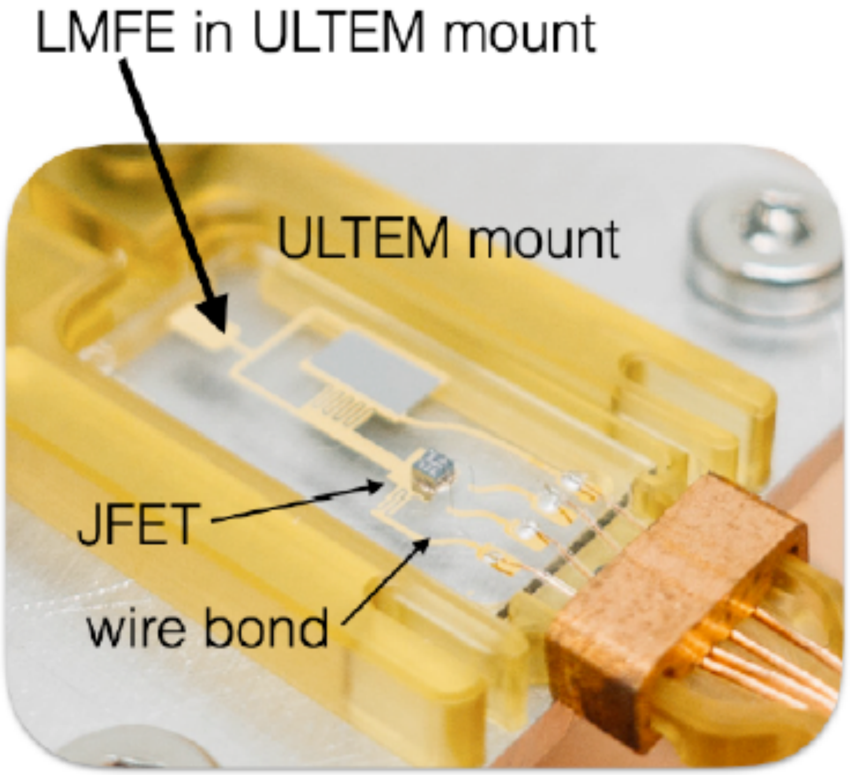

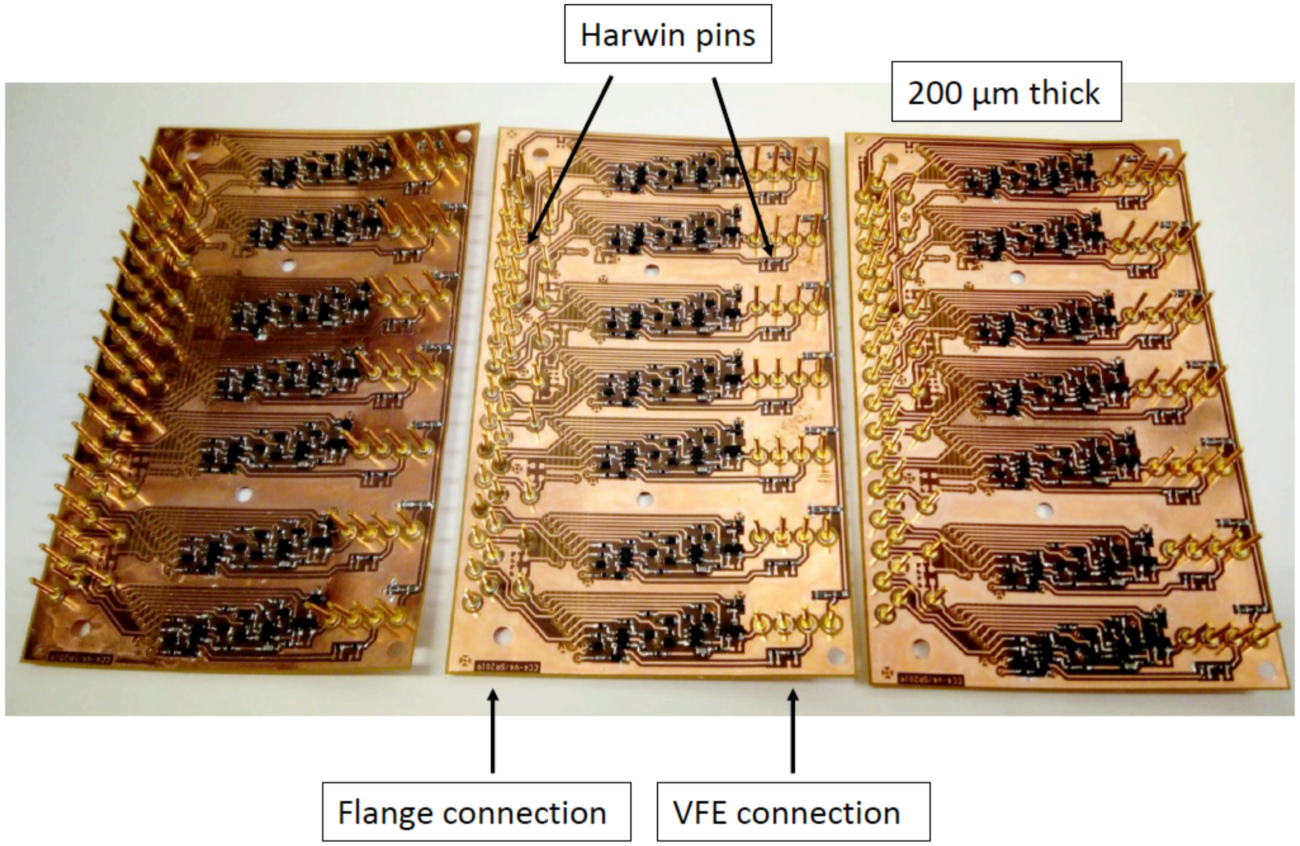

L1000: baseline Front-End design

TABLE V. Specifications for a low-noise, low-capacitance readout ASIC for LEGEND-1000.

https://arxiv.org/abs/2107.11462

Description	Design Specifications
Threshold	1 keV
Dynamic range	10 MeV
Bandwidth	50 MHz
Assumed detector capacitance	5 pF
Cabling	minimal (power, ground, pulser, diff. out)
External components	none
Power supply	single
Reset	internal
Other	observable leakage current, testable warm or cold

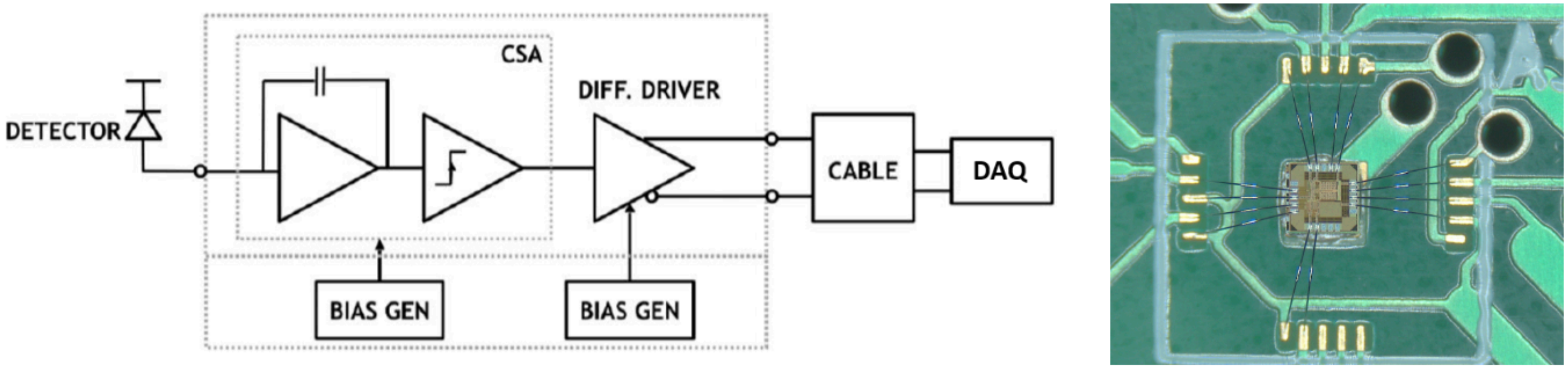

FIG. 30. Left: Block diagram of the L1K charge-sensitive preamplifier ASIC, indicating internal continuous reset, voltage regulation, and differential driver. Right: The wire-bonded 1 mm^2 L1K ASIC on its dedicated testboard.

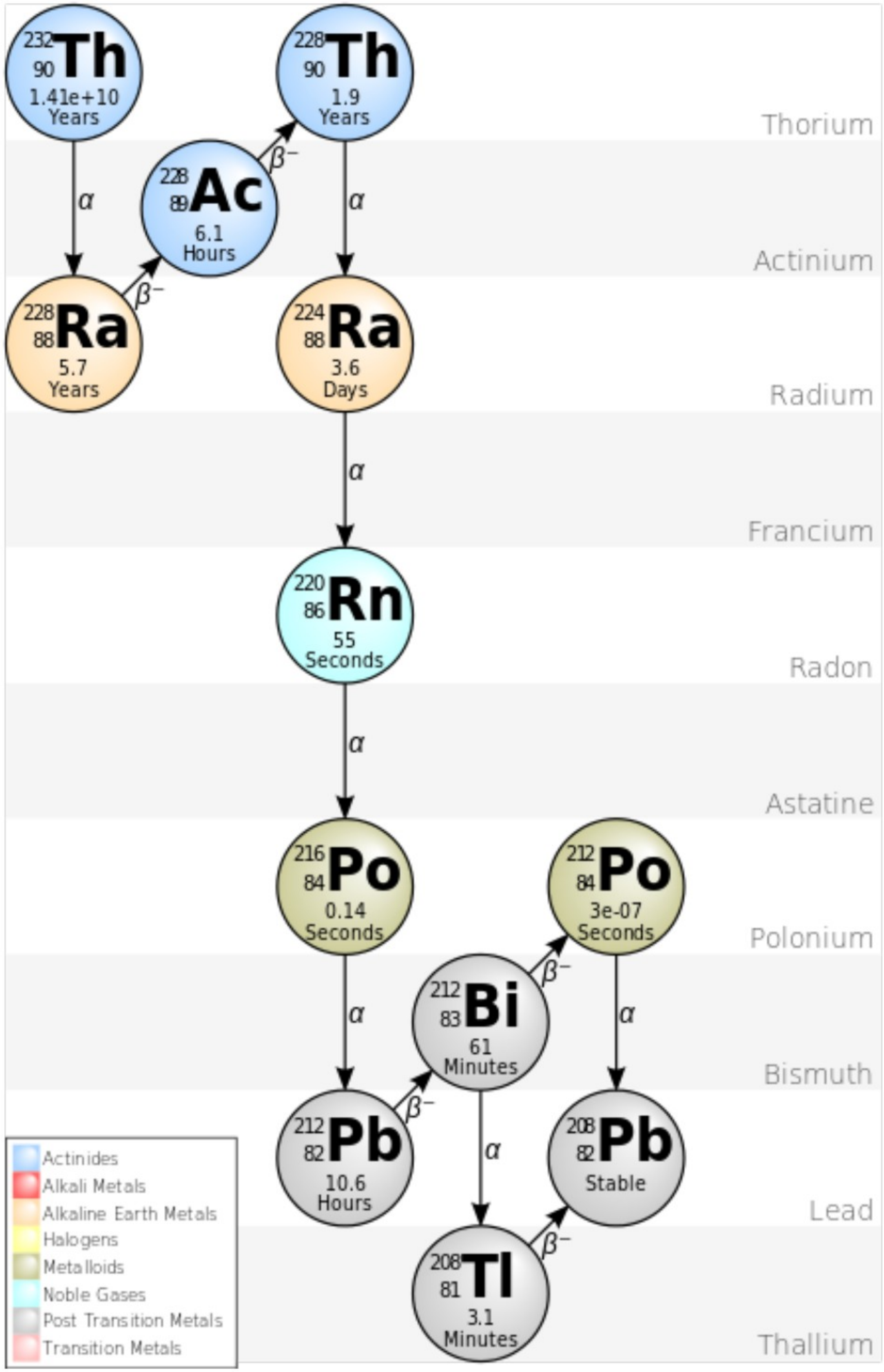

232 90 Th 1.41e+10 Years
228 90 Th 1.9 Years
228 89 Ac 6.1 Hours
228 88 Ra 5.7 Years
224 88 Ra 3.6 Days
220 86 Rn 55 Seconds
216 84 Po 0.14 Seconds
212 84 Po 3e-07 Seconds
212 83 Bi 61 Minutes
212 82 Pb 10.6 Hours
208 82 Pb Stable
208 81 Tl 3.1 Minutes
α
β⁻
Thorium
Actinium
Radium
Francium
Radon
Astatine
Polonium
Bismuth
Lead
Thallium
Actinides
Alkali Metals
Alkaline Earth Metals
Halogens
Metalloids
Noble Gases
Post Transition Metals
Transition Metals

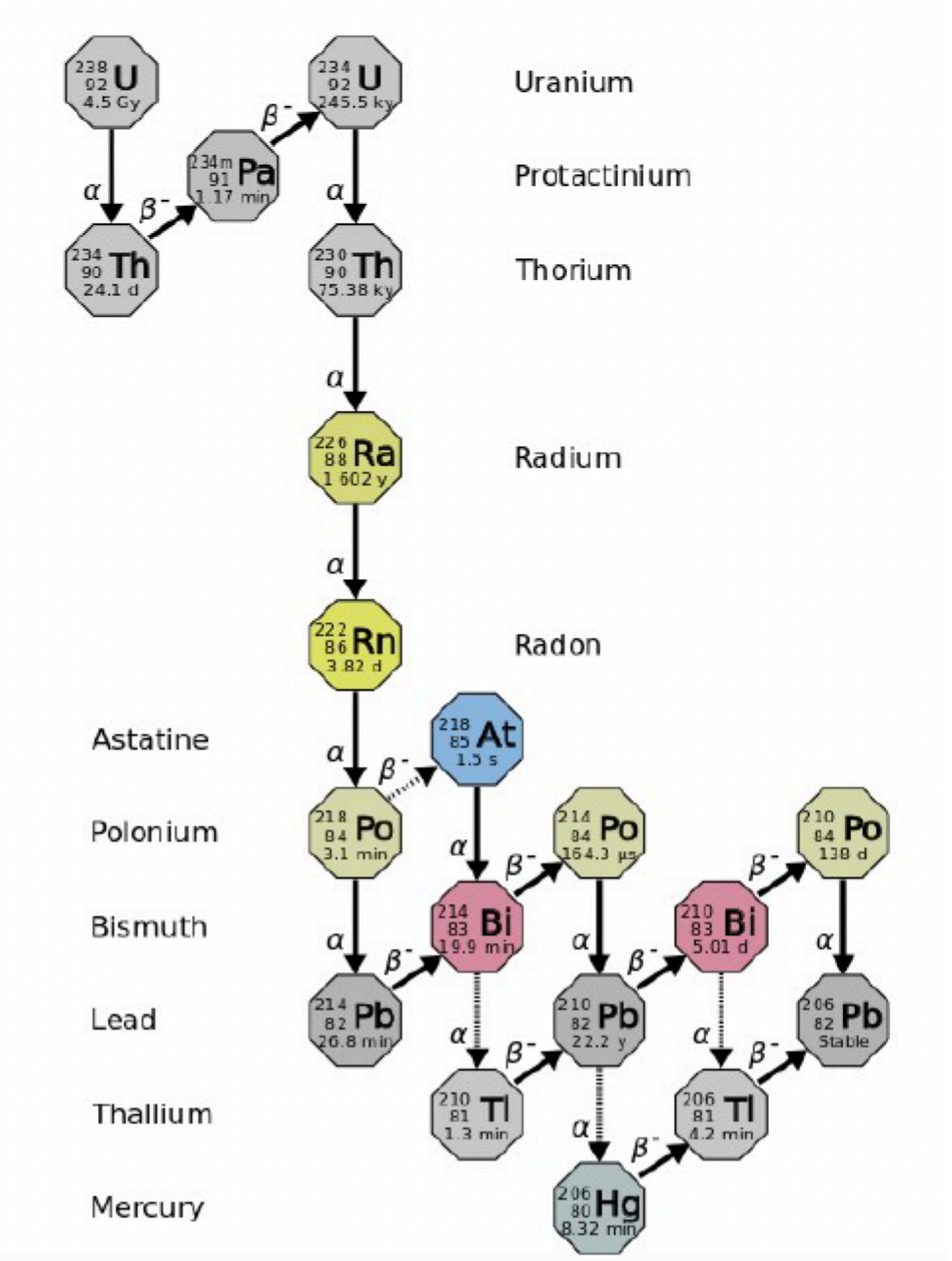

238 92 U 4.5 Gy
234 92 U 245.5 ky
234m 91 Pa 1.17 min
234 90 Th 24.1 d
230 90 Th 75.38 ky
226 88 Ra 1 602 y
222 86 Rn 3.82 d
218 85 At 1.5 s
218 84 Po 3.1 min
214 84 Po 164.3 µs
210 84 Po 138 d
214 83 Bi 19.9 min
210 83 Bi 5.01 d
214 82 Pb 26.8 min
210 82 Pb 22.2 y
206 82 Pb Stable
210 81 Tl 1.3 min
206 81 Tl 4.2 min
206 80 Hg 8.32 min
α
β⁻
Uranium
Protactinium
Thorium
Radium
Radon
Astatine
Polonium
Bismuth
Lead
Thallium
Mercury

Phase II upgrade: BEGe detectors

Broad Energy Germanium

γ interactions:
- multiple Compton scattering (MSE)
- sequence of peaks in current signal
- Double escpape peak (DEP):
  proxy for 0νββ events

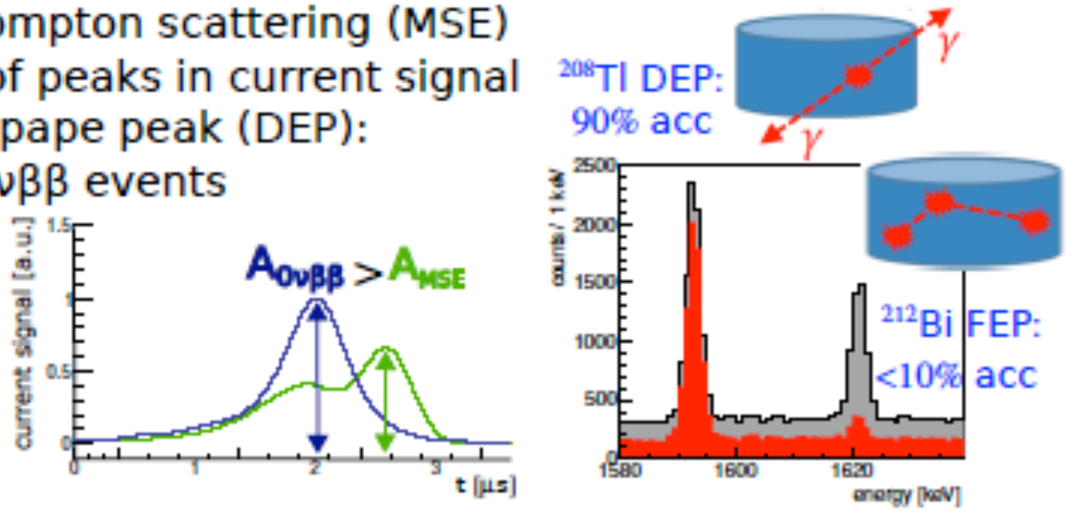

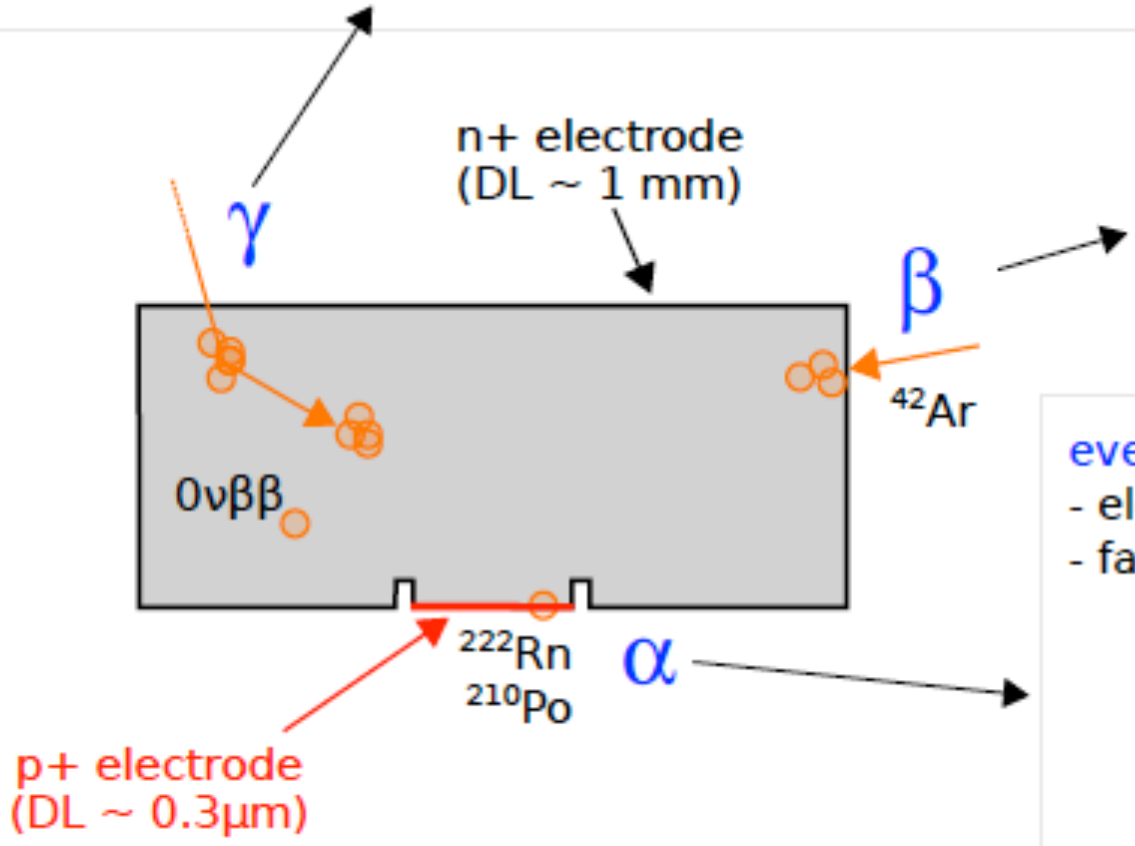
γ

n+ electrode
(DL ~ 1 mm)

β

^{42}Ar

0νββ

^{222}Rn
^{210}Po

α

p+ electrode
(DL ~ 0.3µm)

events on n+ surface:
- semiconductor junction -> weak E field
- slow current signal

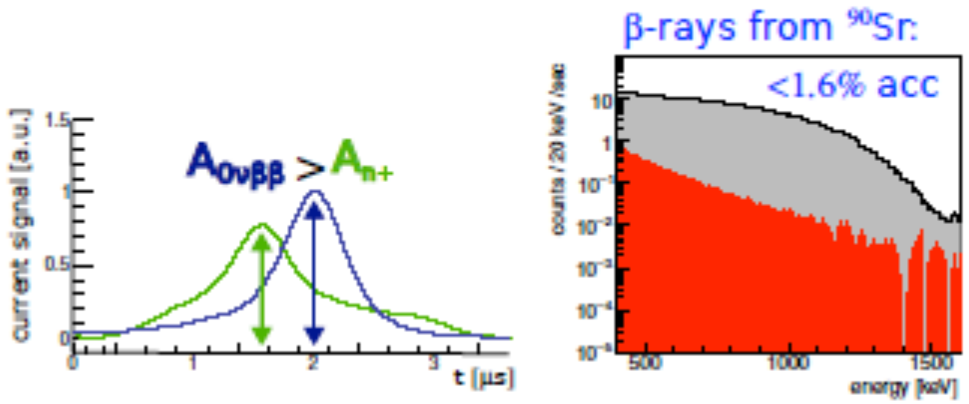

events on p+ electrode:
- electron drift faster then holes
- faster charge signal

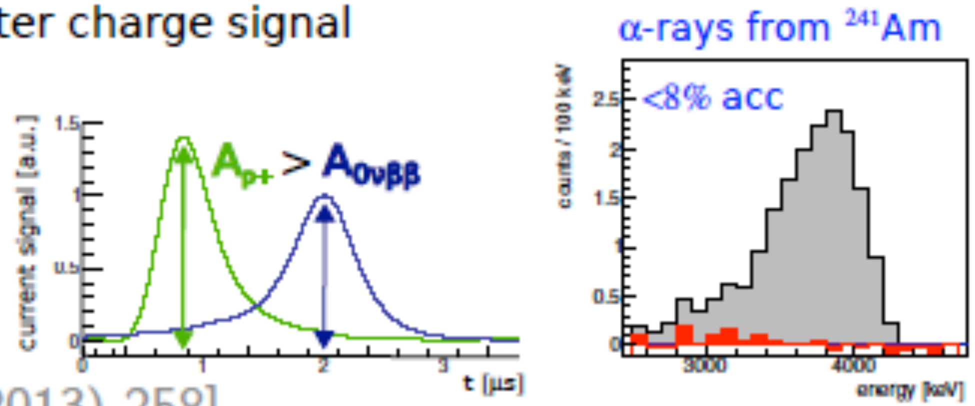

[JINST 6 2011 P03005, JINST 4 2009 P10007, EPJC 73 (2013) 258]

PSD and LAr veto during Phase II commissioning

^{226}Ra calibration run (single BEGe string in GERDA):

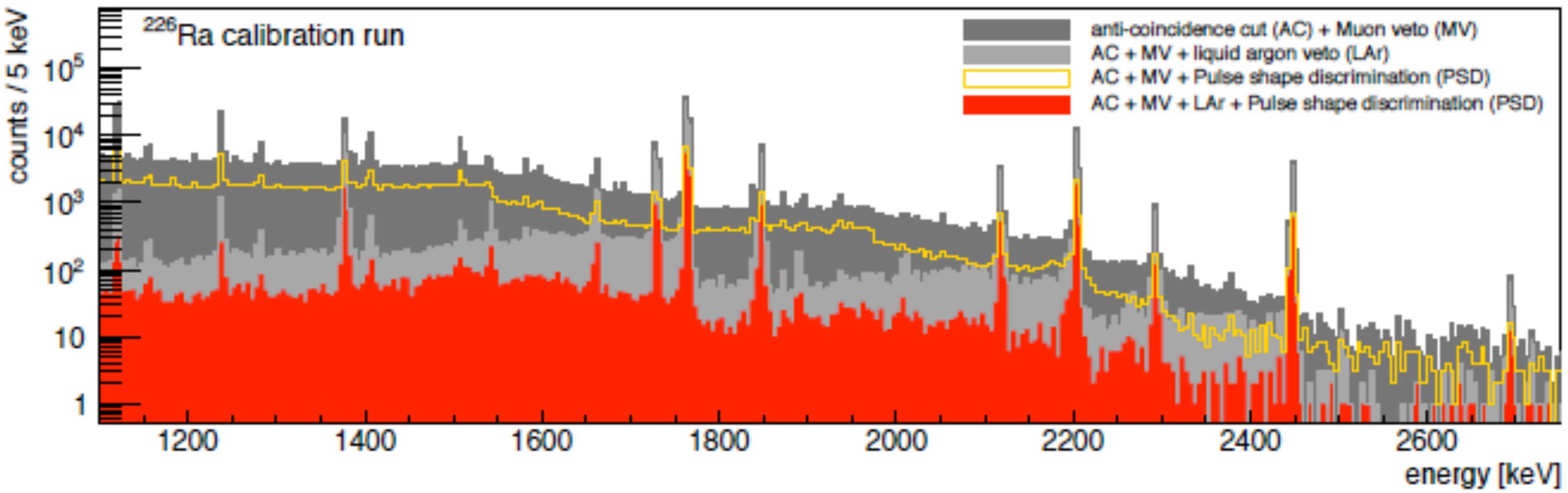

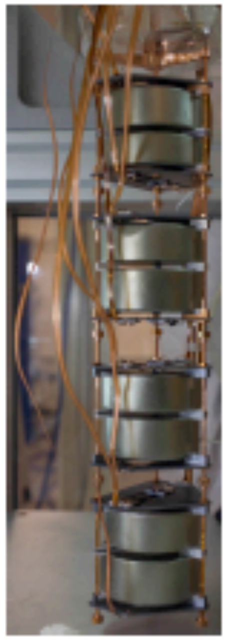

^{228}Th calibration run:

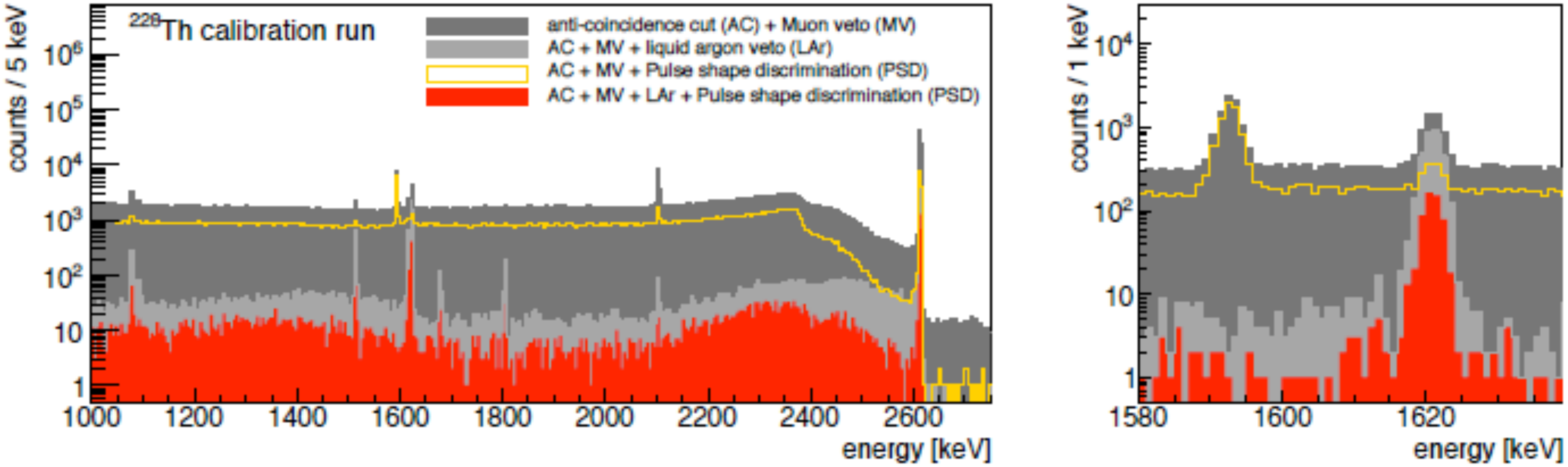

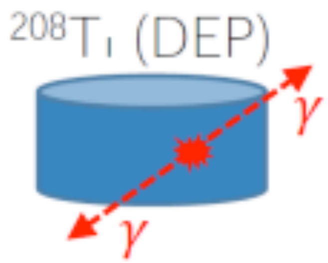

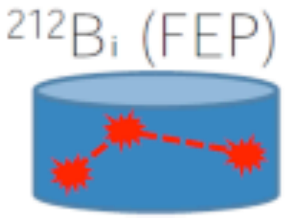

Combined suppression factors: 27±2 (for ^{226}Ra) and 300±28 (for ^{228}Th)

Suppression depends on isotope, location and detector configuration

main components before LAr veto/PSD:
- α from ^{210}Po, ^{226}Ra
- β from ^{42}K
- γ from ^{214}Bi, ^{208}Tl

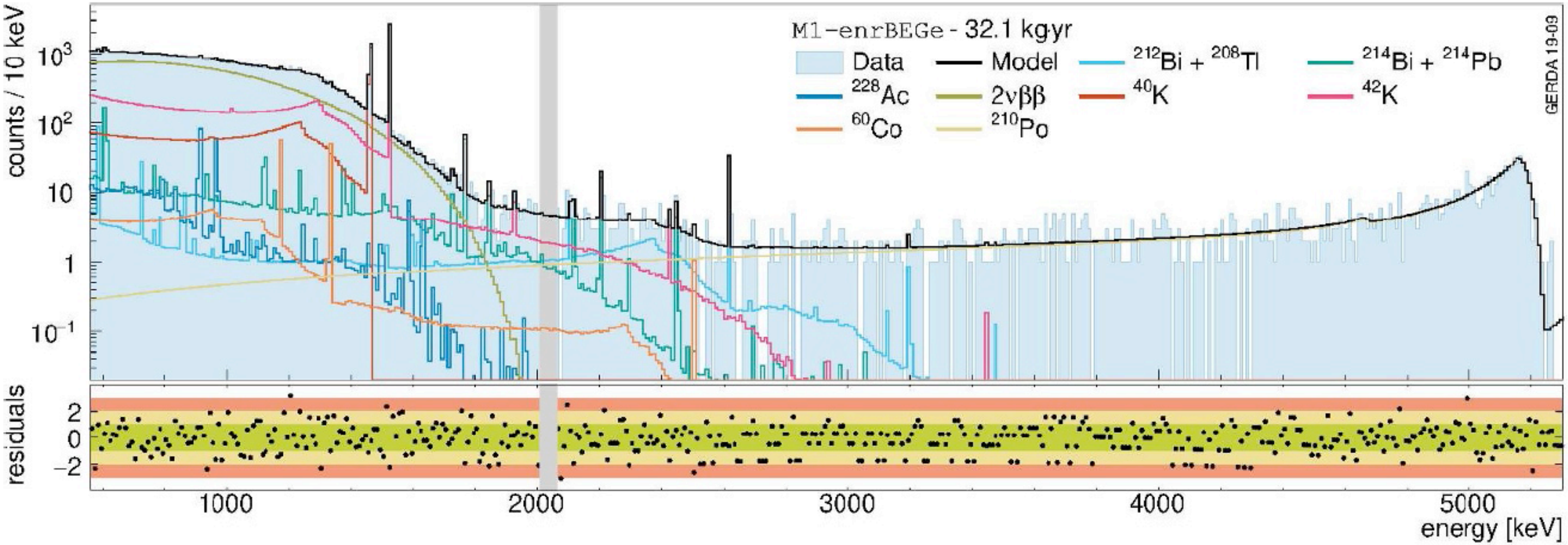

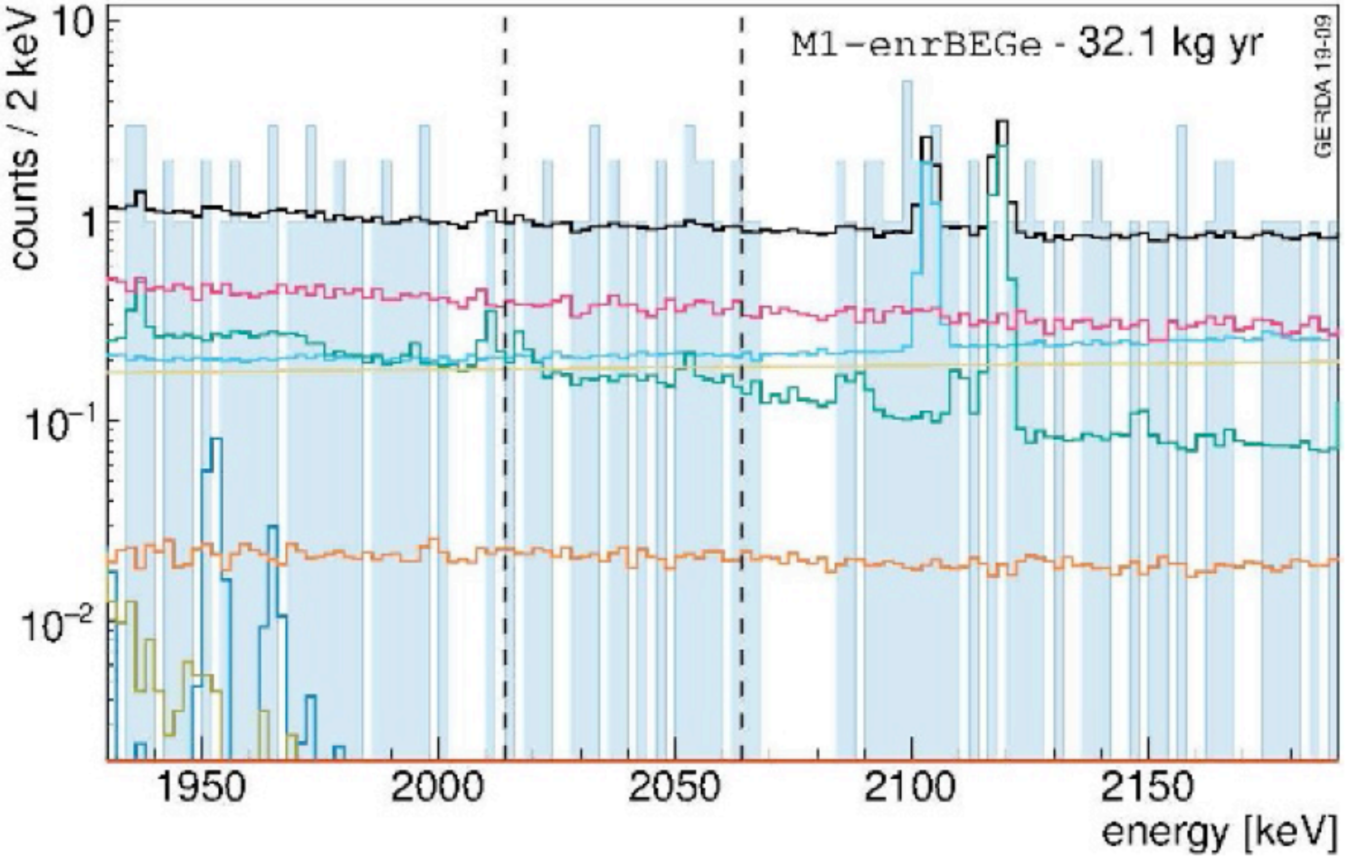

JHEP 2020, 139 (2020)

- same isotopes as in Phase I
- Th/Ra contributions consistent with screening results
- main components before LAr veto/PSD:
  - α from ^{210}Po,^{226}Ra
  - β from ^{42}K
  - γ from ^{214}Bi,^{208}Tl
- flat background in the ROI

https://arxiv.org/pdf/1205.5608.pdf

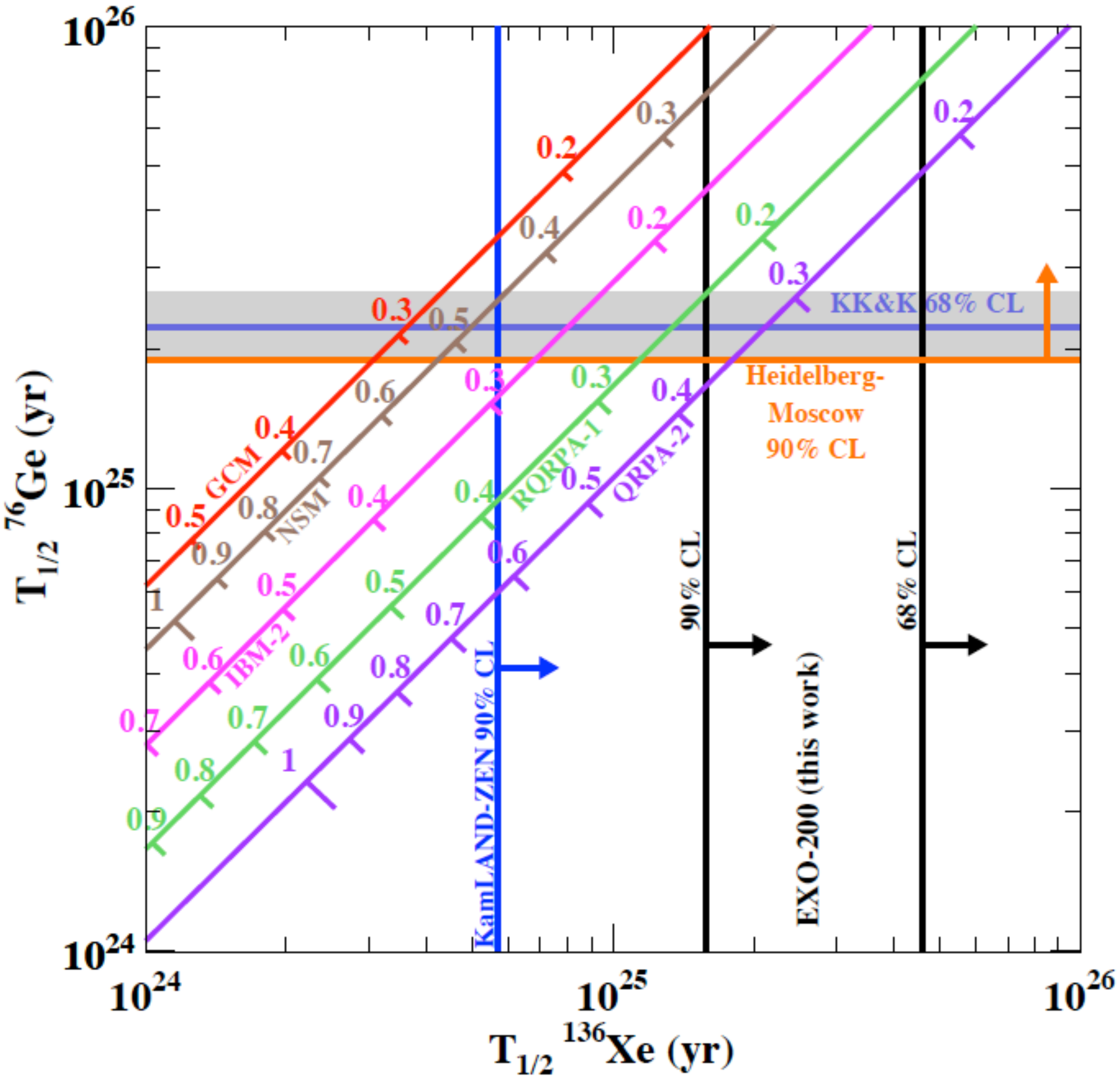

FIG. 6: Relation between the $T_{1/2}^{0\nu\beta\beta}$ in ^{76}Ge and ^{136}Xe for different matrix element calculations (GCM [20], NSM [21], IBM-2 [22], RQRPA-1 [23] and QRPA-2 [5]). For each matrix element $\langle m\rangle_{\beta\beta}$ is also shown (eV). The claim [4] is represented by the grey band, along with the best limit for ^{76}Ge [19]. The result reported here is shown along with that from [7].

Simulated example spectrum, after cuts, from 10 years of data

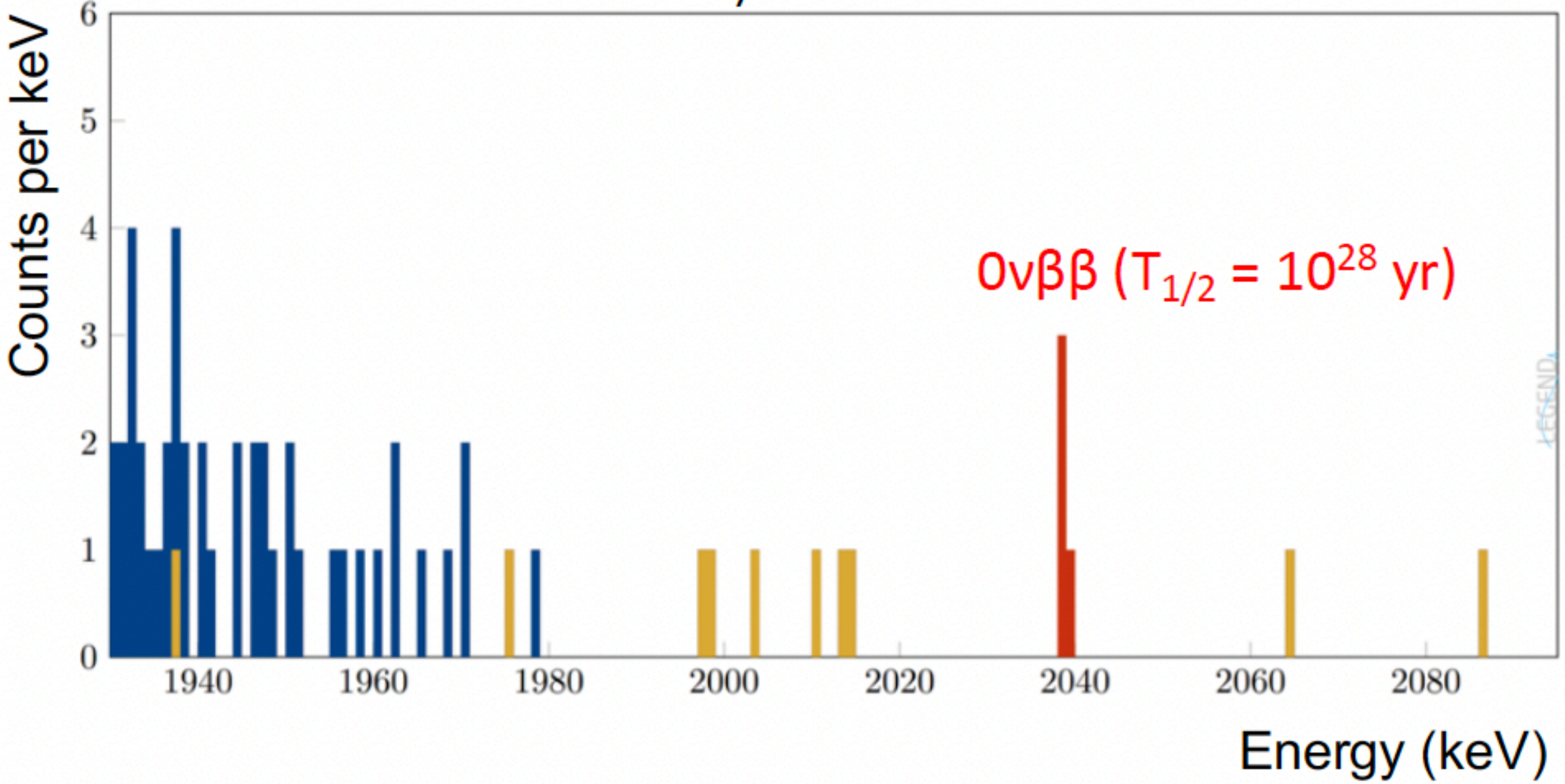

The Baseline Design: Underground Liquid Argon

- L1000 needs 20-25 t of UGLAr
- Builds on pioneering work of DarkSide collaboration
- UGAr will be mined at Urania facility (U.S.) 95 t/y
- Logistics and storage technology under development by DarkSide/ARGO collaboration for LNGS and SNOLAB
- Expression of interest from INFN president[1] and DarkSide leadership
- UGAr production for LEGEND-1000 in 2023 (after DS-20k)

UGAr is depleted in ^{42}Ar (^{39}Ar)

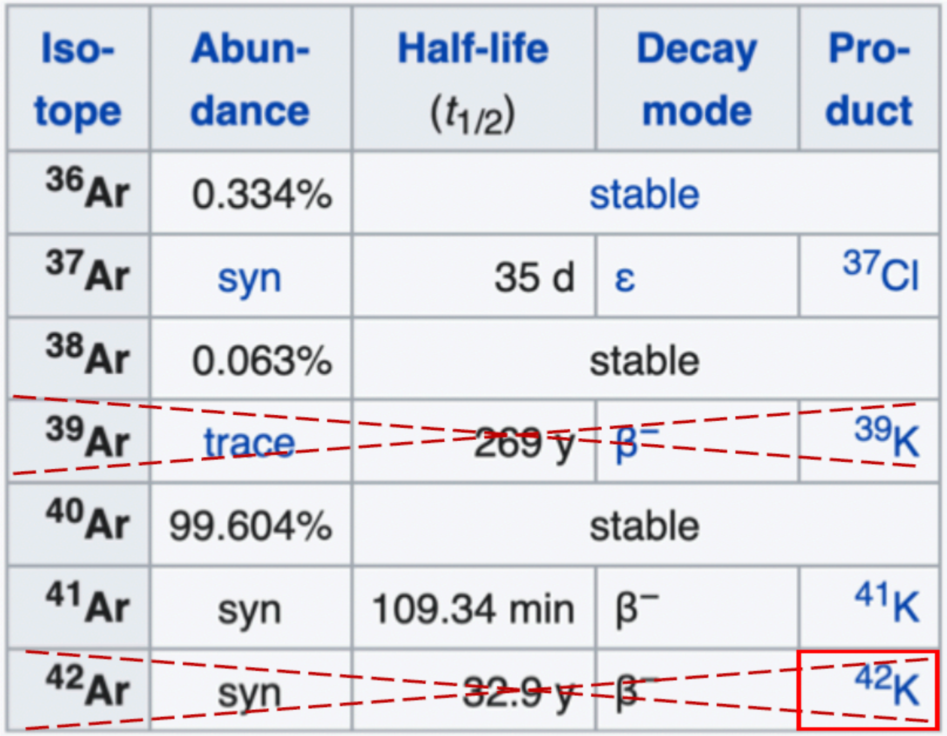

Isotope	Abundance	Half-life ($t_{1/2}$)	Decay mode	Product
^{36}Ar	0.334%	stable		
^{37}Ar	syn	35 d	ε	^{37}Cl
^{38}Ar	0.063%	stable		
~~^{39}Ar~~	~~trace~~	~~269 y~~	~~β⁻~~	~~^{39}K~~
^{40}Ar	99.604%	stable		
^{41}Ar	syn	109.34 min	β⁻	^{41}K
~~^{42}Ar~~	~~syn~~	~~32.9 y~~	~~β⁻~~	~~^{42}K~~

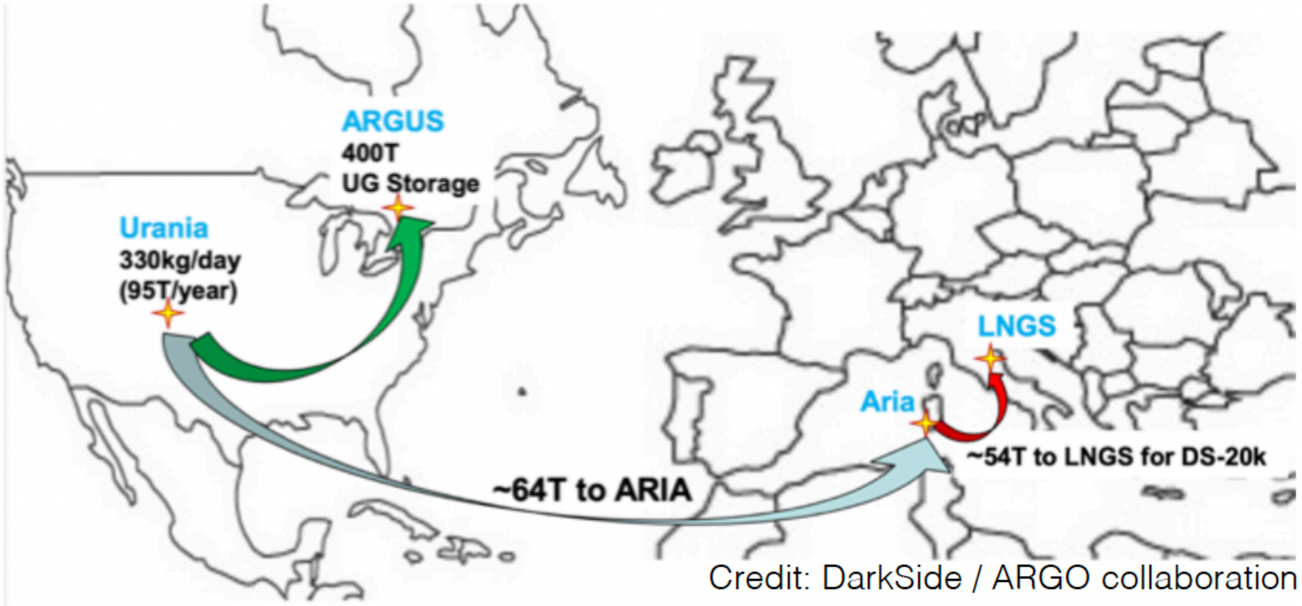

Credit: DarkSide / ARGO collaboration

---

[1] " ...we are confident that the production of the required UAr can be completed in a time scale useful for the accomplishment of the LEGEND-1000 experiment.. The present statement is an expression of interest and availability from INFN..."

BEGe and IC detectors: A/E

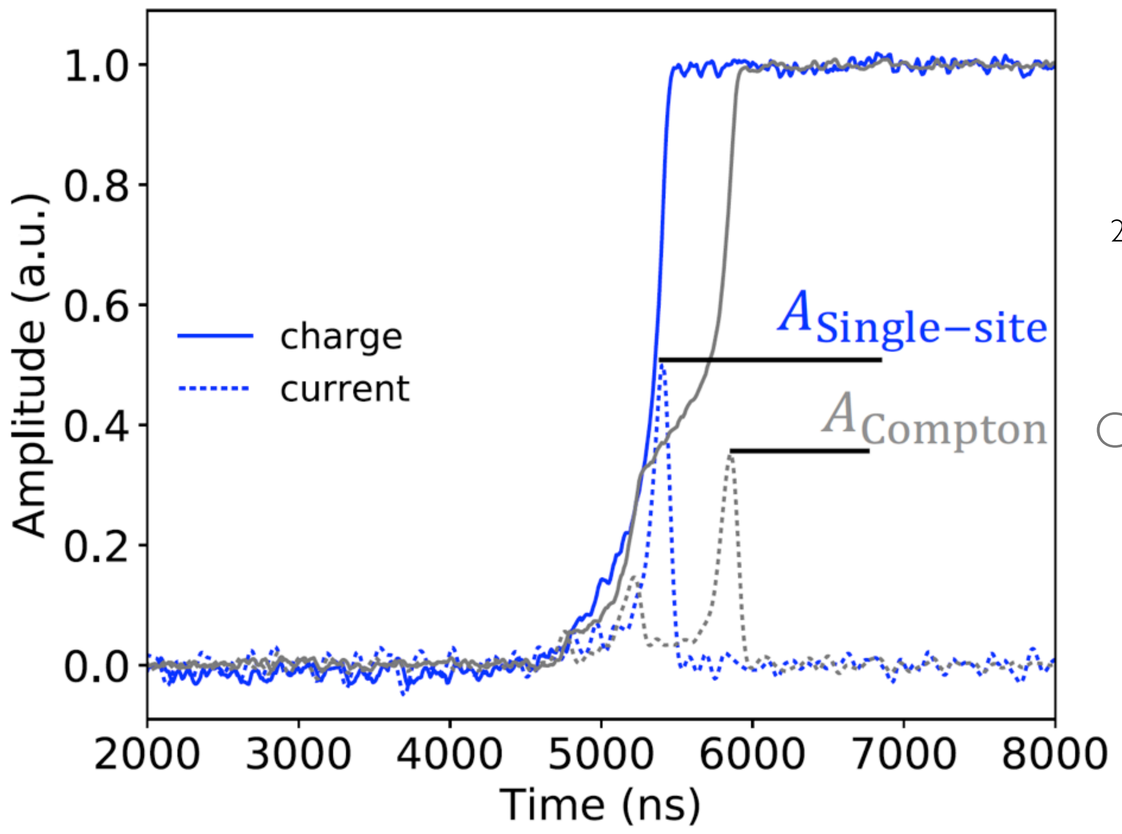

^{208}Tl γ (2614 keV)

DEP from diode

Compton in diode

GERDA

$0\nu\beta\beta$ decay signal efficiency:

- $\epsilon_{\mathbf{PSD}}^{\mathbf{BEGe}} = (\mathbf{88.7} \pm \mathbf{3.2})\%$
- $\epsilon_{\mathbf{PSD}}^{\mathbf{IC}} = (\mathbf{90.0} \pm \mathbf{1.7})\%$
- $\epsilon_{\mathbf{PSD}}^{\mathbf{Coax}} = (\mathbf{68.9} \pm \mathbf{3.1})\%$

Y.Kermaidic, Neutrino '20

See later for L-200 preliminary figures

LEGEND-200: what's new, *in a nutshell*

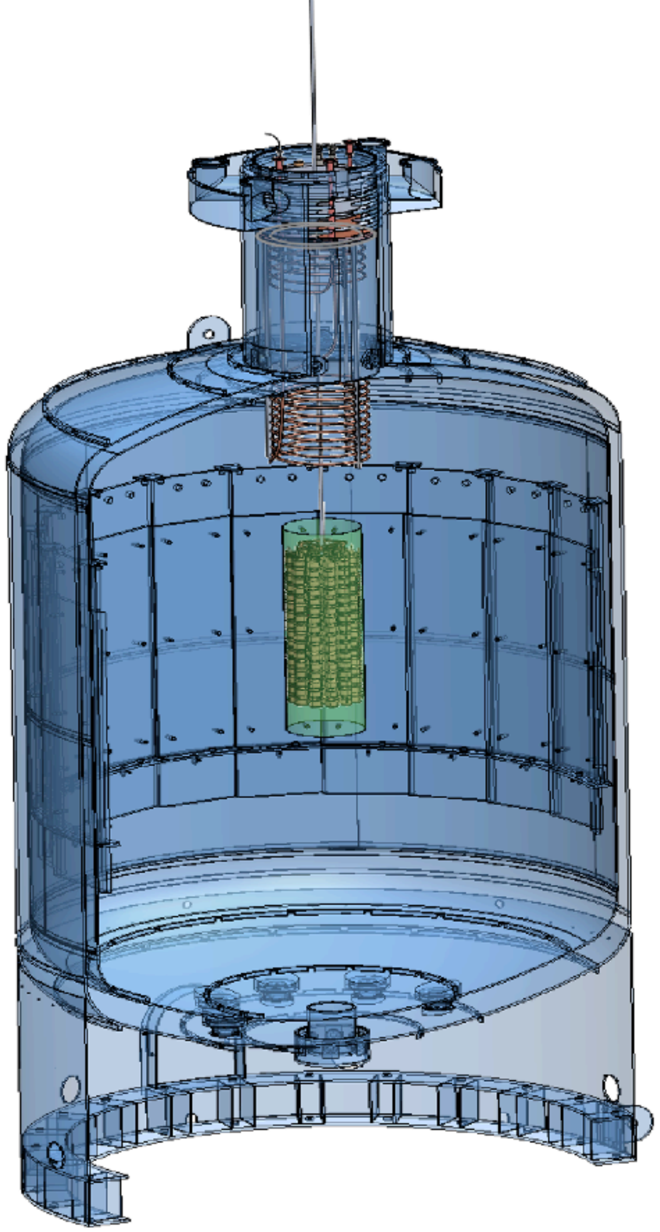

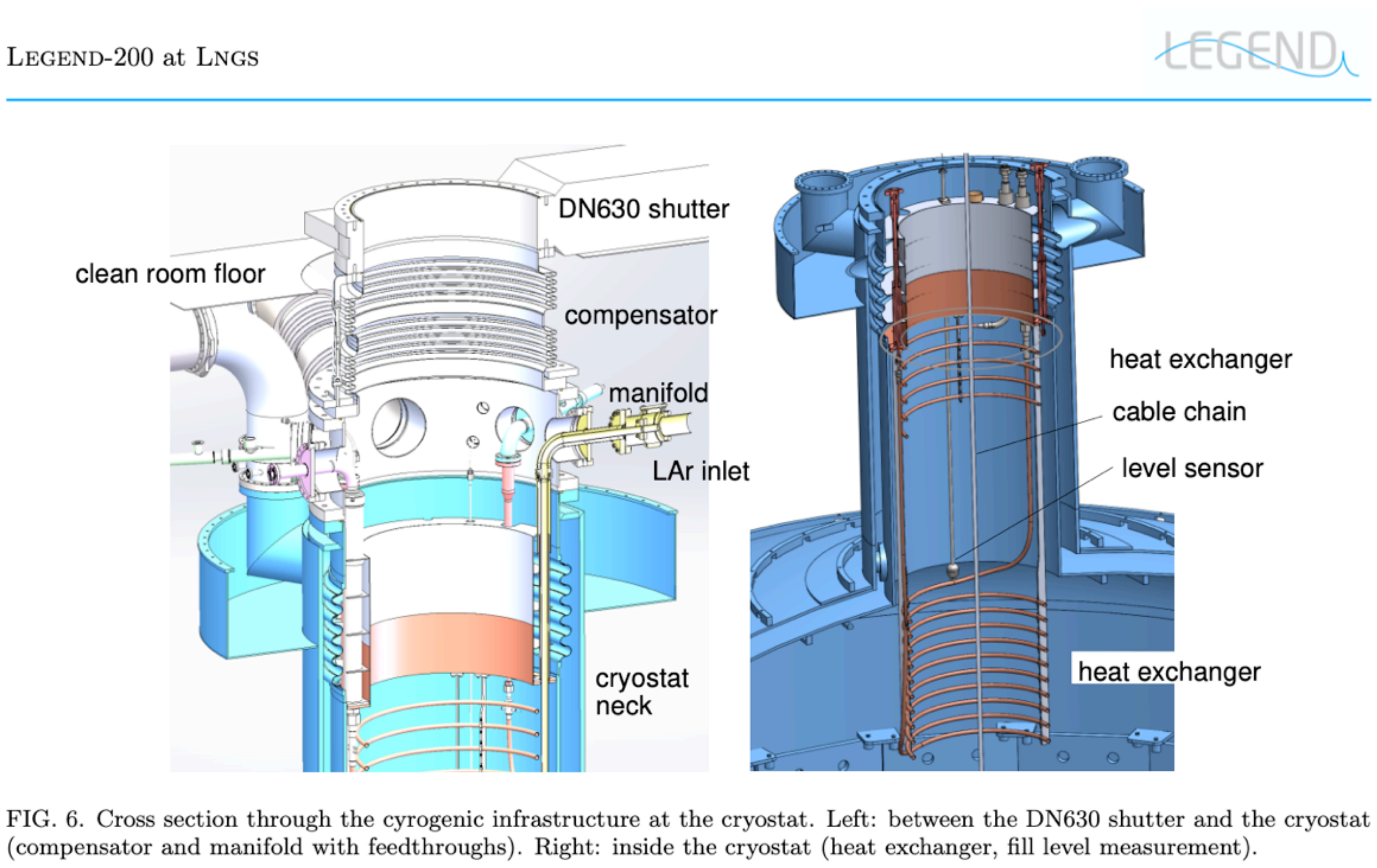

LEGEND-200 at LNGS

FIG. 6. Cross section through the cyrogenic infrastructure at the cryostat. Left: between the DN630 shutter and the cryostat (compensator and manifold with feedthroughs). Right: inside the cryostat (heat exchanger, fill level measurement).

Modifications wrt GERDA infrastructure:

- 14 strings of (mostly) ICPC detectors
- new electronics
- raise clean room roof, new lock
- new cabling, detector suspension, feedthroughs
- Improved LAr light collection

Read also:
Universe **2021**, *7*, 386.